AEAS Report 93-101

(1)

OVERVIEW OF SELECTED UNDERWATER ACOUSTIC PROPAGATION MODELS

L.B. Dozier
R.C. Cavanagh
Science Applications International Corporation
McLean, VA 22102

May 1993

OFFICE OF NAVAL RESEARCH
Advanced Environmental Acoustic
Support Program (AEAS)
Arlington, VA 22217

AEAS Report 93-101

OVERVIEW OF SELECTED UNDERWATER ACOUSTIC PROPAGATION MODELS

May 1993

Prepared by:

Lewis B. Dozier
Raymond C. Cavanagh

Prepared for:

Office of Naval Research
Advanced Environmental Acoustic Support (AEAS) Program
Code 124A
Arlington, VA 22217
Attn: Mr. R. Feden

Contract: N00014-90-D-0250 (D.O. 0005)

SCIENCE APPLICATIONS INTERNATIONAL CORPORATION
1710 Goodridge Drive
McLean, Virginia 22102

TABLE OF CONTENTS

1. INTRODUCTION

1.1 Purpose

The Advanced Environmental Acoustic Support (AEAS) Program, sponsored by the Oceanographer of the Navy (N-96) and managed by the Office of Naval Research (ONR Code 124A), is the Navy's Advanced Development focus for Environmental/Acoustic (EVA) products used for system development/deployment and operational support. Among the more important and visible EVA products are the sound transmission models (often referred to as TL or transmission loss models), which have over the past twenty years made dramatic strides not only in technical capabilities but also in credibility.

Because of the popularity of the EVA models throughout the Navy, AEAS and other projects make day-to-day decisions about these models, such as: which model is best for a given environment, how fast is it likely to run, what computer resources are required, what kind of accuracy is expected, who else uses the model, how does it treat the bottom, fluctuations, etc. This "notebook" was prepared to help transmission model users (including model developers, fleet personnel, wargamers, etc.) answer such questions and make informed decisions.

There is to our knowledge no comparable presentation of information about popular TL models. Our level of detail about the treatment of the physics lies below that of such monographs as DiNapoli and Deavenport (1979) or Tappert (1977) but above that of the wide scope of Etter (1991) or Tango (1988). Much of the computer implementation data were not to be found in any published document, and came from interviews with the model authors and implementers.

1.2 Contents and Format

We have selected nine of the more popular transmission models in use by the Navy today: GSM/FAME, MPP, APL MODE, KRAKEN, RAYMODE, ASTRAL, Standard PE, FFP, and SAFARI. Notice that we have sought to include at least one model for each

"approach," such as MPP for a ray model in a range-dependent environment, ASTRAL as the adiabatic ray model, etc. Note also that the three Navy Standard TL models are included (RAYMODE, PE, ASTRAL).

The format of this report emphasizes utility. The section immediately following this one (Section 2) provides the highest level summary of the attributes of the nine models, in table form. Readers already familiar with the physics of TL models and computer implementations will be able to use these tables directly. Readers in need of more detail will turn to Section 3 to find 6-8 page forms for each model covering everything from history and documentation to users and evaluation.

In both the tabular summary and in the model forms, significant background about the wave equation, its approximations, and its solutions is assumed. For those readers interested in refreshing their background in physics, Sections 4-6 provide a medium level review with references for recommended further reading.

In all cases, we have endeavored to provide the reader with references for the "physics" and for the individual models. Because of the vast literature on the subject, we list what we judge to be representative citations.

1.3 Longevity and Accuracy

Obviously, any tabulation of specific model information can only be a snapshot of the state of the art as of the time it is written. This first edition of the notebook was first drafted at the beginning of FY92; it is anticipated that future editions will appear on a regular basis, in an effort to keep up with the rapidly advancing field of underwater acoustic modeling.

In our survey of models, we have relied not only on published documents, but also on unpublished papers and on conversations with model authors. Nevertheless, we realize that inevitably errors will be made, both of omission and commission. Readers are urged to contact the authors with corrections that will improve future editions.

1.4 Acknowledgments

This work was funded by the Advanced Environmental Acoustic Support (AEAS) Program of the Office of Naval Research, under the sponsorship of the Oceanographer of the Navy (N-96). The authors gratefully acknowledge the support of AEAS and, in particular, Mr. Robert Feden, the AEAS Program Manager.

We also acknowledge and thank the numerous modelers who provided information for Section 3 of the report.

2. SUMMARY TABLES OF MODEL ATTRIBUTES

The tables which follow are intended to provide ready access to concise descriptive information about each model. While by no means exhaustive, the data in the tables answer a broad range of questions about each model's underpinnings and features. Elaboration on most of the contents of these tables can be found first in the model descriptions of Section 3 and in greater detail in the "physics" discussions of Sections 4 through 6.

Table 2-1. Some Basic Properties

Name	Type (RD)	Treatment of Propagation in Range-Dep Env't.	Recommended Frequency Limits (Hz)	Produces Travel Time (Method)
FAME	Ray	--N/A--	5 to 100,000	Yes (Ray "Trace")
MPP	Ray (RD)	Direct Ray Trace	20 to 10,000	Yes (Ray "Trace")
APL/JHU MODE	Normal Mode (RD)	Adiabatic (Modes) or Forward Coupling	5 to 1000$^+$ (Run Time is Limit)	Only From Fourier Synthesis of Many Runs
KRAKEN	Normal Mode (RD)	Adiabatic (Modes) or Forward Coupling	5 to 1000$^+$ (Run Time is Limit)	Only From Fourier Synthesis of Many Runs
RAYMODE	Ray-Mode	None	10 to 100,000	Yes (Ray "Trace")
ASTRAL	Avg'd Ray-Mode (RD)	Adiabatic Mode/Ray Coupling	50 to 10,000$^+$	Yes (Ray "Trace")
Navy Standard PE	PE (RD)	Full Forward Coupling (Subject Only to PE Approximation)	5 to 1000$^+$ (Run Time and FFT Size Limits)	Only From Fourier Synthesis
FFP	FFP	--N/A--	5 to 100,000$^+$	Yes. (Fourier Synthesis)
SAFARI	FFP	--N/A--	5 to 100,000$^+$	Yes. (Fourier Synthesis)

"RD": Capable of Treating Propagation in Range-Dependent Environments

Table 2-2. Historical Data

Name	Type (RD)	Year of Initial Capability	Year of Latest Major Upgrades	Custodian(s)	Sponsor(s)
FAME	Ray	1980	----	NUSC/NLL	NAVSEA
MPP	Ray (RD)	1972	1982	SAIC	AT&T Bell Labs, ONR (AESD)
APL/JHU MODE	Normal Mode (RD)	1974	1991	JHU/APL & SAIC	JHU/APL, CNO (OP-02)
KRAKEN	Normal Mode (RD)	1982	1986	M. Porter (N.J.I.T.)	ONR, NRL, NSF, SACLANTCEN
RAYMODE	Ray-Mode	1969	1985 (Baseline)	SONALYST	NUSC/NLL and NAVSEA
ASTRAL	Avg'd Ray-Mode (RD)	1978	1990 (v. 3.1)	OAML (NAVOCEANO)	ONR-AEAS (originally LRAPP & SEAS)
Navy Standard PE	PE (RD)	1972	1990 (v. 3.4)	OAML (NAVOCEANO)	ONR-AEAS (originally LRAPP & SEAS)
FFP	FFP	1971	1992	SAIC	ONR, NAVSEA
SAFARI	FFP	1982	1990	MIT	SACLANTCEN, ONR (ARCTIC)

Table 2-3. Strengths and Weaknesses

Name	Type (RD)	Notable Strengths	Notable Weaknesses
FAME	Ray	• Popular part of GSM...for eigenray analysis • Relatively fast	• No range dependence in environment • Accuracy limited
MPP	Ray (RD)	• Very accurate ray trace in range-dep. environment • Uniform caustic corrections • Produces arrival structure in angle and time • One of only a small number of range-dep ray trace models not subject to adiabatic coupling constraints (other: GRASS, HARPO, Gaussian Beam)	• Intensity estimates suspect in some cases (e.g., shallow water)
APL/JHU MODE	Normal Mode (RD)	• Range-dependent environment • Full wave solution • Finite element approach	• Run time for deep water/high frequency • Run time for coupled modes • Calculation of broadband propagation
KRAKEN	Normal Mode (RD)	• Range-dependent environment • Full wave solution • Finite difference approaches • Complex eigenfunctions and shear	• Run time for deep water/high frequency • Run time for coupled modes • Calculation of broadband propagation
RAYMODE	Ray-Mode	• Hybrid approach yields applicability over wide range of frequencies, bandwidths • Relatively fast from 10 Hz to 100,000 Hz	• Possible large jumps with frequency • No range dependence allowed in the environment
ASTRAL	Averaged Ray-Mode (RD)	• Very fast (10-1000 times faster than other models reviewed here) • Range-dependent environment • Arrival structure, travel time, and other advantages of ray models • Navy standard and agrees with PE in many cases • TL model in ANDES, AUAMP Baseline, etc.	• Only adiabatic mode coupling • Insensitive to small changes in S/R range, depth, etc. • Incorrect results for resonant double channel • Not valid for very low frequencies • Questionable in shallow water
Navy Standard PE	PE (RD)	• Relatively fast for range-dependent (RD) environment • "Full-wave" solution--including diffraction effects • For full coupling in RD environment, only practical choice for DTC-II, etc.	• Short range (< 1D-2D) is approximated by ray trace or normal mode starter • "Rapid" change in impedance or boundary conditions will cause errors
FFP	FFP	• "Correct" solution of reduced wave equation • Used as benchmark for other models • Good experience with Arctic and broadband applications	• No range-dependence in environment • Run time • Fourier synthesis for broadband • Requires SSP to vary exponentially between tabulated depth points • Requires scientist to test convergence
SAFARI	FFP	• "Correct" solution of reduced wave equations • Readily treats fluid/solid/vacuum layers • Process stable numerically • Used as benchmark for other models	• Run time • User must test for convergence • Fourier synthesis for broadband • No range dependence in environment

Table 2-4. Quantities Predicted

		Quantities Predicted					
Name	**Type (RD)**	**Spectrum of Received Signal From Transmitted Waveform**	**Range Averaged Intensity (Resolution in R)**	**Complex Pressure Field in Range and Depth on λ scale**	**Vertical Angular Arrival Structure (Temporal)**	**Spreads From Scattered Field**	**Broadband Propagation Method**
FAME	Ray	No	Yes (Selectable)	No	Yes (Yes)	No	Ray "Trace"
MPP	Ray (RD)	No	Yes (Selectable)	No	Yes (Yes)	No	Ray "Trace"
APL/JHU MODE	Normal Mode (RD)	No	No	Yes	No (No)*	Angle, Time*	*Fourier Synthesis or Narrowband Approx. (McCann)
KRAKEN	Normal Mode (RD)	No	No	Yes	No (No)*	Angle, Time*	*Fourier Synthesis
RAYMODE	Ray-Mode	No	Yes (Selectable)	No	Yes (Yes)	No	Ray "Trace"
ASTRAL	Avg'd Ray-Mode (RD)	No	Yes (≥ 1 nm)	No	Yes (Yes)	No	Ray "Trace"
Navy Standard PE	PE (RD)	No	Yes (Selectable)	Yes	Yes (No)*	No	*Fourier Synthesis
FFP	FFP	Yes	No	Yes	No (No)*	Angle, Time*	*Fourier Synthesis
SAFARI	FFP	Yes	No	Yes	No (No)*	Angle, Time*	*Fourier Synthesis

Table 2-5. Navy Standard and Evaluation Status

Name	Type (RD)	Operational or R&D	Operational Applications	Status re Navy Standard	Evaluation History
FAME	Ray	R&D	Part of GSM--Used for LFA Projects and CST.	N/A	1989 Evaluation for Shallow Water (McGirr)
MPP	Ray (RD)	R&D	Used as part of EAMOS for LFA. Also tomography.	N/A	McGirr et al (1985) Evaluation
APL/JHU MODE	Normal Mode (RD)	R&D	LFA assessments	N/A	Some comparisons with data and KRAKEN
KRAKEN	Normal Mode (RD)	R&D	Used as part of WRAP for noise and active sonar predictions.	N/A	Extensive comparisons by SACLANTCEN and Boden et al (1991)
RAYMODE	Ray-Mode	OP'L	Part of SFMPL, ASWTDA, SIMAS, ICAPS, TESS, etc. for APP and FNOC uses.	Navy Standard (Rev. 8.05 Baseline)	Extensive including: 1976 Bakeoff by POSSM; 1981 Bartberger; 1988 Papas
ASTRAL	Avg'd Ray-Mode (RD)	OP'L	Part of SPARS, ASAPS, AUAMP, ANDES, ICECAP.	Navy Standard (Vers 3.1)	Extensive comparisons by King (1986)
Navy Standard PE	PE (RD)	OP'L	Part of SPARS, ASAPS, FNOC Forecasts.	Navy Standard (Vers 3.4)	Extensive Comparison by King (1986)
FFP	FFP	R&D	Arctic applications for Kutschale version.	N/A	Often used as benchmark for evaluation of models in range-independent environments, since accurate solution of full wave equation
SAFARI	FFP	R&D	Applications include seismics and simulations.	N/A	Extensive comparisons by SACLANTCEN.

Table 2-6. Boundary Interaction

Name	Type (RD)	Treatment of Sea Surface Interaction			Treatment of Bottom Interaction			
		"Loss" vs. θ_i	Scattering Kernel (Loss vs. θ_i and θ_R)	Spectral Effects	"Loss" vs. θ	Layered Geo-Acoustic	Shear	Rough Surface Scatter at Sediment Layer & BSMT
FAME	Ray	Yes	No	No	Yes	Yes	No	No
MPP	Ray (RD)	Yes	No	No	Yes	No	No	No
APL/JHU MODE	Normal Mode (RD)	Yes	No	No	Yes	Yes	No	No
KRAKEN	Normal Mode (RD)	No	Yes	No	No	Yes	Yes (KRAKENC)	Possible
RAYMODE	Ray-Mode	Yes	No	No	Yes	Yes	No	No
ASTRAL	Avg'd Ray-Mode (RD)	Yes	No	No	Yes	No	No	No
Navy Standard PE	PE (RD)	Yes	No	No	Yes	Yes	Only as "Loss" term	No
FFP	FFP	Yes	Yes	No	Yes	Yes	No	Yes
SAFARI	FFP	No	Yes	No	Yes	Yes	Yes	Yes

θ_i = Incident (Grazing) Angle θ_R = Reflected Angle θ = Grazing Angle

Table 2-7. Some Limitations

Name	Type (RD)	Limits On: Minimum Water Depth		Treatment of Bottom		Rough Surface Scatter (Vice "Loss")	Min. Range	Min/Max Frequency (f)
		Flat Bottom	Sloping Bottom	Geoacoustic	Shear			
FAME	Ray	10λ	---	Yes	No	No	≥ D	f > 50 Hz
MPP	Ray (RD)	10λ	10λ	No	No	No	≥ D	f ≥ 10 Hz
APL/JHU MODE	Normal Mode (RD)	2λ	2λ	Yes	No	No	≥ D/10	f ≤ 1000+ Hz (Run Time Limit)
KRAKEN	Normal Mode (RD)	2λ	2λ	Yes	Yes (KRAKEN C)	Yes	≥ D/10	f ≤ 1000+ Hz (Run Time Limit)
RAYMODE	Ray-Mode	2λ	2λ	Yes	No	No	≥ D/10	5 ≤ f < 100,000
ASTRAL	Avg'd Ray-Mode (RD)	10λ	10λ	Yes	No	No	≥ D*	f > 50 Hz
Navy Standard PE	PE (RD)	2λ	2λ	Yes	No	No	≥ D	f ≤ 1000 Hz (unless expanded FFT)
FFP	FFP	2λ	---	Yes	No	Yes (Ice)	≥ D	Up to 100+ kHz
SAFARI	FFP	2λ	---	Yes	Yes	Yes	≥ D	Up to 100+ kHz

D ≡ WATER DEPTH λ ≡ Acoustic Wavelength

Table 2-8. Some Estimated Running Times

Assume SUN DTC II, Range 200 nm, 1 source, 1 receiver, CW source, frequency as noted

Name	Type (RD)	Range-Independent, Deep Water Case	Range-Dependent, Deep Water Case
FAME	Ray	10 seconds for 10 ≤ f ≤ 1000 Hz	N/A
MPP	Ray (RD)	10 seconds for 10 ≤ f ≤ 1000 Hz	40 seconds for 10 ≤ f ≤ 1000 Hz
APL/JHU MODE	Normal Mode (RD)	Estimate for deep water at about 1.5 * f seconds, where f is frequency in Hz. Case4 of interest is thus about 75 seconds at 50 Hz.	Directly dependent on number of different environmental provinces.
KRAKEN	Normal Mode (RD)	20 minutes on VAX 8600 at f = 1000 Hz for water depth of 2500 m	Directly dependent on number of different environmental provinces.
RAYMODE	Ray-Mode	10 seconds for f ≤ 45 Hz 4 seconds for 45 < f ≤ 1000 Hz	N/A
ASTRAL	Avg'd Ray-Mode (RD)	< 0.1 seconds for any f.	< 0.5 seconds for any f.
Navy Standard PE	PE (RD)	16 seconds for f = 20 Hz 40 minutes for f = 1000 Hz	16 seconds for f = 20 Hz, 40 minutes for f = 1000 Hz
FFP	FFP	60 seconds	N/A
SAFARI	FFP	10 seconds for f ≤ 1000 Hz (20 minutes for typical broadband case)	N/A

Table 2-9. Running Time Relationships (Approximate)

		Additional Time Factor Over a Single Run If There is a Doubling In						
Name	Type (RD)	Water Depth	Maximum Frequency	# Frequencies	Range	Range Steps (Output)	# Fixed Points	# Moving Points
FAME	Ray	~1x	~1x	~2x	~2x	~1x	~2x	~2x
MPP	Ray (RD)	~1x	~1x	~2x	~2x	~2x	~2x	~2x
APL/JHU MODE	Normal Mode (RD)	~2x	~4x	~2x	~1x	~1x	~1x	~1x
KRAKEN	Normal Mode (RD)	~2x	~4x	~2x	~1x	~1x	~1x	~1x
RAYMODE	Ray-Mode	~1x	~1x	~2x	~2x		~2x	~2x
ASTRAL	Avg'd Ray-Mode (RD)	~1x	~1x	~2x	~2x	~2x	~2x	~2x
Navy Standard PE	PE (RD)	~2x	~4x	~2x	~2x	~1x	~2x	~1x
FFP	FFP	~2x	~2x	~2x	~1x	~1x		~2x
SAFARI	FFP	~2x	~2x	~2x	~1x	~1x		~1x

Table 2-10 Input Data

Name	Type (RD)	Can Use Navy Standard (OAML) Data Bases	Connected To Them	Alternative Input Data Bases Included
FAME	Ray	Yes	Yes (via GSM)	Via GSM
MPP	Ray (RD)	Yes	No	Via EAMOS operating system to GDEM, LFBL, etc.
APL/JHU MODE	Normal Mode (RD)	Yes	No	Via EAMOS operating system to GDEM, LFBL, etc.
KRAKEN	Normal Mode (RD)	Yes	No	In WRAP applications there is connection to data bases.
RAYMODE	Ray-Mode	Yes	Yes (via APP systems)	None
ASTRAL	Avg'd Ray-Mode (RD)	Yes	Yes	Arctic GDEM, Ice Roughness, etc. in ICECAP
Navy Standard PE	PE (RD)	Yes	Yes	Arctic GDEM, Ice Roughness, etc. in ICECAP
FFP	FFP	Yes	No	None
SAFARI	FFP	Yes	No	None

Table 2-11. Computer Implementation

Name	Type (RD)	High-Level Development Language	Executable Lines of Code	Host Computers					
				Intel 80X86 PC	VAX	SUN (DTC-II)	HP	CRAY	Other
FAME	Ray	FORTRAN	TBD	Yes	Yes	Yes	No	No	
MPP	Ray (RD)	FORTRAN	TBD	Yes	Yes	Yes	No	No	
APL/JHU MODE	Normal Mode (RD)	FORTRAN	~10K	Yes	Yes	No	No	Yes	
KRAKEN	Normal Mode (RD)	FORTRAN	TBD	Yes	Yes	No	No	No	
RAYMODE	Ray-Mode	FORTRAN/ BASIC	~35K	No	Yes	Yes	9020	No	
ASTRAL	Avg'd Ray-Mode (RD)	FORTRAN	~18K	Yes	Yes	Yes	9020	No	
Navy Standard PE	PE (RD)	FORTRAN	~9K	Yes	Yes	Yes	9020	No	
FFP	FFP	FORTRAN	~20K	Yes	Yes	No	No	No	
SAFARI	FFP	FORTRAN	~30K	Yes	Yes	Yes	No	Yes	• Hypercube • Connection Machine • ALLIANT • CONVEX

Table 2-12. Approaches

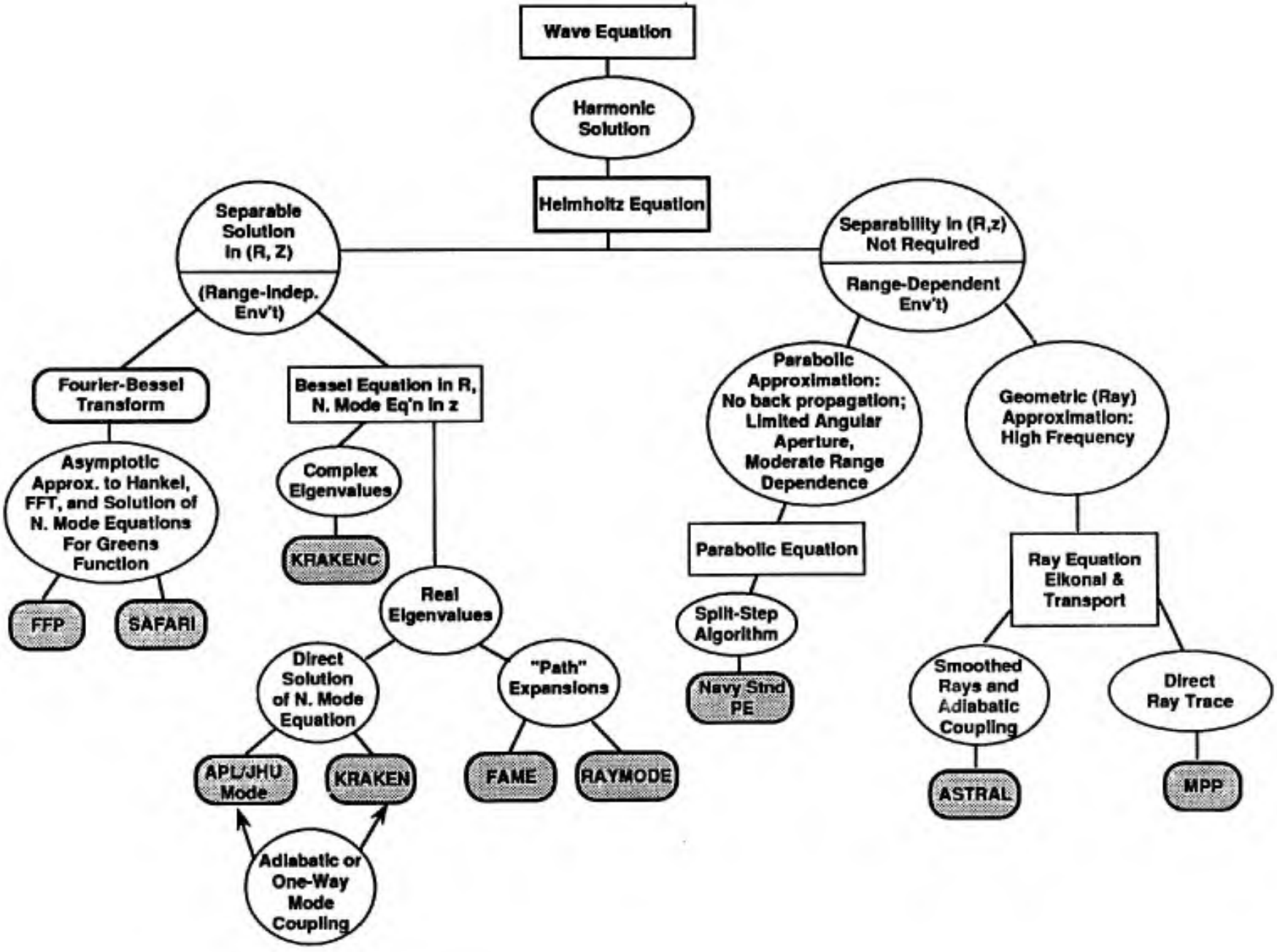

3. SUMMARY MODEL DESCRIPTIONS

In this section we give eight page forms for each model, covering everything from history and documentation to users and evaluation. The order of presentation is as follows:

FAME	Section 3.1
MPP	Section 3.2
APL/JHU MODE	Section 3.3
KRAKEN	Section 3.4
RAYMODE	Section 3.5
ASTRAL	Section 3.6
PE	Section 3.7
FFP	Section 3.8
SAFARI	Section 3.9


FAME
Fast Multipath
Expansion

Historical and Bibliographic Data

Common Names:

FAME

Fast Multipath Expansion

Name or Acronym: FAME

Full Name: Fast Multipath Expansion

Concept Developer: L. Felsen

Algorithm Developer: Henry Weinberg

Software Developer: Henry Weinberg

Year of Initial Capability: 1980

Years of Major Upgrades: None

Related and Derivative Models: MPE (Multipath Expansion)

Custodian: NUWC; Henry Weinberg is the developer, but FAME is usually distributed only as part of the Generic Sonar Model, for which contact E. Jensen at NUWC, New London, CT.

Sponsors: NAVSEA [Carey Smith]

References: H. Weinberg, "Effective Range Derivative for Acoustic Propagation Loss in a Horizontally Stratified Ocean," J. Acoust. Soc. Am. 70, 1736-1742 (1981).

H. Weinberg, "Generic Sonar Model," NUSC Technical Document 5971D (NUSC, New London, CT, 6 June 1985).

"The CST Program Modeling Subsystem: Generic Sonar Model (GSM)," Undersea Applications Modeling Division, SAIC, McLean, VA, November, 1991.

Historical Notes: FAME was developed in order to speed up the computer running time of the original MPE (Multipath Expansion) model; typically, FAME runs 10 times faster than MPE. Today its primary use is as one of several propagation loss models used by the Generic Sonar Model (GSM). It is perhaps the most used of the TL models because it also provides eigenray arrival structures which are generally quite accurate (but see "Restrictions and Warnings," next page).

The primary documentation of FAME physics is the original journal article by Weinberg (see Ref. above). The available GSM user's manuals contain only brief descriptions of FAME inputs and outputs.

Summary of Model Physics, Attributes, and Restrictions

Common Names:

FAME

Fast Multipath Expansion

Phenomenon Modeled:	**Approach:**
Ray Paths, Intensities, & Travel Times	Ray Equations (WKB)
Bottom Loss	LFBL, Geoacoustic Parameters, or Loss vs. Angle
Surface Loss	AEAS model (input: wind speed) Beckmann-Spizzichino model (input: wind speed)
Diffraction / caustic corrections	Effective range derivative technique; results in imaginary eigenrays (occur in pairs)

Notable Attributes and Discriminants: It is easier and faster numerically to evaluate the integrals used at low frequency (because the integrands oscillate more slowly).

Domain of Application (Frequency, range, water depth, range-dependence, etc.):
Range independent. Shear is not included.

Restrictions and Warnings:

(1) Do not use if extreme TL accuracy is required.

(2) The automatic eigenray selection is sensitive to the eigenray tolerance (a user input). The smaller it is made, the more eigenrays are found, but if it is made too small, some of the eigenrays are spurious.

(3) The automatic eigenray selection is sensitive to the (fixed) range step (a user input). A smaller range step will usually result in more eigenrays being found. In reality, the number of eigenrays found should be independent of the range step.

(4) Cases have been observed in which ducted arrivals dropped out for the width of a convergence zone, as the deep cycling rays returned to the duct, and then reappeared beyond the convergence zone. The dropout surely is an error.

(5) In reverberation applications at short range from the source, one is concerned with arrivals even 30 or 40 dB below peak levels (if they come in at different times). FAME, however, typically only gives a couple of bottom bounces. FAME finds eigenrays that bracket an angular interval and interpolates perhaps a couple of eigenrays within the interval. This is not enough; either more eigenrays need to be found within the interval, or the interval needs to be made smaller, so that higher order bottom bounce can be included.

(6) A change in algorithm at 100 Hz causes a frequency discontinuity in transmission loss results there.

Model Components

Common Names:
FAME
Fast Multipath Expansion

Input Data Bases/Existing Interfaces: As part of the Generic Sonar Model, it interfaces with the following data bases:

DBDB5
GDEM/HOP
LFBL

Acoustic Submodels:

Bottom loss - uses LFBL
Surface loss - uses AEAS model, or Beckman-Spizzichino model

System Submodels/Extensions:

(1) It is perhaps *the* key range-independent transmission loss and eigenray model within the Generic Sonar Model (GSM).

(2) Eigenray model used in the Activated Bottom Sensor (ABS) model developed by SAIC for AEAS, and running on IBM PCs.

Display and Output Routines: Output routines include:

(1) Stacked plots of arrival structures at successive (user-input) ranges
(2) Total transmission loss (can be either coherent or incoherent sum)
(3) Eigenray component plots
- **(a)** Time vs. range
- **(b)** Time vs. source angle in degrees
- **(c)** Spacing in degrees vs. range
- **(d)** Phase in degrees vs. source angle in degrees
- **(e)** Level in dB vs. range in nm
- **(f)** Level in dB vs. source angle

The graphics currently available differ depending on the computer system, and whether FAME is being run from within GSM, ABS, or otherwise. GSM on the VAX has complete graphics of the above outputs (using DISSPLA). GSM on the SUN has no graphics yet. ABS on the PC has all but eigenray plots.

Use and User Data

Common Names:

FAME

Fast Multipath Expansion

Major Installations (Activity/Computer Version):

NUWC
SAIC
NOSC
JHU/APL and other participating CST organizations
All locations where the Generic Sonar Model is installed.

Fleet (Users and Uses): Anywhere the Generic Sonar Model is used.

System Design/Development (Users and Uses):

NOSC (C. Reed) - LFA systems analysis

JHU/APL: For the CST experiments, in direct support of the LFA program, SAIC has adapted the Generic Sonar Model to provide acoustic predictions for bistatic system configurations in a range-independent environment. (See Reference below.) FAME is a key ingredient of these predictions.

EVA R&D (Users and Uses):

NUWC: Henry Weinberg and Roy Deavenport (model comparisons)
SAIC: Anthony Eller and Marilyn Blodgett (eigenray analyses and arrival structures)

Reference: "The CST Program Modeling Subsystem: Generic Sonar Model (GSM)," Undersea Applications Modeling Division, SAIC, McLean, VA, November, 1991.

Computer Implementation
Data-I

Common Names:

FAME

Fast Multipath Expansion

Host Computer System: Univac, VAX running VMS, SUN, IBM PCs

Displays: VAX: standard Tektronix graphics
IBM PCs: EGA/VGA

Mass Storage: TBD

High-Level Language(s): FORTRAN

Lines of Executable Code: TBD

Data Bases: Only through Generic Sonar Model, including DBDB5, LFBL, etc.

Mass Storage (by Data Base): Not applicable.

Modes (Batch/Interactive): Batch, through Generic Sonar Model.

Running Time/Memory Data -- Single Case Execution

Henry Weinberg claims that a typical single source--single receiver transmission loss run takes about 10 sec on a SUN (DTC). The more eigenrays present, the longer the run time.

Running Time/Memory Data -- Multiple Case Execution:

Multiple Fixed Point Depths: each fixed point depth is a separate run.

Multiple Moving Point Depths: each moving point depth is a separate run.

Multiple Frequencies: each frequency is a separate run.

Multiple Array Response Patterns: virtually free in Generic Sonar Model.

Computer Implementation
Data-II

Common Names:

FAME

Fast Multipath Expansion

System Developer (POC/Sponsor): Henry Weinberg (NUWC, New London, CT).

Custodian (POC/Sponsor): Henry Weinberg (NUWC, New London, CT),

Configuration Management (POC): Only as part of the Generic Sonar Model. Contact E. Jensen (NUWC, New London, CT).

Documentation:

Physics Description: H. Weinberg, "Effective Range Derivative for Acoustic Propagation Loss in a Horizontally Stratified Ocean," J. Acoust. Soc. Am. 70, 1736-1742 (1981).

Software Documentation: H. Weinberg, "Generic Sonar Model," NUSC Technical Document 5971D (NUSC, New London, CT, 6 June 1985).

"The CST Program Modeling Subsystem: Generic Sonar Model (GSM)," Undersea Applications Modeling Division, SAIC, McLean, VA, November, 1991.

User's or Operator's Guides: H. Weinberg, "Generic Sonar Model," NUSC Technical Document 5971D (NUSC, New London, CT, 6 June 1985).

"The CST Program Modeling Subsystem: Generic Sonar Model (GSM)," Undersea Applications Modeling Division, SAIC, McLean, VA, November, 1991.

Degree of Automation: None except as part of GSM. In its ordinary implementation, GSM is not very automated either, requiring a detailed ASCII input file. As part of LFA support for CST, SAIC has written a menu-driven front end for GSM that runs under UNIX.

Comments: FAME is not normally distributed as a stand-alone model, but only as part of the Generic Sonar Model.

Evaluation and Standardization Status

Common Names:

FAME

Fast Multipath Expansion

Mod or Version: No numbered version. See current version of Generic Sonar Model.

Implementation Type: FORTRAN.

Evaluation Event: Evaluation of models for 17 shallow water test cases in range dependent environments.

Results: FAME was evaluated against SAFARI, SNAP, PE, and ASTRAL, and performed very well.

References: Robert McGirr and David King, "Review of candidate shallow water propagation loss models," NORDA Technical Note 346, January 1989.

Evaluation (POC): Henry Weinberg (NUWC); David King (NOARL); Anthony Eller (SAIC).

Evaluation (POC) Guides: None.

Degree of Automation: None except as part of GSM. In its ordinary implementation, GSM is not very automated either, requiring a detailed ASCII input file. As part of LFA support for CST, SAIC has written a menu-driven front end for GSM that runs under UNIX.

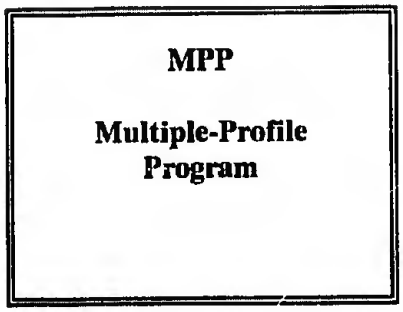
MPP
Multiple-Profile
Program

Historical and Bibliographic Data

Common Names:

MPP

Multiple-Profile Program

Name or Acronym: MPP

Full Name: Multiple-Profile Program

Concept Developers: C. W. Spofford;
Y. A. Kratsov and D. Ludwig (caustic corrections)

Algorithm Developers: C. W. Spofford and J. A. Polak

Software Developers: C. W. Spofford and J. A. Polak; also H. S. Garon, E. S. Holmes, and J. L. Spiesberger

Year of Initial Capability: 1972

Years of Major Upgrades: 1979: Garon introduced MPP2, alternate submodel for TL
1982: Spiesberger and Holmes converted code to double precision

Related and Derivative Models: None.

Custodian: SAIC (POC: C. W. Spofford)

Sponsors: AT&T Bell Laboratories, ONR Code AESD (Acoustic Environmental Support Detachment)

References: (1) C. W. Spofford, "The Bell Laboratories Multiple-Profile Ray-Tracing Program," Reference 3 in *Continuation of LRAPP: Final Report (U)*, Bell Laboratories Technical Report, Contract N00014-71-C-0088, 1972. (CONFIDENTIAL)

(2) J. L. Spiesberger and K. Metzger, "Basin-Scale Tomography: A New Tool for Studying Weather and Climate," J. Geophys. Res. 96, C3, 4869-4889, March 15, 1991. See especially Appendix B.

(3) D. Ludwig, "Uniform Asymptotic Expansions at a Caustic," Commun. Pure Appl. Math. 19, 215-250 (1966).

(4) Yu. A. Kratsov, "One Modification of the Geometric Optics Method," Soviet Radio Physics 1, 104-111 (1964).

Historical Notes: MPP was originally developed at AT&T Bell Laboratories for use both in system-studies applications (to characterize acoustic performance of proposed systems) and in research applications. MPP followed the development of an early ray-tracing program by Norris and Walkinshaw in 1960, and a more automated, user-friendly version, which added the concept of "sequential signatures" (keeping track of histories of ray path bounces, in order to correctly associate rays by families), by Polak and Spofford in the late 1960s. MPP then added range dependence, the Kravtsov-Ludwig uniform asymptotic corrections at real caustics, and an automated processing of false caustics associated with sound-speed gradient discontinuities.

Since about 1980, the emphasis in use of MPP has shifted to tomographic research. Attention has been given to the precision with which eigenrays can be computed in range-dependent environments. The portion of MPP which computes transmission loss has not been improved in many years and is today not highly regarded in comparison with most other

Summary of Model Physics, Attributes, and Restrictions

Common Names:

MPP

Multiple-Profile Program

(Historical Notes Continued)
models in this notebook. For example, MPP does not include algorithms which estimate the intensity of nongeometric rays in the shadow zone of a caustic (see discussion on p. 4884 of Ref. 2 above). On the other hand, MPP has proven remarkably accurate for eigenrays (again, see p. 4884 of Ref. 2), quite valuable in tomographic research, and useful for supplementing models such as PE (which do not give arrival structures when run in CW mode).

Phenomenon Modeled	Approach
Ray Paths, Intensities, & Travel Times	Ray "Trace"
Range Dependence in Environment	Ray "Trace"
Caustic corrections	Kratsov-Ludwig uniform asymptotics
False caustic elimination	Automated processing using sequential signature groups
Eigenrays	Look between 2 traced rays with same sequential signature (history)
Intensity along eigenray	(1) Original MPP: geometric ray divergence (2) MPP2: "smearing" out of energy associated with ray bundle (like Gaussian beam)
Transmission loss	Coherent or incoherent sum of eigenray intensities
Arrival structure	Careful computation of travel time along eigenrays
Bottom loss	Tabulated function or modified Rayleigh reflection coefficient
Surface-image interference	Sequential signatures used to identify up/down pairs of rays

Notable Attributes and Discriminants:

Eigenray and associated travel time calculations are extremely accurate (see evaluation by Spiessberger, Ref. on p. 3.2-7).

Domain of Application (Frequency, range, water depth, range-dependence, etc.):

Eigenrays are independent of frequency. Using the double precision version of the code, eigenrays are precise to within 1.5 m, and travel times are precise to within 0.1 ms, for ranges up to 3000 km (see p. 4884 of Ref. 2, p. 3.2-1).

Restrictions and Warnings:

In general, do not use MPP to compute transmission loss. The part of the code that computes acoustic intensity can be unreliable and is known to give errors in some cases. For example, in the 1985 evaluation (see p. 31 of Ref. 1 on p. 3.2-7), in a shallow-water range-independent case, MPP is seen to give too high an intensity because of a failure to include fully coherent bottom reflections (with phase change). The surface-image interference is also incorrectly done in this case, causing the details of the MPP transmission loss curve not to match those of the normal mode benchmark curve.

Model Components

Common Names:

MPP

Multiple-Profile Program

Input Data Bases/Existing Interfaces: As part of EAMOS, it interfaces with the following data bases:

LFBL (Low Frequency Bottom Loss) with LFBLTAB to compute L(θ)
Sound speed profiles (Wright-Colborn, GDEM)
Sediment thickness database (GEOSED)
Bathymetry (SYNBAPS, DBDB5, and DBDBC)

Acoustic Submodels:

Surface-image interference (assumes equal amplitudes for the two paths, and rays locally straight lines)
Bottom reflection loss (tabulated function of angle, or "modified Rayleigh" bottom reflection coefficient)

System Submodels:

Source and receiver vertical directivity patterns

Display and Output Routines:

Ray "Trace"
Eigenray plots
Arrival Angle vs Range
Arrival Time & Intensities by Path
Contoured TL vs Range & Depth
TL vs Range for Given Depths

Use and User Data

Common Names:

MPP

Multiple-Profile Program

Major Installations (Activity/Computer Version):

SAIC
A&T
Woods Hole
NRL (Stennis Space Center)
NOSC
NAVOCEANO

(All as part of EAMOS model operating system on PC and DTC)

Fleet (Users and Uses): None.

System Design/Development (Users and Uses):

NOSC: In conjunction with use of SAIC EAMOS for LFA systems analysis.

EVA R&D (Users and Uses):

SAIC: part of EAMOS Model Operating System on IBM PCs and SUNs
A&T: part of EAMOS Model Operating System on IBM PCs and SUNs
Woods Hole (POC: J. L. Spiesberger): tomographic research (see Ref. below)

References: L. Boden, J. B. Bowlin, and J. L. Spiesberger, "Time domain analysis of normal mode, parabolic, and ray solutions of the wave equation," J. Acoust. Soc. Am. 90, 954-958 (1991).

Computer Implementation
Data-I

Common Names:

MPP

Multiple-Profile Program

Host Computer Systems: VAX, SUN, IBM PCs

Array Processor: None.

Displays: High-resolution color display (e.g., EGA or VGA for IBM-PC compatible systems)

Mass Storage:

High-Level Languages: FORTRAN

Lines of Executable Code: TBD

Data Bases: None in stand-alone form. As part of EAMOS, it is linked to several data bases: LFBL, Wright-Colburn, GDEM, HOP, SYNBAPS, DBDB5, DBDBC and GEOSED.

Mass Storage (by Data Base): TBD

Modes (Batch/Interactive): TBD

Running Time/Memory Data -- Single Case Execution

Problem A: TBD

Problem B: TBD

Problem C: TBD

Running Time/Memory Data -- Multiple Case Execution:

Multiple Fixed Point Depths: TBD

Multiple Moving Point Depths: TBD

Multiple Frequencies: TBD

Multiple Array Response Patterns: TBD

Computer Implementation
Data-II

Common Names:

MPP

Multiple-Profile Program

System Developer (POC/Sponsor): Bell Laboratories.

Custodian (POC/Sponsor): SAIC (POC: C. W. Spofford)

Configuration Management (POC): None.

Documentation:

Physics Description:

(1) C. W. Spofford, "The Bell Laboratories Multiple-Profile Ray-Tracing Program," Reference 3 in *Continuation of LRAPP: Final Report (U),* Bell Laboratories Technical Report, Contract N00014-71-C-0088, 1972. (CONFIDENTIAL)

(2) J. L. Spiesberger and K. Metzger, "Basin-Scale Tomography: A New Tool for Studying Weather and Climate," J. Geophys. Res. 96, C3, 4869-4889, March 15, 1991. See especially Appendix B.

Software Documentation: None.

User's or Operator's Guides: None, except via Model Operating Systems such as EAMOS.

Degree of Automation: None except where implemented within Model Operating Systems (EAMOS on IBM PCs and SUNs).

Comments:

Evaluation and Standardization Status

Common Names:

MPP

Multiple-Profile Program

Mod or Version: Not applicable.

Implementation Type: FORTRAN.

Evaluation Event: (1) 1985 evaluation to determine whether any of 4 range-dependent ray theory models could satisfy operational needs at the Fleet Numerical Oceanography Center. GRASS, MEDUSA, MPP, and UNIMOD were compared.

(2) Spiesberger's evaluations (p. 4884 of Ref. 2 below).

Results: (1) MEDUSA was judged best at tracing rays. None of the models was judged satisfactory for computing TL.

(2) Double precision version of code computes eigenrays to within 1.5 m and travel times to within 0.1 ms for ranges up to 3000 km.

References: (1) R. W. McGirr, D. B. King, J. A. Davis, and J. Campbell, "An Evaluation of Range-Dependent Ray Theory Models," NORDA Report 115, September 1985.

(2) J. L. Spiesberger and K. Metzger, "Basin-Scale Tomography: A New Tool for Studying Weather and Climate," J. Geophys. Res. 96, C3, 4869-4889, March 15, 1991. See especially Appendix B.

Evaluation (POC): David King (NOARL)

Evaluation (POC) Guides: None.

Degree of Automation: Under Model Operating Systems such as EAMOS, MPP can be run without much scientist intervention. However, interpretation of results can be non-trivial.

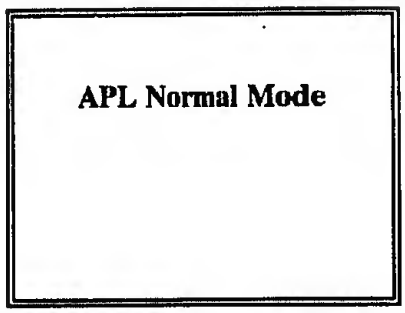
APL Normal Mode

Historical and Bibliographic Data

Common Name:

APL Normal Mode

Name or Acronym: APL Normal Mode

Full Name: APL Normal Mode

Concept Developers: David Stickler

Algorithm Developers: David Stickler, Allan Boyles, Lewis Dozier, Paul Vidmar, Kevin McCann, Marcelle Ladd

Software Developers: Allan Boyles, Lewis Dozier, Paul Vidmar, Hyrum Laney, Shawna Laney, Ruth Keenan, Kevin McCann, Marcelle Ladd

Year of Initial Capability: 1974

Years of Major Upgrades:

1981: Dozier implemented exponent-mantissa arithmetic to avoid overflows

1983: Dozier sped up mode normalization by a factor of 10 by introducing analytic formulas for integrals of products of Airy functions, replacing the numerical integration previously being done.

1987: JHU/APL added group velocity and broadband capability

1987: Dozier, Vidmar, and H. Laney wrote a text-based menu-driven front end for the code, including automatic generation of a geoacoustic bottom from LFBL inputs. Since then, the user has been freed from having to use a text editor to prepare ASCII input files.

1991: S. Laney and R. Keenan integrated the model into EAMOS, the IBM PC based model operating system.

Related and Derivative Models: (1) Stickler's original code, documented in Ref. 1 below; not known to be actively used in the community today

(2) Broadband versions of the code at JHU/APL (see Ref. 3 below) and at SAIC

Custodians: Ruth Keenan (SAIC), Allan Boyles (JHU/APL).

Sponsors: JHU/APL, OP-02 (SSBN Security Program)

References: (1) D. Stickler, "Normal mode program with both the discrete and branch line contributions," J. Acoust. Soc. Am. 57, 856-861 (1975).

(2) C. A. Boyles, *Acoustic Waveguides* (John Wiley, New York, 1984), Chapter 4.

(3) K. J. McCann and F. Lee-McCann, "A narrow-band approximation to the acoustic pressure field," J. Acoust. Soc. Am. 89, 2670-2676 (1991).

Historical Notes: In the early 1980s, SAIC was sponsored by JHU/APL to supply a numerically stable implementation of JHU/APL's alteration of Stickler's original model. Their alteration terminates the problem with a perfectly reflecting boundary at finite depth, thereby giving a purely discrete spectrum of modal eigenvalues. After the 1983 Dozier upgrade, SAIC and JHU/APL, although working together on coupled mode codes, have internally carried out different modifications to the 1983 code, so that different SAIC and JHU/APL versions now exist.

Summary of Model Physics, Attributes, and Restrictions

Common Name:

APL Normal Mode

Phenomenon Modeled	**Approach**
Complex pressure field in range and depth	Normal mode solution of separable Helmholtz equation
Range dependence	Adiabatic (SAIC version)
Attenuation	Perturbation theory
Problem termination	Rigid boundary condition below last layer
Broadband (pulse) waveforms	(1) Frequency synthesis, or (2) Narrowband approximation (Ref. 3 , page 3.3-1)

Notable Attributes and Discriminants: This normal mode code takes a *finite element* approach, as contrasted with the finite difference approach of KRAKEN. The finite elements are Airy functions, the elementary solutions within each layer of discretization of the sound speed profile, where the square of refraction is assumed linear (rather than the sound speed itself). Thus, even at high frequencies, the number of layers, and hence Airy functions, remains the same. On the other hand, KRAKEN must sample the water column ever more densely, on a sub-wavelength scale, as frequency increases. For this reason, it appears (based on a few actual runs) that this code may offer a run time advantage over KRAKEN at higher frequencies, although this point remains to be further investigated.

Propagation in range-dependent environments is treated adiabatically.

Domain of Application (Frequency, range, water depth, range-dependence, etc.): In principle, any frequency can be treated as long as at least one mode is trapped. However, extremely high frequencies become quite time-consuming, and see the warning below.

Adiabatic range dependence is included. Stronger range dependence can be treated via an SAIC special version of the code that includes forward (one-way) coupling. Also, backscatter (reverberation) can be treated by either of two codes jointly developed by SAIC and JHU/APL, one for rough surface scatter and one for rough bottom scatter. These codes are *not* part of the "APL normal mode" model, however. They are distinct codes which merely use the APL normal mode model to compute background modes.

Restrictions and Warnings:

The code can give wrong answers in the case of a slow bottom (sound speed less at top of sediment than at bottom of water column) in deep water at high frequencies, above about 500 Hz. This situation contains, in effect, a double duct not seen by the longer wavelengths at low frequencies. Research is currently underway at JHU/APL to solve this problem.

The code can also give wrong answers in shallow water if one attempts to terminate the problem too quickly with a highly absorbing bottom layer. The high attenuation violates the perturbation theory used to compute the modal attenuation constants. Since all modes are bottom interacting, the result is that all modes suffer too much attenuation, and computed transmission loss can fall many dB below the truth.

Model Components

Common Name:
APL Normal Mode

Input Data Bases/Existing Interfaces: The SAIC version of the code has for several years had a front end that would compute a geoacoustic bottom from LFBL input. In 1991 SAIC integrated the code into an internal version of EAMOS, the IBM PC-based Model Operating System which also contains ASTRAL, Navy Standard PE, and MPP. As part of EAMOS, it is interfaced to several data bases:

LFBL (Low Frequency Bottom Loss)
Sound speed profiles (Wright-Colborn, HOP, GDEM)
Sediment thickness database (GEOSED)
Bathymetry (SYNBAPS, DBDB5, and DBDBC)

Acoustic Submodels:

Bottom Loss: A front-end program written at SAIC will convert LFBL parameters into the geoacoustic input required by the mode code. In addition, a recent modification allows one to directly specify $L(\theta)$ [loss as a function of grazing angle], thus bypassing the perturbation theory used by the code. This is useful for some shallow water cases (see "Restrictions and Warnings" on previous page).

System Submodels: None.

Display and Output Routines: As part of SAIC's internal version of EAMOS, the following can be obtained:

Plots of transmission loss (TL) as a function of range/depth at fixed depth/range
Full field color contour plot of TL(r,z)
Mode shape plots
Color contour plot of FOM(r,z) ["Figure of Merit": equal to TL plus or minus a constant]

Use and User Data

Common Name:

APL Normal Mode

Major Installations (Activity/Computer Version):

SAIC
JHU/APL
Raytheon Co. (Submarine Signal Division, Portsmouth, RI) POC: Susan Bates
AT&T Technologies, Inc. (Arlington, VA) POC: R. F. Henrick

Fleet (Users and Uses): None.

System Design/Development (Users and Uses):

SAIC: extensive use in ONT's High Gain Initiative (HGI) program as a replica generator for matched field processing. The normal mode model has performed quite well. Results are being used to design future high gain array systems.

JHU/APL: for comparison with broadband sea test data, the broadband version of the mode code (Ref. 1 below) treats vertical source and receiving arrays.

EVA R&D (Users and Uses):

SAIC: Recent incorporation into internal version of EAMOS (Environmental Acoustic Model Operating System) running on IBM-compatible PCs. Specific motivation is use in modeling of Arctic propagation.

SAIC: Recent extension into a broadband version, still somewhat experimental.

JHU/APL: Extension into a broadband version (see Ref. 1 below).

JHU/APL: Computation of group velocities (see Ref. 2 below).

SAIC and JHU/APL: use in computing modes for *coupled mode codes* (for scattering from rough ocean surfaces and rough bottom interfaces).

References:

(1) M. E. Ladd, "APL Normal Mode Pulse Propagation Model," STD-N-525, JHU/APL, September 1987.

(2) M. E. Ladd, "Group Velocity Added to Normal Mode Code," STD-N-524, JHU/APL, September 1987.

Computer Implementation
Data-I

Common Name:

APL Normal Mode

Host Computer System: CRAY, VAX, IBM PC.

CPUs: CRAY; VAX; Intel 8088, 80286, 80386 (+coprocessor in each case), or 80486DX

Array Processor: None.

Displays: High-resolution color display (e.g., EGA or VGA for IBM-compatible PCs) is required for color contour plots.

Mass Storage: Size of executable depends entirely on dimension of key arrays, i.e., the maximum number of normal modes and layers allowed.

High-Level Language(s): FORTRAN

Lines of Executable Code: About 3000

Data Bases: None in usual stand-alone form. As part of EAMOS, it is linked to several data bases: LFBL, Wright-Colborn, HOP, GDEM, SYNBAPS, and GEOSED.

Mass Storage (by Data Base): for EAMOS, Compressed Data Bases ~ 14 Mb, Decompressed Data Bases ~ 63 Mb.

Modes (Batch/Interactive): Either. Generally interactive on PCs, batch on VAXes.

Running Time/Memory Data -- Single Case Execution

To compute modes in deep water (5 km) takes typically on the order of one second per mode on a fast (33 MHz) 486DX PC. Lower numbered modes trapped in the water column usually require less time than more complicated modes that interact with the bottom. Run time will increase with the number of profile discretization layers, since the number of Airy functions (finite elements) increases. Run time in shallow water will typically be less than in deep water, in part because the number of such elements is usually smaller.

Running Time/Memory Data -- Multiple Case Execution:

Multiple Fixed Point Depths: Virtually free.

Multiple Moving Point Depths: Virtually free.

Multiple Frequencies: Run time proportional to number of frequencies.

Multiple Array Response Patterns: Virtually free.

Computer Implementation
Data-II

Common Name:

APL Normal Mode

System Developer (POC/Sponsor): JHU/APL, OP02.

Custodian (POC/Sponsor): SAIC (POC: Lewis Dozier)
JHU/APL (POCs: Allan Boyles, Kevin McCann)

Configuration Management (POC): None.

Documentation:

Physics Description: C. A. Boyles, *Acoustic Waveguides* (John Wiley, New York, 1984), Chapter 4.

Software Documentation: M. E. Ladd, "APL Normal Mode Pulse Propagation Model," STD-N-525, JHU/APL, September 1987.

User's or Operator's Guides: M. E. Ladd, "APL Normal Mode Pulse Propagation Model," STD-N-525, JHU/APL, September 1987.

Degree of Automation: Depends entirely on whether one is running "stand-alone" APL normal mode, or APL normal mode from within SAIC's EAMOS Model Operating System for IBM PCs. In the former case, there is an optional text-based menu-driven front end, but not linked to environmental data bases (although it will convert LFBL input supplied by the user). In the latter case, there is a high degree of automation, both of user input and of linkage with data bases.

Evaluation and Standardization Status

Common Name:

APL Normal Mode

Mod or Version: Not applicable.

Implementation Type: FORTRAN.

Evaluation Event: No formal evaluation, but SAIC has compared a number of low-frequency cases with KRAKEN.

Results: Mode eigenvalues typically agree to seven significant figures.

References: None.

Evaluation (POC): None.

Evaluation (POC) Guides: None.

Degree of Automation: Depends entirely on whether one is running "stand-alone" APL normal mode, or APL normal mode from within SAIC's EAMOS Model Operating System for IBM PCs. In the former case, there is an optional text-based menu-driven front end, but not linked to environmental data bases (although it will convert LFBL input supplied by the user). In the latter case, there is a high degree of automation, both of user input and of linkage with data bases.

KRAKEN

KRAKENC

Historical and Bibliographic Data

Common Names:

KRAKEN

KRAKENC

Name or Acronym: KRAKEN

Full Name: KRAKEN
(KRAKENC refers to the version with complex eigenvalues)

Concept Developers: Richardson, Newton, Brent, Sturm (authors of classical numerical methods used in KRAKEN -- see numerical analysis texts)

Algorithm Developers: Michael B. Porter, W. A. Kuperman (3-D WRAP, noise)

Software Developers: Michael B. Porter, W. A. Kuperman (3-D WRAP, noise)

Year of Initial Capability: 1982

Years of Major Upgrades: 1985, 1986

Related and Derivative Models: KRAKENC

Custodian: Michael Porter (New Jersey Institute of Technology)

Sponsors: ONR, NRL, NSF, SACLANTCEN

References: (1) M. B. Porter, "The KRAKEN Normal Mode Program," (a complete physics documentation and computer code user's manual), SACLANT Technical Memorandum, 1991.

(2) W. A. Kuperman, M. B. Porter, J. S. Perkins, and R. B. Evans, "Rapid computation of acoustic fields in three-dimensional ocean environments," J. Acoust. Soc. Am. 89, 125-133(1991).

(3) M. B. Porter and E. L. Reiss, "A numerical method for bottom-interacting ocean acoustic normal modes," J. Acoust. Soc. Am. 77, 1760-1767 (1985).

(4) M. B. Porter and E. L. Reiss, "A numerical method for ocean acoustic normal modes," J. Acoust. Soc. Am. 76, 244-252 (1984).

Historical Notes: The name "KRAKEN", according to a draft of the user's manual, is "a fabulous Scandinavian sea monster." The name is not an acronym and bears no relation to the model.

Porter profited from previous numerical mode solutions by others (e.g., see the references to Dozier and Biesner in Ref. 4 above). His primary contribution in KRAKEN is a collection of numerical methods from various sources, all tested for maximal reliability and efficiency for real ocean environments. In KRAKENC, he goes beyond the usual normal mode capability and directly computes complex modes and eigenvalues, and treats shear.

Summary of Model Physics, Attributes, and Restrictions

Common Names:

KRAKEN

KRAKENC

Phenomenon Modeled	Approach
Complex pressure field in range & depth	Normal mode solution of separable Helmholtz equation
Propagation of shear waves in the bottom	Full elastic treatment
Interfacial roughness	Modified boundary condition on flat surface
Surface & bottom loss	Tabulated complex reflection coefficient input
Range dependence	Forward (one-way) coupling or adiabatic
Evanescent (leaky) modes	Complex residue series, as for non-evanescent modes
Attenuation	Perturbation theory (KRAKEN) Direct complex eigenfunction calculation (KRAKENC)
Problem termination	Choice of free, rigid, or half-space boundary conditions
3-D environments	Nx2D approximation, plus adiabatic horizontal refraction option [Gaussian beams]
Pulse (broadband) propagation	Frequency synthesis

Notable Attributes and Discriminants:

Unlike many normal mode codes, KRAKEN treats shear waves and optionally (KRAKENC) can compute fully complex eigenfunctions. In addition, its 3-D capability has led to its being the nucleus of the Wide-Area Rapid Acoustic Prediction (WRAP) model developed at NRL. Within WRAP it is even used to model noise.

Kraken uses a finite difference approach to solving the depth equations. Propagation in range-dependent environments is handled adiabatically.

Domain of Application (Frequency, range, water depth, range-dependence, etc.):

In theory, KRAKEN can be used for any combination of frequency, range, and water depth, although like any normal mode code, computer time will become excessive at high frequencies in deep water. KRAKEN has an option to treat range dependence adiabatically, and another option to include one-way forward coupling. Thus, KRAKEN can handle forward scatter, but not backscatter. KRAKEN is, however, used to generate normal modes for Richard Evans' coupled mode model, which does treat backscatter.

Restrictions and Warnings:

KRAKENC is not as reliable as KRAKEN, since complex root-finders are inherently much less robust than real ones. One should be fairly certain that the complex eigenfunctions are really required before using KRAKENC.

Model Components

Common Names:
KRAKEN
KRAKENC

Input Data Bases/Existing Interfaces: None in KRAKEN *per se*. It is used as the nucleus of the WRAP model at NRL, which is interfaced to environmental databases.

Acoustic Submodels:

(1) Twersky scatter model for under-ice scattering
(2) Kirchhoff scatter model for open ocean surface scattering
(3) Kuperman-Ingenito boundary condition for interface roughness
(4) Gaussian beams for horizontal refraction and 3-D capability

System Submodels: None in KRAKEN *per se*. It is used as the nucleus of the WRAP model at NRL, which includes options to predict array performance in complex 3-D environments.

Display and Output Routines:

(1) Plots of sound speed profile inputs
(2) Plots of coherent transmission loss vs. range at a given depth
(3) Plots of coherent transmission loss vs. depth at a given range
(4) Plots of amplitude of Green's function vs. horizontal wavenumber k for a given source-receiver combination
(5) Full field contour plots of transmission loss vs
    (a) range-depth (vertical plane)
    (b) range-range (horizontal plane): 3-D view from above
(6) Plots of individual normal mode functions vs. depth

Use and User Data

Common Names:

KRAKEN

KRAKENC

Major Installations (Activity/Computer Version):

(1) SACLANTCEN runs KRAKEN thousands of times in an operational mode, connected to databases including DBDB5 and GDEM.

(2) NRL runs KRAKEN as an integral part of WRAP, which is connected to databases including DBDB5 and GDEM.

Fleet (Users and Uses): None

System Design/Development (Users and Uses):

SACLANTCEN (Terry Peebles): operational mode -- finding optimal paths for platforms to move and avoid detection

EVA R&D (Users and Uses):

NRL (W. A. Kuperman): WRAP (for both TL and Kuperman-Ingenito noise) matched field processing
NRL: Arctic group uses it for reverberation modeling
NOSC (B. Williams): matched field processing, as starter field for PE
Scripps (W. Hodgkiss): matched field processing
JHU/APL (C. A. Boyles)
SAIC (R. B. Evans, H. A. Freese): matched field processing, coupled modes
MITRE (T. Foreman)
Woods Hole (L. Boden *et al.* - see Reference 2 below): tomography
National Center for Physical Acoustics (K. Gilbert)
NOAA, Boulder, CO (E.C. Shang): matched field processing
Norwegian Defense Research Establishment (J. Glattetre): 3-D modeling
ARE [Admiralty Research Establishment, England] (H. Ashworth)
GERDSM [French equivalent of NRL] (R. Ancey)

References:

(1) W. A. Kuperman, M. B. Porter, J. S. Perkins, and R. B. Evans, *Rapid computation of acoustic fields in three-dimensional ocean environments*, J. Acoust. Soc. Am. 89, 125-133 (1991). This describes WRAP and its use of KRAKEN.

(2) Linda Boden, James Bowlin, and John Spiesberger, "Time domain analysis of normal mode, parabolic, and ray solutions of the wave equation," J. Acoust. Soc. Am. 90, 954-958 (1991). This describes the use of KRAKEN in broadband mode to compute arrival time structures for tomographic applications.

Computer Implementation
Data-I

Common Names:

KRAKEN

KRAKENC

Host Computer Systems: VAX, IBM-compatible PCs, IRIS workstations

CPUs: VAX, IRIS, Intel 80386+80387 (or 80486DX)

Array Processor: None

Display: Immaterial

Mass Storage: Less than 2 MB for KRAKEN and FIELD (plotting) executables

High-Level Language: FORTRAN

Lines of Executable Code: 2 1.44 MB IBM floppy disks hold all source incl. companion models not part of KRAKEN (BELLHOP, etc.)

Data Bases: None

Mass Storage (by Data Base): Not applicable

Modes (Batch/Interactive): Either

Running Time/Memory Data -- Single Case Execution

Problem A: Arctic problem, 50 Hz, 5 km depth, 20 sec on VAX 8600

Problem B: Arctic problem, 1 kHz, 2.5 km depth, 20 min on VAX 8600

Running Time/Memory Data -- Multiple Case Execution:

Multiple Fixed Point Depths: virtually free except for forward coupling option

Multiple Moving Point Depths: these are virtually free

Multiple Frequencies: run time proportional to number of frequencies

Multiple Array Response Patterns: not directly implemented

Computer Implementation
Data-II

Common Names:

KRAKEN

KRAKENC

System Developer (POC/Sponsor): Michael Porter

Custodian (POC/Sponsor): Michael Porter (New Jersey Institute of Technology), phone 201-596-2995

Configuration Management (POC): Not applicable

Documentation:

Physics Description:

(1) M. B. Porter and E. L. Reiss, *A numerical method for bottom-interacting ocean acoustic normal modes*, J. Acoust. Soc. Am. 77, 1760-1767 (1985).
(2) M. B. Porter and E. L. Reiss, *A numerical method for ocean acoustic normal modes*, J. Acoust. Soc. Am. 76, 244-252 (1984).
(3) M. B. Porter, *The KRAKEN Normal Mode Program*, SACLANT Technical Memorandum, 1991.

Software Documentation: M. B. Porter, *The KRAKEN Normal Mode Program*, SACLANT Technical Memorandum, 1991.

User's or Operator's Guides: M. B. Porter, *The KRAKEN Normal Mode Program*, SACLANT Technical Memorandum, 1991.

Degree of Automation: None. User must prepare ASCII input set according to specification in User's Guide.

Evaluation and Standardization Status

Common Names:

KRAKEN

KRAKENC

Mod or Version: Not applicable. Maintained through 1991 as of this writing.

Implementation Type: Standard FORTRAN, currently on VAX, IBM-compatible PC, and IRIS workstation running UNIX

Evaluation Event: No formal evaluation, but SACLANTCEN has run many thousands of cases in an operational mode. Also, Boden *et al.* (see Reference below) compared arrival structures predicted by broadband KRAKEN with those predicted by Navy Standard PE and MPP.

Results: KRAKEN found to be extremely reliable by SACLANTCEN. Boden *et al.* obtained generally good results but found that small phase errors in high order modes do cause errors in travel time computations at long ranges. These errors are of little or no consequence for ordinary single-frequency KRAKEN runs.

References: Linda Boden, James B. Bowlin, and John L. Spiesberger, "Time domain analysis of normal mode, parabolic, and ray solutions of the wave equation," J. Acoust. Soc. Am. 90, 954-958 (1991).

Evaluation (POC): No formal POC, but Terry Peebles at SACLANTCEN has been involved in the heavy operational use of KRAKEN.

Evaluation (POC) Guides: None.

RAYMODE;
Passive RAYMODE;
Range-independent
passive baseline
RAYMODE

Historical and Bibliographic Data

Common Names:
RAYMODE;
Passive RAYMODE;
Range-independent passive baseline RAYMODE

Name or Acronym: RAYMODE or Passive RAYMODE

Full Name: Range-independent passive baseline RAYMODE

Concept Developers: G. A. Leibiger, L. Felsen

Algorithm Developers: G. A. Leibiger [NUWC/NLL]; John Jakacky, Richard Somes, Lisa Gaito, Katharine Clark, Jane Murphy [all from Sonalyst]

Software Developers: Jane Murphy, Richard Somes, Lisa Gaito, Katharine Clark [all from Sonalyst]

Year of Initial Capability: 1969

Years of Major Upgrades:
1972 (Fast Model RAYMODE II)
1974 (RAYMODE 4)
1976 (RAYMODE X)
1982 (configuration management, first baseline)
1985 (new baseline)

Related and Derivative Models: Active RAYMODE
Range-dependent RAYMODE

Custodian: SONALYST (Waterford, CT)

Sponsors: NUWC, NAVSEA

References: (1) "1985 Baseline Passive RAYMODE Propagation Loss Prediction Computer Program Performance Specification Rev. 8.05," (SONALYST, Waterford, CT, December, 1991)

(2) C. L. Bartberger, "An Investigation of the Physics of the RAYMODE Model," Report No. NADC-82009-30 (NADC, Warminster, PA, 24 November 1981)

(3) "History of the RAYMODE Propagation Loss Model," NUSC Technical Document 7125 (Combat Systems Analysis Staff, NUSC, New London, CT, 5 September 1984).

(4) G. A. Leibiger, "Wave Propagation in an Inhomogeneous Medium with Slow Spatial Variation," Ph.D. Dissertation, Stevens Institute of Technology, 1968.

(5) G. A. Leibiger, "A Combined Ray Theory - Normal Mode Approach to Long Range Low Frequency Propagation Loss Prediction," NUSC Technical Memorandum PA3-0109-71 (NUSC, New London, CT, 13 August 1971).

(6) T. T. Papas, "A Description of the RAYMODE Propagation Loss Program with an Analysis of its Frequency Characteristics," A&T Report No. P9623-88-1 (Analysis & Technology, Arlington, VA, undated but circa 1988)

(7) G. A. Leibiger, "The Acoustic Propagation Model RAYMODE: Theory and Numerical Treatment," NUSC TR (1978).

(8) J. A. Davis and O. P. Council, "Passive Raymode," PSI Technical Report TR-S310046, January, 1985.

Historical and Bibliographic Data (Continued)

Common Names:
RAYMODE;
Passive RAYMODE;
Range-independent passive baseline RAYMODE

Historical Notes: All of the RAYMODE models are outgrowths of the 1968 Ph.D. dissertation by Leibiger (Ref. 4 above). To our knowledge none of them has ever been described (in terms of the basic physics) in the open literature. There are, however, numerous documents on the subject (see References on p. 3.5-1) and overviews of the RAYMODE model are given in Etter (1991) and Deavenport and DiNapoli (1979). For the configuration-managed active and passive baseline RAYMODE models, detailed DOD standard documentation is available, e.g., Ref. 1 on p. 3.5-1.

Summary of Model Physics, Attributes, and Restrictions

Common Names:
RAYMODE;
Passive RAYMODE;
Range-independent passive baseline RAYMODE

Phenomenon Modeled:	**Approach:**
Complex pressure in range and depth for a range-dependent environment	Hybrid normal mode and ray solution
Upward refracting environments (surface duct, Arctic half channel)	Uses normal (virtual) modes if no more than 10 trapped. Otherwise, a recursive integration method is used which reduces computation time by 80%.
Surface loss	Beckman-Spizzichino (water), Keenan hybrid model (ice)
Bottom loss	LFBL (up to 1000 Hz), MGS (above 1000 Hz)

Notable Attributes and Discriminants:
Passive RAYMODE is a hybrid model (hence its name--uses both ray and mode concepts). It begins with the representation of the acoustic pressure as a Hankel transform of the Green's function, as in Eq. (5-56). The integration over wavenumber is then split into several subintervals, corresponding to "ducts," or subchannels, of the sound velocity profile. Within each duct, an independent decision is made to evaluate the wavenumber integral, as follows:

1. If no more than 10 modes are trapped in the duct, the mode sum is computed.
2. Else, if f≤1000 Hz,
   (a) If the duct is bottom bounce, if f≤45 Hz, compute the mode sum, or
   if f>45 Hz, use stationary phase/Fresnel integral.
   (b) If the duct is not bottom bounce, use "quadratic" stationary phase/Fresnel int.
3. If f>1000 Hz, use faster Fresnel integral routines.

Because of this logic tree with cutoffs at specific frequencies (explicit, and implied by mode cutoffs), there can be relatively large differences in RAYMODE results even for small differences in frequency (see "Evaluation" section). On the other hand, because the model includes both rays and modes, it is very general and can handle a wide range of cases (e.g., almost any frequency) quite efficiently (see "Running Time" section).

Domain of Application (Frequency, range, water depth, range-dependence, etc.):
Documentation states validity for frequencies from 10 to 100,000 Hz. There is no specific restriction on range, but the user is limited to output at 400 range points.

Restrictions and Warnings:
1. If most or all of water column approximately isovelocity: for accuracy, model might need to trace more rays than a hard-wired limit which is in the computer code.
2. RAYMODE may not do as well in shallow water because of possible inadequacies in its shallow water bottom loss model, which could be changed or upgraded at any time.

Model Components

Common Names:
RAYMODE;
Passive RAYMODE;
Range-independent passive baseline RAYMODE

Input Data Bases/Existing Interfaces:
RAYMODE itself simply reads an ASCII input file. It is interfaced to all Navy Standard data bases through its inclusion in performance prediction systems such as APP. These include DBDB5, LFBL, and GDEM.

Acoustic Submodels: RAYMODE is consistent with the other Navy Standard propagation loss models with regard to:

1. Surface loss: Beckman-Spizzichino (water), hybrid model (ice) [Ruth Keenan, "Ice Surface Loss Models, Evaluation and Recommendation," SAIC Report 89/1456, June 1989]
2. Bottom loss: BLUG up to 1000 Hz, MGS above 1000 Hz

System Submodels: System correction factor SYSCOR (same as in Navy Standard PE)

Display and Output Routines: With RAYMODE itself, only simple "courtesy" graphics (using basic graphics routines always supplied by host, e.g, VAX, if any) are provided. When RAYMODE is embedded in performance prediction systems, its output is fed into much more elaborate displays.

The primary output is transmission loss as a function of range, which can be either coherent or incoherent. In practice, the incoherent loss is typically used.

Transmission loss can also be output separately for individual ray paths.

Use and User Data

Common Names:
RAYMODE;
Passive RAYMODE;
Range-independent passive baseline RAYMODE

Major Installations (Activity/Computer Version):
NUWC
FNOC
Fleet applications (see below)

Fleet (Users and Uses):
The fleet gets RAYMODE as part of larger systems, including SFMPL, SIMAS, ICAPS, and ASWTDA. Also, RAYMODE is a part of all fleet trainers. Fleet users include:

SUBDEVRON 12
SUBPAC
PATWING5
WINGSLANT
WINGSPAC
CTF66
All ASWOCs
All surface ships with SIMAS
All units receiving FNOC forecasts

System Design/Development (Users and Uses):
RAYMODE is run on Intel 80486DX laptops aboard P3 aircraft for sonobuoy performance prediction. In particular, the LAPS system runs RAYMODE under the OS/2 operating system in multi-tasking mode. Other systems include ICAPS, TESS, GFMPL, SFMPL, ASWTDA, and SIMAS.

EVA R&D (Users and Uses):
Roy Deavenport (NUWC/NLL)
Diane McCammon (Penn State) - target strength (primarily active RAYMODE)
Chris Eggen (APL/UW) - high frequency boundary loss work
FNOC
Analysis & Technology (ASWTDA applications)

Computer Implementation
Data-I

Common Names:
RAYMODE;
Passive RAYMODE;
Range-independent passive baseline RAYMODE

Host Computer System: VAX running VMS, SUN, HP Unix **Array Processor:** None
Also runs on Intel 80486DX CPUs [OS/2 operating system] for LAPS

Display(s): **Mass Storage:** VAX executable 111K bytes

High-Level Language(s): FORTRAN
Rocky Mountain Basic (non-configuration managed version)

Lines of Executable Code: Source code is 700K bytes

Data Bases: DBDB5, DBDBC, LFBL, HOPS, GDEM (as part of APP; not required for stand-alone RAYMODE)

Mass Storage (by Data Base): DBDBC 2.7 MB, LFBL 2.7 MB, GDEM 2.7 MB per ocean per season for temperature, salinity, and sound speed.

Modes (Batch/Interactive): Either

Running Time/Memory Data -- Single Case Execution (VAX 8000 series)
[Single fixed depth, single moving point depth]

Problem A: (below 45 Hz -- modal sum used) 10 sec

Problem B: (45 to 1000 Hz) 4 sec

Problem C: (above 1000 Hz) 2 sec

Running Time/Memory Data -- Multiple Case Execution:

Multiple Fixed Point Depths: N times the single fixed point case.

Multiple Moving Point Depths: N times the single moving point case.

Multiple Frequencies: each additional frequency requires about 85% of the run time of the first frequency, if the same submodels of RAYMODE are used (i.e., for frequencies falling within the same category of Problem A, B, or C above)

Multiple Array Response Patterns: No directional source implemented. Each additional array response pattern increases run time by about 15%.

Computer Implementation
Data-II

Common Names:
RAYMODE;
Passive RAYMODE;
Range-independent passive baseline RAYMODE

System Developer (POC/Sponsor): SONALYST

Custodian (POC/Sponsor): Rick Somes (SONALYST, Waterford, CT),

Configuration Management (POC): Bruce Incze (NUSC, New London, CT),

Documentation:

Physics Description: T. T. Papas, "A Description of the RAYMODE Propagation Loss Program with an Analysis of its Frequency Characteristics," A&T Report No. P9623-88-1 (Analysis & Technology, Arlington, VA, undated but circa 1988).

J. A. Davis and O. P. Council, "Passive RAYMODE," PSI Tech. Report TR-S310046 (Planning Systems Inc., Slidell, LA, January 1985)

Software Documentation: "1985 Baseline Passive RAYMODE Propagation Loss Prediction Computer Program Performance Specification Rev. 8.05," (SONALYST, Waterford, CT, December, 1991)

J. A. Davis and O. P. Council, "Passive RAYMODE," PSI Tech. Report TR-S310046 (Planning Systems Inc., Slidell, LA, January 1985)

User's or Operator's Guides: "1985 Baseline Passive RAYMODE Propagation Loss Prediction Computer Program Performance Specification Rev. 8.05," (SONALYST, Waterford, CT, December, 1991)

Degree of Automation: None for RAYMODE itself. Automation occurs when RAYMODE is embedded in performance prediction systems.

Comments: As of December 1991 the fleet still has version 8.00. It will take some time for distribution of the updated version 8.05 to the fleet.

Evaluation and Standardization Status

Common Names:
RAYMODE;
Passive RAYMODE;
Range-independent passive baseline RAYMODE

Mod or Version: Rev. 8.05 passive baseline as of December 1991

Implementation Type: FORTRAN

Evaluation Event: (1) Dec. 1976: RAYMODE 4 and RAYMODE X were compared against CONGRATS V, FACT, and NISSM II by the NAVSEA POSSM (Panel on Sonar System Models). Comparison was made against PARKA data and FFP runs.

(2) 1981 by Bartberger.

(3) 1988 by Papas.

Results: (1) RAYMODE X was found most accurate.

(2) Bartberger recommended corrections and improvements in 8 areas. Several significant errors and omissions were uncovered, e.g, sign error in integration routine, omission of certain surface duct modes, lack of earth curvature, unsatisfactory algorithm for determining number of ray cycles in bottom bounce region.

(3) Papas found large changes in transmission loss for small changes in frequency due to: (a) Passing through one of the transition frequencies at which the approximation used by RAYMODE changes;

(b) Crossing of a mode cutoff frequency (especially mode 1)

(c) Large variations in the coherent sum at ranges which are not an integer multiple of 1000 yd, due to phase substitution methods used.

References: (1) "History of the RAYMODE Propagation Loss Model," NUSC Technical Document 7125 (Combat Systems Analysis Staff, NUSC, New London, CT, 5 September 1984), p. 14.

(2) C. L. Bartberger, "An Investigation of the Physics of the RAYMODE Model," Report No. NADC-82009-30 (NADC, Warminster, PA, 24 November 1981).

(3) T. T. Papas, "A Description of the RAYMODE Propagation Loss Program with an Analysis of its Frequency Characteristics," A&T Report No. P9623-88-1 (Analysis & Technology, Arlington, VA, undated but circa 1988).

Evaluation (POC): Richard Somes (SONALYST, Waterford, CT).

Evaluation (POC) Guides: None.

ASTRAL

CZ ASTRAL

Historical and Bibliographic Data

Common Names:

ASTRAL

CZ ASTRAL

Name or Acronym: ASTRAL

Full Name: ASEPS TRANSMISSION LOSS

Concept Developers: A. D. Pierce, D. M. Milder, P. W. Smith, D. E. Weston, C. Spofford

Algorithm Developers: C. W. Spofford, D. White, F. Ryan, R. Holt

Software Developers: D. White, L. S. Blumen, R. Holt, B. Scaife

Year of Initial Capability: 1978

Years of Major Upgrades:
1983: LFBL interface
1986: surface duct treatment added
1986: convergence zone treatment added
1990: double duct & surface duct upgrades (Version 3.1)
1992: software improvements (Version 4.1)

Related and Derivative Models: ASTRAL is the TL model in the AUAMP Baseline Active Model, in the ICECAP Arctic Model, in the ANDES Noise Model, and others.

Custodian: OAML (NAVOCEANO)

Sponsor: ONR/AEAS (originally LRAPP)

References: **(1)** DeWayne White and Richard J. Moore, "System Design Description for the ASTRAL Model," OAML-SDD-23 (OAML, May 1991).

(2) DeWayne White and Richard J. Moore, "Software Test Description for the ASTRAL Model," OAML-STD-23 (OAML, May 1991).

(3) DeWayne White, "Software Requirements Specification for the ASTRAL Model," OAML-STD-23 (OAML, May 1991).

(4) "User's Guide for ASTRAL 3.0 and the ASTRAL 3.0 Preprocessor (PASTRL)," Tech. Report No. 446-440 (Planning Systems, Inc., McLean, VA, May 1990).

(5) DeWayne White, "ASTRAL 2.0: A Preliminary Report, Surface Ducts and Convergence Zone Modifications," Report SAIC-86/6562 (SAIC, McLean, VA, December 1986).

(6) C. W. Spofford, "The ASTRAL Model, Vol. I: Technical Description," Report No. SAI-79-742-WA (Science Applications, McLean, VA, January 1979).

(7) L. S. Blumen and C. W. Spofford, "The ASTRAL Model, Vol. II: Software Implementation," Report No. SAI-79-743-WA (Science Applications, McLean, VA, January 1979).

(8) A. D. Pierce, "Extension of the Method of Normal Modes to Sound Propagation in an Almost-Stratified Medium," J. Acoust. Soc. Am. 37, 19-27 (1965).

(9) D. M. Milder, "Ray and Wave Invariants for SOFAR Channel Propagation," J. Acoust. Soc. Am. 46, 1259-1263 (1969).

Historical and Bibliographic Data (Continued)

Common Names:

ASTRAL

CZ ASTRAL

References (Continued):

(10) P. W. Smith, "Averaged sound transmission in range-dependent channels," J. Acoust. Soc. Am. 55, 1197-1204 (1974).

(11) D. E. Weston, "Guided Propagation in a slowly varying Medium," Proc. Phys. Soc. (London) 73, 365-384 (1959).

Historical Notes: The key to ASTRAL is "adiabatic" ray theory--as discussed first for underwater sound by Pierce (Ref. 8, p. 3.6-1) and Milder (Ref. 9, p. 3.6-1)--and the use of range-averaged ray/mode intensities in tracking the adiabatic evolution of the paths in range. ASTRAL was originally developed to meet the need for an accurate, high-speed automated model capable of predicting range-smoothed (over 30-40 nm, i.e., no convergence zones) transmission loss in a range-dependent environment. Subsequently, approximate treatments of surface ducts and convergence zones were included without sacrificing the high speed for which ASTRAL is known.

Summary of Model Physics, Attributes, and Restrictions

Common Names:

ASTRAL

CZ ASTRAL

Phenomenon Modeled:	**Approach:**
Range-averaged transmission loss (TL)	hybrid mode-ray
Range-dependent environments	adiabatic ray invariant
Convergence zones	does not include phased effects of individual modes within a smoothed mode ("smode") bundle
Temporal arrival structure	ray "trace"
Vertical angular arrival structure	ray "trace"
Bottom loss	averaged phased bottom loss (averaged impedance matching), e.g., LFBL
Surface ducts	incoherent normal mode theory
Depressed (double) duct	effect of each duct computed separately
Underice scattering loss	ICECAP surface loss model
Rough surface loss	modified Kirchhoff for loss

Notable Attributes and Discriminants:

Ray-trace done in near field to handle sloping bottoms via angle conversion ($\theta_{out} = \theta_{in} - 2\theta_{slope}$) upon bottom reflection. (This will be abandoned in ASTRAL 4.0 in favor of "smode" coupling.)

Domain of Application (Frequency, range, water depth, range-dependence, etc.):

$f \geq 50$ Hz (approx.)
water depth $\geq 10\lambda$ (approx.) (λ = acoustic wavelength)
range-dependent environments, except see warning below

Restrictions and Warnings:

1. Do not use if environment changes rapidly enough to cause *strong mode coupling* (significant coupling between widely separated mode numbers).

2. ASTRAL cannot correctly compute TL in the case of a *resonant* double channel, where 2 modes have approximately the same eigenvalue (a rare case).

Model Components

Common Names:
ASTRAL
CZ ASTRAL

Input Data Bases/Existing Interfaces: ASTRAL can be run stand-alone with a user-generated ASCII input file. As part of several Model Operating Systems (e.g., EAMOS, AUAMP), it is interfaced to standard data bases:

LFBL (Low Frequency Bottom Loss) and MGS (for frequencies above 1000 Hz)
Sound speed profiles (Wright-Colborn, HOP, GDEM)
Sediment thickness database (GEOSED)
Bathymetry (SYNBAPS, DBDB5, DBDBC)

As part of ICECAP, ASTRAL is interfaced to:

ARCTIC GDEM (classified)
LFBL
DBDB5 (unclassified)
LeSchack data base of ice roughness and keel spacing

Acoustic Submodels:

Bottom loss - needs averaged phased bottom loss input, currently taken from LFBL

Ice loss - ICECAP surface loss model [Ruth Keenan, "Ice Surface Loss Models, Evaluation and Recommendation," SAIC Report 89/1456, June 1989]

Surface duct - incoherent version of FACT surface duct model

System Submodels: System Correction Factor (SYSCOR) model for Bottom Loss (same as in Navy Standard PE)

Display and Output Routines:

Transmission loss (TL) as a function of range, at a given depth
Temporal and spatial arrival structure versus range at a given depth
Travel time can be printed (after sorting). A spreadsheet can be used to view it.

Use and User Data

Common Names:

ASTRAL

CZ ASTRAL

Major Installations (Activity/Computer Version):

There are numerous installations of ASTRAL (usually along with Navy Standard PE) on PCs, VAXes, and SUNs, often as part of Model Operating Systems, ICECAP, SPARS, or performance prediction systems such as APP. Many specific installation locations are given below.

Fleet (Users and Uses):

Comsubdevron 12, New London, CT: tactical decision aid
Comsubdevron 13, San Diego, CA: tactical decision aid
PATWING5 and Naval Air Station, Brunswick, Maine
COSL/COSP/NOPF/NOSC - SPARS

System Design/Development (Users and Uses):

ARL/UT: SPARS system includes ASTRAL
Naval Training Systems Center (Orlando): POC is Mike Egnor
SI: OPTAMAS uses ASTRAL

EVA R&D (Users and Uses):

SAIC (POC: DeWayne White): continuing model upgrades for AEAS
NRL/SSC: Dave King compares ASTRAL with other models and has included ASTRAL in AEAS Model Operating System
UCSD MPL/SIO
PSU: Robert Holt (developed preprocessor to convert ASTRAL 2.4 input to ASTRAL 3.0 input)
SAIC (POC: William Renner): ASTRAL is used in the ANDES noise model
SAIC (POC: Anthony Eller): ASTRAL is used in the AUAMP Baseline performance prediction model
SAIC (POCs: John Hanna, Chris Pearson): incoherent scattering has been added to ASTRAL for more accurate TL in ice-covered environments (see Reference below).

Reference: L. B. Dozier, J. S. Hanna, and C. R. Pearson, "Treatments of Incoherent Scattering for the Parabolic Equation and ASTRAL Propagation Models," in *Ocean Variability & Acoustic Propagation*, edited by J. Potter and A. Warn-Varnas (Kluwer Academic Publishers, the Netherlands, 1991).

Computer Implementation
Data-I

Common Names:

ASTRAL

CZ ASTRAL

Host Computer Systems: VAX 11/780 (or similar),
Navy Standard HP9020, SUN DTC-II,
IBM-compatible PC with coprocessor
(or 80486DX alone)
Code is quite transportable (ANSI 1978 FORTRAN)
and should be easily implementable on other CPUs
and other operating systems.

CPUs: VAX; HP9020; SUN; Intel 8088, 80286, 80386 (+coprocessor in each case), or 80486DX

Array Processor: None **Mass Storage:** 500K for executables

Displays: EGA/VGA for simple plots on IBM PC systems; none otherwise

High-Level Languages: FORTRAN (ANSI 1978 standard)

Lines of Executable Code: 18,000 (approx.)

Data Bases: ASTRAL can be run stand-alone with a user-generated ASCII input file. As part of Model Operating Systems, it is linked to several data bases: LFBL, Wright-Colborn, HOP, GDEM, SYNBAPS, and GEOSED. Also, see page 3.6-4 for ICECAP data bases.

Mass Storage (by Data Base): (to be filled in)

Modes (Batch/Interactive): Interactive in Model Operating Systems; can be run batch as a stand-alone model

Running Time/Memory Data -- Single Case Execution

Run times are independent of frequency. Typical single case execution times: 1.5 to 25.5 sec for installation test cases on a 33 MHz IBM-compatible PC (80386 CPU + 80387 coprocessor). Times increase for more complicated environments, e.g., double ducts.

Running Time/Memory Data -- Multiple Case Execution:
ASTRAL run time T (in seconds) can be estimated as:

$$T = MD * [4.1 + (0.138)(NR)(NF)(NS) + (0.176)(NE)]$$

where NR, NF, NS, NE are the numbers of range steps, frequencies, source depths, and provinces respectively. MD is a computer-dependent factor with typical values of 1 (for an HP 9020) to 4 (for an 8086 PC).

Multiple Array Response Patterns: ASTRAL can convolve a VLA beam pattern with the intensity field.

Computer Implementation
Data-II

Common Names:

ASTRAL

CZ ASTRAL

System Developer (POC/Sponsor): AEAS (ONR Code 124A): E. D. Chaika

Custodian (POC/Sponsor): SAIC: DeWayne White

Configuration Management (POC): OAML (NAVOCEANO): Mark Boston

Documentation:

Physics Description: DeWayne White, "Software Requirements Specification for the ASTRAL Model," OAML-STD-23 (OAML, May 1991).

Software Documentation: DeWayne White and Richard J. Moore, "System Design Description for the ASTRAL Model," OAML-SDD-23 (OAML, May 1991).

User's or Operator's Guides: DeWayne White and Richard J. Moore, "Software Test Description for the ASTRAL Model," OAML-STD-23 (OAML, May 1991).

"User's Guide for ASTRAL 3.0 and the ASTRAL 3.0 Preprocessor (PASTRL)," Tech. Report No. 446-440 (Planning Systems, Inc., McLean, VA, May 1990).

Degree of Automation: Depends entirely on whether one is running "stand-alone" ASTRAL or ASTRAL from within a "Model Operating System" such as the unclassified one SAIC has developed for IBM-compatible PCs and SUNs, or the classified one (also for IBM PCs) developed by Dave King of NOARL.

Comments: For the last year a significant rewrite of ASTRAL has been underway. The new version will be known as ASTRAL 4.2.

Evaluation and Standardization Status

Common Names:

ASTRAL

CZ ASTRAL

Mod or Version: Version 4.1

Implementation Type: FORTRAN (ANSI 1978 Standard)

Evaluation Event: Range-dependent Model Evaluation conducted in 1986 (supervised by Dave King of NOARL)

Results: ASTRAL was compared against Navy Standard PE, Range-dependent RAYMODE, and a special frequency-extrapolated version of PE submitted by PSI. ASTRAL was second only to Navy Standard PE, being most accurate in 10 of 32 test cases (Navy Standard PE was most accurate in 16 of the 32 cases, and the other two models were most accurate in 3 cases each). As a result, Navy Standard PE and ASTRAL were designated as Navy Standard Range Dependent Propagation Models.

References: (1) David King and Darlene Currie, "Evaluation of Range-Dependent Models Resident on Navy Standard Desk-Top Computer," NORDA Report 205, September 1986. (CONFIDENTIAL)
(2) CNO Washington DC R 051542Z OCT 1987 ZYB (Message to the fleet designating PE and ASTRAL as Navy Standard Range Dependent Propagation Models)

Evaluation (POC): Dave King, NOARL.

Evaluation (POC) Guides: None.

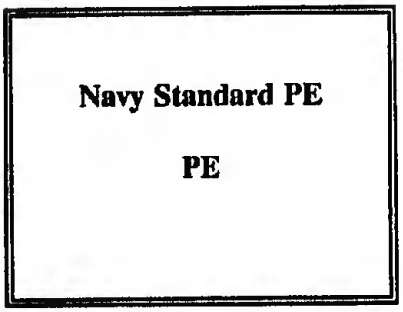
Navy Standard PE
PE

Historical and Bibliographic Data

Common Names:

Navy Standard PE

PE

Name or Acronym: Navy Standard PE

Full Name: Navy Standard Parabolic Equation Model

Concept Developers: Leontovich and Foch,
F. Tappert, Ronald Hardin

Algorithm Developers: Frederick Tappert and Ronald Hardin. Also: Harvey Brock, Charles Spofford, John Hanna, Lewis Dozier, Eleanor Holmes.

Software Developers: Frederick Tappert and Ronald Hardin. Also, Harvey Brock, Howard Garon, Robert Buchal, Eleanor Holmes, Laurie Gainey.

Year of Initial Capability: 1972

Years of Major Upgrades:

1977: band-limited wavenumber source function
1977: CMOD phase correction
1983: wide-angle split-step algorithm by Thomson/Chapman
1987-1990: added/improved interfaces to environmental databases, e.g, LFBL, GDEM

Related and Derivative Models:

1. Other split-step models: (a) "Miami-PE" (F. Tappert, Lan Nghiem-Phu);
   (b) OPTAMAS PE; (c) PAREQ (F. Jensen, SACLANTCEN)
2. Finite difference PE (Ding Lee, NUWC; R. Greene, SAIC)
3. Broadband PE models: (a) Ordinary CW PE run in a loop (SAIC, Univ. of Miami)
   (b) Time Domain PE (M. Collins, W. Kuperman)
4. Finite Element PE: FEPE, NRL-SSC

Custodian: OAML (NAVOCEANO)

Sponsor: AEAS (ONR Code 124A)

References: **(1)** R. H. Hardin and F. D. Tappert, SIAM Rev. (Chronicle) 15, 423 (1973).

(2) F. D. Tappert, SIAM Rev. (Chronicle) 16, 140 (1974).

(3) F. D. Tappert and R. H. Hardin, Proc. Eighth Inter. Congress on Acoustics (London, 1974), Vol. 2, p. 452.

(4) F. D. Tappert, "The Parabolic Approximation Method," in *Lecture Notes in Physics* No. 70, *Wave Propagation in Underwater Acoustics*, edited by J. B. Keller and J. S. Papadakis (Springer, New York, 1977).

(5) E. S. Holmes and L. A. Gainey, "Software Product Specification for the Parabolic Equation Model Version 3.3," OAML-SPS-22, September 10, 1991.

(6) E. S. Holmes and L. A. Gainey, "Software Test Description for the Parabolic Equation Model Version 3.3," OAML-STD-22, September 10, 1991.

(7) E. S. Holmes and L. A. Gainey, "Software Requirements Specification for the Parabolic Equation Model Version 3.3," OAML-SRS-22, September 10, 1991.

(8) V.A. Fock, *Electromagnetic Diffraction and Propagation Problems*, Pergamon Press, 1965.

(9) J.F. Claerbout, Geophys. 35 (1970), 407-418.

Historical and Bibliographic Data (Continued)

Common Names:

Navy Standard PE

PE

Historical Notes: PE was introduced into underwater acoustics in 1972 by F. Tappert and R. Hardin, following their earlier use of the parabolic approximation in seismics (Ref. 9) and radar physics (Ref. 8). At the same time, they introduced the split-step Fourier algorithm as an efficient and unconditionally stable means of numerical solution. Rapid proliferation of PE research and models followed, and today there are a large number (many not maintained) of PE models, all direct descendants of the original Tappert-Hardin model.

Summary of Model Physics, Attributes, and Restrictions

Common Names:

Navy Standard PE

PE

Phenomenon Modeled	Approach
Complex pressure field in range and depth	Full solution of the parabolic equation by finite difference techniques and the split-step Fourier algorithm
Diffraction (full-wave effects)	Inherent in the direct solution of the PE
Range dependence	Variable coefficient wave equation is solved directly; no adiabatic approximation
Bottom loss	Uses geoacoustic bottom inputs, e.g., from LFBL
Underice scattering loss	ICECAP surface loss model
Rough surface loss	Uses transform over small depth region near surface to get angular energy distribution; then an input loss versus angle function can be applied
Broadband (pulse) propagation	Frequency synthesis

Notable Attributes and Discriminants: The PE approach is, as explained in Section 4.4 and 6.5, unique. This PE model differs from other PEs in that it has been designated the Navy Standard PE. It has benefitted from many detailed comparisons with data and other models, and many upgrades have now been added to handle special environments. Today it typifies the state-of-the-art in parabolic equation modeling, although occasional upgrades are still being made, e.g., following comparisons with other split-step PEs listed on page 3.7-1.

Domain of Application (Frequency, range, water depth, range-dependence, etc.):
As frequency and water depth increase, so does the FFT size required by PE. Not only does this require more computer memory, but FFT computation time (which is perhaps 80% of the total PE run time for large FFTs, say 2^{10} and above) goes up with FFT size 2^N as NlogN. Thus, the FFT size is commonly limited to about 2^{12}, which allows frequencies of about 1 kHz in deep (5 km) water. In principle, however, given enough memory and computer time, PE should be able to handle almost any frequency/water-depth combination.

Restrictions and Warnings: The parabolic approximation will be violated (and PE will give wrong answers) when:

1. Significant amounts of energy are carried in very steep angle paths (e.g., above 40 degrees from horizontal). This is always true in the very near field of the source, where PE currently is supplemented by an approximate ray trace to avoid a temporary "drop-out" of the pressure which occurs if only angles of, say, 40 degrees and below are included. Other methods are being considered to increase the accuracy of this near-field computation.
2. Impedance (ρc) changes rapidly with range or depth. For example, this is usually indicated by a bottom loss curve $L(\theta)$ with large slope $dL/d\theta$ over some interval of θ within the beamwidth used for a given PE run.
3. Shear is included only as an approximate loss term; care should be taken at VLF.

Model Components

Common Names:
Navy Standard PE
PE

Input Data Bases/Existing Interfaces: PE can be run stand-alone with a user-generated ASCII input file. As part of a Model Operating System (e.g., EAMOS), it is interfaced to several data bases:

LFBL (Low Frequency Bottom Loss)
Sound speed profiles (Wright-Colborn, HOP, GDEM)
Sediment thickness database (GEOSED)
Bathymetry (SYNBAPS, DBDB5)

As part of ICECAP on the HP9020, Navy Standard PE is interfaced to:

Arctic GDEM (classified)
LFBL
DBDB5 (unclassified)
LeSchack data base of ice roughness and keel spacing

Acoustic Submodels:

Bottom loss: BLGTAB to convert LFBL input to loss versus angle.
Ice loss: ICECAP loss model.

System Submodels:

System Correction Factor (SYSCOR) for bottom loss
Directional source
Beamformer (not part of configuration-managed PE): user can select a subset of the vertical PE mesh to simulate a vertical array, and perform certain beam-forming algorithms on this data. This is an optional post-processor of the complex pressure field computed and (optionally) saved by PE.

Display and Output Routines:

Transmission loss (TL) as a function of range/depth at fixed depth/range
Full field color contour plot of TL(r,z)
Area coverage plot of TL(r,ϕ) at fixed depth z over azimuth ϕ
Color contour plot of FOM(r,z) ["Figure of Merit": equal to TL plus or minus a constant]
For broadband (multi-frequency) PE runs:
Contour plot of TL(f,r) at fixed depth z
Time spread (arrival structure) - normalized TL(t) at a fixed z

Use and User Data

Common Names:

Navy Standard PE

PE

Major Installations (Activity/Computer Version):

There are numerous installations of Navy Standard PE (usually along with ASTRAL) on PCs, VAXes, and SUNs, often as part of Model Operating Systems, ICECAP, SPARS, or performance prediction systems such as APP. Many specific installation locations are given below.

Fleet (Users and Uses):

Comsubdevron 12, New London, CT: tactical decision aid
Comsubdevron 13, San Diego, CA: tactical decision aid
PATWING5 and Naval Air Station, Brunswick, Maine
COSL/COSP/NOPF/NOSC - SPARS

System Design/Development (Users and Uses):

ARL/UT: SPARS system includes Navy Standard PE.
NOSC: LFA system design

EVA R&D (Users and Uses):

A&T (POC: E. S. Holmes) and SAIC (POC: L. A. Gainey): continuing model upgrades for AEAS, and many others.

EAMOS (Model Operating System) Users of PE:

SAIC (developer)
NOSC: C. Reed and A. D'Amico using for performance prediction, model-data comparison, decision aid, and pre-assessments
JHU/APL: Fred Newman for preassessments
A&T: Eleanor Holmes
NAVOCEANO: Martha Head

Model-data comparisons using ICECAP

SAIC (POC: Ruth Keenan)
NOCF (Naval Oceanographic Command Facility) in Brunswick, Maine; San Diego; and Keflavik, Iceland
NAVPOLAR (Naval Polar Oceanographic Center), Washington, DC
Naval Air Station, Moffit Field, CA
Naval Postgraduate School
ARL/UT
ARL/UW
NOARL
NAVOCEANO (POC: Mark Jarrett)
NUSC (POC: Bruce Incze)
NOSC (POC: Barbara Sotirin)
PSI

Tomographic applications (using broadband PE for travel time predictions)

Woods Hole [Linda Boden, James Bowlin, & John Spiesberger, "Time domain analysis of normal mode, parabolic, and ray solutions of the wave equation," J. Acoust. Soc. Am. 90, 954-958 (1991).

Computer Implementation
Data-I

Common Names:

Navy Standard PE

PE

Host Computer System: VAX 11/780 (or similar),
Navy Standard HP9020, SUN DTC-II,
IBM-compatible PC with coprocessor
(or 80486DX alone)
Code is quite transportable (ANSI 1978 FORTRAN)
and should be easily implementable on other CPUs
and other operating systems.

CPUs: VAX; HP9020; SUN; Intel 8088, 80286, 80386 (+coprocessor in each case), or 80486DX

Array Processor: Typically none, but the key algorithm, an FFT (or sine transform), cries out for such an aid. Specialized implementations, e.g., using DSP chips, have been carried out experimentally.

Display: High-resolution color display (e.g., EGA or VGA for IBM-PC compatible systems) is required for color contour plots.

Mass Storage: Executable is approx. 500K bytes (although on IBM PC systems there exist programs that can compress the executable on disk to another running executable which is just over 100K bytes; it expands dynamically when loaded into memory). Size of the output transmission loss file is approximately 500 + 4*(# of ranges)*(1+ # of output depths) bytes.
The size of the complex pressure field which can optionally be saved is approximately
500 + 8*(# of ranges)*(1/2 + # of output depths).
If PE is run in broadband mode, there is a separate complex pressure file for each frequency.

High-Level Languages: FORTRAN

Lines of Executable Code: 8,665 (approx.)

Data Bases: PE can be run stand-alone with a user-generated ASCII input file. As part of Model Operating Systems, it is linked to several data bases: LFBL, Wright-Colborn, HOP, GDEM, SYNBAPS, DBDB5, and GEOSED. Also, see ICECAP data bases above.

Mass Storage (by Data Base): for EAMOS, Compressed Data Bases ~ 14 Mb, Decompressed Data Bases ~ 63 Mb.

Modes (Batch/Interactive): Batch in stand-alone version; interactive in Model Operating Systems but may run so slow that effectively it is batch -- multitasking operating systems are obviously a help here.

Running Time/Memory Data -- Single Case Execution

PE run times generally vary linearly with maximum bottom depth and range, and as the square of the frequency. Following are run times for each of the seven test cases in the Software Test Description for PE (see Ref. 6, page 3.7-1) on a 33 MHz 80386 PC with 80387 coprocessor, and on a SUN DTC-II:

Computer Implementation
Data-II

Common Names:

Navy Standard PE

PE

Frequency	Bottom Depth	Max Range	PC Run Time	DTC-II Run Time
12 Hz	16000 ft	100 nm	10 sec	2 sec
23 Hz	18000 ft	500 nm	93 sec	16 sec
600 Hz	5000 ft	20 nm	3 min 46 sec	47 sec
60 Hz	12000 ft	465 nm	3 min 33 sec	49 sec
200 Hz	15800 ft	40 nm	7 min 37 sec	97 sec
1400 Hz	6560 ft	0.1 nm	33 sec	7 sec
200 Hz	6500 ft	0.2 nm	4 sec	1 sec

Running Time/Memory Data -- Multiple Case Execution:

Multiple Fixed Point Depths: separate run for each such depth

Multiple Moving Point Depths: no extra cost

Multiple Frequencies: separate run for each different frequency

Multiple Array Response Patterns: fixed point: one pattern per run. Moving points: multiple depths can be saved in the same run (at multiple ranges) for subsequent beamforming (post processing).

System Developer (POC/Sponsor): AEAS (ONR Code 124A): E. D. Chaika

Custodian (POC/Sponsor): A&T (E. S. Holmes) and SAIC (L. A. Gainey)

Configuration Management (POC): Mark Boston (NAVOCEANO)

Documentation:

Physics Description: (1) E. S. Holmes and L. A. Gainey, "Software Requirements Specification for the Parabolic Equation Model Version 3.3," OAML-SRS-22, Sept. 10, 1991.

(2) F. D. Tappert, "The Parabolic Approximation Method," in *Lecture Notes in Physics* No. 70, *Wave Propagation in Underwater Acoustics*, edited by J. B. Keller and J. S. Papadakis (Springer, New York, 1977).

Software Documentation: E. S. Holmes and L. A. Gainey, "Software Product Specification for the Parabolic Equation Model Version 3.3," OAML-SPS-22, Sept. 10, 1991.

User's or Operator's Guides: E. S. Holmes and L. A. Gainey, "Software Test Description for the Parabolic Equation Model Version 3.3," OAML-STD-22, Sept. 10, 1991.

Degree of Automation: Depends entirely on whether one is running "stand-alone" PE or PE from within a "Model Operating System" such as EAMOS, which SAIC has developed for IBM-compatible PCs and SUNs, or the classified one (also for IBM PCs) developed by Dave King of NRL/SSC.

Evaluation and Status
Standardization

Common Names:

Navy Standard PE

PE

Mod or Version: Version 3.3

Implementation Type: FORTRAN (ANSI 1978 Standard)

Evaluation Event: Range-dependent Model Evaluation conducted in 1986 (supervised by Dave King of NRL/SSC)

Results: Navy Standard PE was compared against ASTRAL, Range-dependent RAYMODE, and a special frequency-extrapolated version of PE submitted by PSI. Navy Standard PE was most accurate in 16 of 32 test cases, ASTRAL in 10 of the 32 cases, and the other two models were most accurate in 3 test cases each. As a result, Navy Standard PE and ASTRAL were designated as Navy Standard Range Dependent Propagation Models.

References: (1) David King and Darlene Currie, "Evaluation of Range-Dependent Models Resident on Navy Standard Desk-Top Computer," NORDA Report 205, September 1986. (CONFIDENTIAL)
(2) CNO Washington DC R 051542Z OCT 1987 ZYB (Message to the fleet designating PE and ASTRAL as Navy Standard Range Dependent Propagation Models)

Also see results of 1981 workshop: J.A. Davis, D. White, R. Cavanagh, "NORDA Parabolic Equation Workshop, 31 March - 3 April 1981," NORDA Tech Note 143 and 1991 Workshop: Chin-Bing, S., King, D., Davis, J. and Evans, R. (Eds.) (1993), "PE Workshop II: Proceedings of the 2nd Parabolic Equation Workshop (May 6-9, 1991)," NRL/BE/7181-93-0001, Naval Research Laboratory, Washington, D.C.

Evaluation (POC): Dave King, NOARL.

Evaluation (POC) Guides: None.

FFP

Fast Field Program

Historical and Bibliographic Data

Common Names:

FFP

Fast Field Program

Name or Acronym: FFP

Full Name: Fast Field Program

Concept Developers: H. W. Marsh, F. R. DiNapoli

Algorithm Developer: F. R. DiNapoli

Software Developers: F. R. DiNapoli, Joanne Kelly

Year of Initial Capability: 1971

Years of Major Upgrades:
1989: modified to create complex pressure arrays and loop on frequency (pulse propagation)
1990: added postprocessor to plot CW and broadband outputs
1990: attenuation no longer required to vary linearly with freq
1992: ongoing effort to increase automation of exponential fit to sound speed profile

Related and Derivative Models: Arctic acoustic FFP [H. W. Kutschale, Refs. 5-7]
Time-domain FFP [M. B. Porter, Ref. 8]
FFP for sound propagation in the atmosphere [Ref. 9]

Custodian: Fred DiNapoli, SAIC, New London, CT.

Sponsors: ONR, NAVSEA

References: (1) F. R. DiNapoli and R. L. Deavenport, "Theoretical and numerical Green's function field solution in a plane multilayered medium," J. Acoust. Soc. Am. 67, 92-105 (1980)

(2) F. R. DiNapoli, "A Fast Field Program for Multilayered Media," NUSC Technical Report 4103, 26 August 1971.

(3) F. R. DiNapoli, "Acoustic Propagation in a Stratified Medium," NUSL Report 1046, 13 August 1969 [doctoral thesis].

(4) H. W. Marsh and S. R. Elam, Internal Document, Raytheon Co., Marine Research Laboratory, New London, CT, 1967.

(5) H. W. Kutschale, "The integral solution of the sound field in a multi-layered liquid-solid half-space with numerical computations for low-frequency propagation in the Arctic Ocean," Tech. Rep. No. 1 (CU1-1-70, ONR Contract N00014-67-A-0108-0016), Lamont-Doherty Geological Observatory, Columbia University, Palisades, NY, 1970.

(6) H. W. Kutschale, "Rapid computation by wave theory of the propagation loss in the Arctic Ocean," Tech. Rep. No. 8, Lamont-Doherty Geological Observatory, Columbia University, Palisades, NY, 1981.

(7) H. W. Kutschale, "Relation of ice cover to onshore detection of underwater sources," Final Report under Contract N60921-80-C-0096, Lamont-Doherty Geological Observatory, Columbia University, Palisades, NY, 1981.

(8) M. B. Porter, "The time-marched fast-field program (FFP) for modeling acoustic pulse propagation," J. Acoust. Soc. Am. 87, 2013-2023 (1990).

(9) R. Raspet *et al.*, "A fast-field program for sound propagation in a layered atmosphere above an impedance ground," J. Acoust. Soc. Am. 77, 345-352 (1985).

Common Names:

FFP

Fast Field Program

Historical Notes: The essential idea of the FFP is to evaluate the Hankel transform, (see Section 5), by replacing it by its far-field asymptotic expansion and then using a Fast Fourier transform. The idea was conceived by Marsh (Ref. 4, previous page) and extended by DiNapoli, who devised an elegant recursion technique which allows the calculation of the Green's function for many values of the transform variable simultaneously [Ref. 1, previous page]. FFP early on gained a good reputation for accuracy, and was used by the NAVSEA POSSM (Panel on Sonar System Models) as a benchmark in a 1976 comparison of ray models (see Section 3.5 for more details). Although FFP is well known in the community, most current use and development of FFP appears still to lie with DiNapoli, the original developer of the model.

Summary of Model Physics, Attributes, and Restrictions

Phenomenon Modeled	Approach
Complex CW pressure versus range and depth	Numerical solution of the Fourier-Bessel transform of the Helmholtz equation with Hankel approximation
Rough surface loss	Effective impedance boundary condition
Broadband (pulse) propagation	Frequency synthesis

Notable Attributes and Discriminants:
FFP has for years been used as the benchmark or standard for propagation in a range-independent environment. It has a very well developed broadband capability, including a wide variety of plotting options. Run time is independent of frequency, so broadband runs are feasible even at very high frequencies.

Domain of Application (Frequency, range, water depth, range-dependence, etc.):
Range independent only. Can be run at extremely high frequency -- has agreed well with ray models at 100 kHz.

Restrictions and Warnings:
Use of far-field asymptotic expansion of the Hankel function implies that there may be significant errors at very close range to the source. The magnitude of the errors is dependent on details of the propagation geometry, sound speed profile, frequency, and boundary losses, according to p. 105 of Ref. 1 on the previous page.

Model Components

Common Names:

FFP

Fast Field Program

Input Data Bases/Existing Interfaces: None.

Acoustic Submodels:

Attenuation: Thorp
Scattering loss: Marsh-Mellon

System Submodels:

LFM source waveform or Gaussian pulse can be designated as input options and will be computed automatically by FFP.

Display and Output Routines: A postprocessor program can provide plots of:

Transmission loss
Kernel
Transfer function
Time history of pulse
Power spectral density of a pulse
Waveform pressure response
Impulse response of the channel

Use and User Data

Common Names:

FFP

Fast Field Program

Major Installations (Activity/Computer Version):
SAIC (New London, CT): Fred DiNapoli
NUWC (New London, CT): Roy Deavenport

Fleet (Users and Uses): None.

System Design/Development (Users and Uses): None.

EVA R&D (Users and Uses):
SAIC: comparison with Arctic data
NUSC: comparison with other models

Computer Implementation
Data-I

Common Names:

FFP

Fast Field Program

Host Computer System: VAX, IBM PC. **CPUs:** VAX, Intel 80386+80387 or 80486DX
Array Processor: None.

Displays: IBM EGA or VGA for postprocessor

Mass Storage: Executable size depends on array dimensions, perhaps 1 MB.

High-Level Language: FORTRAN **Lines of Executable Code:** Source code, incl. postprocessor graphics, is 128K bytes

Data Bases: None.

Mass Storage (by Data Base): Not applicable.

Modes (Batch/Interactive): Main program runs batch. Interactive postprocessor on IBM PCs.

Running Time/Memory Data -- Single Case Execution

IBM 80386+80387: Deep water problem, 1 minute, independent of frequency.

Running Time/Memory Data -- Multiple Case Execution:

Multiple Fixed Point Depths: each fixed point depth is a separate run.

Multiple Moving Point Depths: each moving point depth is a separate run.

Multiple Frequencies: each frequency is a separate run.

Multiple Array Response Patterns: not directly implemented.

Computer Implementation
Data-II

Common Names:

FFP

Fast Field Program

System Developer (POC/Sponsor): None currently.

Custodian (POC/Sponsor): F. R. DiNapoli (SAIC, New London, CT)

Configuration Management (POC): None.

Documentation:

Physics Description: F. R. DiNapoli and R. L. Deavenport, "Theoretical and numerical Green's function field solution in a plane multilayered medium," J. Acoust. Soc. Am. 67, 92-105 (1980).

Software Documentation: Some contained in user's notes available from DiNapoli.

User's or Operator's Guides: Informal user's notes available directly from DiNapoli.

Degree of Automation: None. User must prepare ASCII input set according to specification in User's Notes available from DiNapoli. At the moment the required exponential fit to the desired sound speed profile must be done by hand. DiNapoli is currently involved in an effort to automate this part of the process.

Evaluation and Status
Standardization

Common Names:

FFP

Fast Field Program

Mod or Version: Not applicable. Maintained through 1991 as of this writing.

Implementation Type: FORTRAN.

Evaluation Event: Although FFP itself was not formally evaluated, it was used as a benchmark in the 1976 evaluation of ray models carried out by the NAVSEA POSSM (Panel on Sonar System Models). Also, Raspet *et al.* (see Reference below) have compared their atmospheric FFP with Kutschale's FFP, which is closely related to DiNapoli's, with excellent results.

Results: Generally quite good comparisons.

References: R. Raspet *et al.*, "A fast-field program for sound propagation in a layered atmosphere above an impedance ground," J. Acoust. Soc. Am. 77, 345-352 (1985).

Evaluation (POC): None.

Evaluation (POC) Guides: None.

Degree of Automation: None. User must prepare ASCII input set according to specification in User's Notes available from DiNapoli. At the moment the required exponential fit to the desired sound speed profile must be done by hand. DiNapoli is currently involved in an effort to automate this part of the process.

SAFARI

OASES

Historical and Bibliographic Data

Common Names:

SAFARI

OASES

Name or Acronym: SAFARI

Full Name: Seismo-Acoustic Fast Field Algorithm for Range Independent Environments

Concept Developers: Pekeris; Ewing, Jardetsky, and Press; Kutschale; DiNapoli; Schmidt

Algorithm Developer: Henrik Schmidt

Software Developer: Henrik Schmidt

Year of Initial Capability: 1982

Years of Major Upgrades: 1987: boundary roughness & noise modeling
1990: automated wavenumber sampling

Related and Derivative Models: (1) SAFARI noise model (Ref. 6; developed for matched field processing)
(2) OASES: SAFARI renamed after 1990 upgrade to automate wavenumber integration

Custodian: Henrik Schmidt, Massachusetts Institute of Technology

Sponsors: SACLANTCEN, ONR Arctic Acoustics

References: (1) H. Schmidt, "SAFARI User's guide," SACLANT ASW Research Centre, La Spezia, Italy, July 29, 1987.

(2) H. Schmidt, "OASES Upgrade Notes," MIT, 1990, available from author.

(3) H. Schmidt and F. B. Jensen, "A full wave solution for propagation in multilayered viscoelastic media with application to Gaussian beam reflection at fluid-solid interfaces," J. Acoust. Soc. Am. 77, 813-825 (1985).

(4) H. Schmidt and F. B. Jensen, "Efficient numerical solution technique for wave propagation in horizontally stratified environments," Comp. and Maths. with Appls. 11, 699-715 (1985).

(5) B. E. Miller and H. Schmidt, "Observation and inversion of seismo-acoustic waves in a complex arctic ice environment," J. Acoust. Soc. Am. 89, 1668-1685 (1991).

(6) H. Schmidt and W. A. Kuperman, "Estimation of surface noise source level from low-frequency seismoacoustic ambient noise measurements," J. Acoust. Soc. Am. 84, 2153-2162 (1988).

(7) F. B. Jensen and H. Schmidt, "Subcritical penetration of narrow Gaussian beams into sediments," J. Acoust. Soc. Am. 82, 574-579 (1987).

(8) W. M. Ewing, W. S. Jardetsky, and F. Press, *Elastic Waves in Layered Media* (McGraw-Hill, New York, 1957).

(9) H. W. Kutschale, "Rapid computation by wave theory of propagation loss in the Arctic Ocean," Rep. CU-8-73, Columbia University, NY (1973).

Historical and Bibliographic Data (Continued)

Common Names:

SAFARI

OASES

Historical Notes: SAFARI was developed as an efficient numerical implementation of the original solution technique of Ewing, Jardetsky, and Press [Ref. 8 on page 3.9-1] but using modern finite-element numerical approaches. It followed by roughly a decade the Fast Field Program (FFP) and, although it solves the same depth-dependent Green's function, includes shear and offers other advantages (see next page).

Summary of Model Physics, Attributes, and Restrictions

Common Names:

SAFARI

OASES

Phenomenon Modeled:	**Approach:**
Complex CW pressure versus range and depth in a range-independent environment	Fourier-Bessel transform of separable Helmholtz equation
Shear	Full elastic treatment
Scattering due to rough interfaces	Perturbation theory for coherent scatter Incoherent scatter: under development
Attenuation in sediment	Uses complex Lamé constants and assumes attenuation increases linearly with frequency.
Broadband (pulse) propagation	Frequency synthesis

Notable Attributes and Discriminants: Uses a *global matrix approach* to solve for the depth-dependent Green's function, rather than the propagator matrix approach of FFP. Advantages include:

1. Field produced by multiple sources (e.g., phased array) is easily determined by superimposing fields produced by individual sources.

2. Field can be computed at any number of receiver depths simultaneously.

3. Mixed problems with fluid, solid, and vacuum layers are efficiently treated.

4. No numerical stability problems within a layer because of choice of coordinate system and organization of global system of equations.

5. Solution unconditionally numerically stable for any number of layers.

6. Global nature of solution leads to easy vectorization on array processors.

In principle, SAFARI provides an exact solution to the wave equation in a horizontally stratified environment. It is highly regarded and, like FFP, is frequently used as a benchmark for range-independent ocean acoustic problems, especially those with complicated bottoms.

Domain of Application (Frequency, range, water depth, range-dependence, etc.):
Range-independent (no adiabatic version yet)

Restrictions and Warnings: (1) The model can be run at high frequencies but requires substantial RAM and computer time.

(2) If source and receiver are at the same, or about the same, depth, a much wider wavenumber spectrum is required for the integration.

(3) To be safe, one should always test for convergence of the integration, e.g., by doing it again with one-half the wavenumber mesh spacing to make sure the answer does not change significantly.

Model Components

Common Names:
SAFARI
OASES

Variants of OASES model:
OASP: Pulsed Source
OAST: TL at single frequency
OASR: Reflection coefficient
OASN: Noise model
OASM: Matched field processing
OASS: includes incoherent scattering (under development)

All of these use the same *kernel* program that computes the Green's function at different wavenumbers, given environmental and propagation geometry inputs.

Input Data Bases/Existing Interfaces: None.

Acoustic Submodels:
Scattering/reverberation from object in bottom
Model of coherent scattering loss at rough interface
Model that keeps incoherently scattered energy in the waveguide and allows it to propagate [under development]
Noise model [in use at NRL-DC and SSC]: Kuperman-Ingenito approach + discrete shipping

System Submodels/Extensions:
Matched field processing (modified version OASM): SAFARI computes signal, OASES computes noise and noise correlations. Beamformer allows specification of arbitrary 3-D array geometry.

Display and Output Routines:
OASES includes an interactive processor (menu-oriented system). The user can choose center frequencies, bandwidths, and source and receiver depth, see the result, and then choose again.
Frequency spectra at individual receivers
Frequency-wavenumber diagrams or time-domain equivalents
Stacking of results in depth or range
Movie of snapshots at successive times t, $t+\Delta t$, $t+2\Delta t$, ...
Full-field contour plots of intensity

Use and User Data

Common Names:

SAFARI

OASES

Major Installations (Activity/Computer Version)
NUWC
NOSC
NRL
NRL/SSC
NSWC (White Oak)
NCSC (Naval Coastal Systems Center)
DREP and DREA, Canadian labs
German lab in Kiel
Two French labs
Labs in Australia and New Zealand
Schlumberger [Ridgefield, CT and Cambridge, England]: commercial seismic applications

Fleet (Users and Uses):
Cmdr. Bruce Miller, Corpus Christi runs SAFARI on a PC.

System Design/Development (Users and Uses):
Alliant Techsystems [Arlington, VA]: SAFARI is kernel of ATSS [Alliant Time Series Simulator], used in beamformers for evaluation of active and passive signal processing algorithms
Krupp-Atlas [Germany]: battlefield surveillance research

EVA R&D (Users and Uses):
1. Universities doing research in seismics and underwater acoustics, including:
    APL/UW
    ARL/UT
    Univ. of Miami
    Scripps
    Woods Hole
    Penn. State
    Colorado School of Mines
    Universities in Taiwan, Korea, and Europe
2. Government labs as listed above

References:
SAFARI and OASES have been distributed to over 200 users, of which the above is a synopsis of the most important. Dr. Henrik Schmidt maintains a complete user list.

Computer Implementation
Data-I

Common Names:
SAFARI
OASES

Host Computer Systems and CPUs:
VAX with VMS operating system
Unix Workstations [SUNs, etc.]
IBM 9000 RISC machines
Mini supercomputers: Convex, Alliant
CRAY supercomputers
Intel Hypercube: optimized for this parallel architecture & for Caltech DELTA 528-node mesh
Connection Machine
IBM-compatible PCs with Intel 80386+80387, or 80486DX processors

Array Processor: Original implementation at SACLANT used FPS164 and FPS264

Display(s): Immaterial

Mass Storage: Executable sizes vary with key array dimensions; typically, 400K bytes for OASP, OAST, or OASR, somewhat more for OASN, OASM, or OASS

High-Level Language(s): FORTRAN

Data Bases: None.

Lines of Executable Code: Source code, incl. graphics, is 400K bytes

Mass Storage (by Data Base): Not applicable

Modes (Batch/Interactive): Either

Running Time/Memory Data -- Single Case Execution

Problem A: Max 10 sec for single freq. ≤ 1000 Hz, 1000 to 2000 ranges, 100 depths, on a SPARCSTATION II or DEC 5000 or IBM 9000

Problem B: Rule of thumb: about 100 times as long for a broadband case; perhaps 30 minutes on SPARCSTATION II or DEC 5000 or IBM 9000

Problem C: Caltech DELTA (528-node i860 mesh) can do time domain computation with moving sources and receivers in *real time* 2 seconds for the most complicated broadband case.

Running Time/Memory Data -- Multiple Case Execution:

Multiple Fixed Point Depths: virtually free

Multiple Moving Point Depths: virtually free

Computer Implementation
Data-II

Common Names:

SAFARI

OASES

Multiple Frequencies: Run time scales linearly with number of frequencies on scalar machine. On massively parallel machine such as Caltech DELTA, every wavenumber is done on a different node with no inter-nodal communication! Thus, every single frequency or broadband case scales *directly* with the number of nodes.

Multiple Array Response Patterns: Beam patterns can be input at source and/or receiver. Multiple patterns are virtually free. At longer range, more wavenumber sampling is required, but this can be offset by limiting the wavenumber spectrum to cover only the smaller angles that will remain at long range. Thus, a run to 1 km but with the full spectrum may take the same run time as a run to 1000 km but including only shallow angles.

System Developer (POC/Sponsor): Henrik Schmidt.

Custodian (POC/Sponsor): Henrik Schmidt (Massachusetts Institute of Technology)

Configuration Management (POC): Not applicable.

Documentation:

Physics Description: H. Schmidt and F. B. Jensen, "A full wave solution for propagation in multilayered viscoelastic media with application to Gaussian beam reflection at fluid-solid interfaces," J. Acoust. Soc. Am. 77, 813-825 (1985).

Software Documentation: see User's Guides below.

User's or Operator's Guides:

(1) H. Schmidt, "SAFARI User's guide," SACLANT ASW Research Centre, La Spezia, Italy, July 29, 1987.

(2) H. Schmidt, "OASES Upgrade Notes," MIT, 1990, available from author.

Degree of Automation: None, in the sense that the user must prepare an ASCII input set according to specifications in User's Guides. OASES has automated the wavenumber integration. There are no automated interfaces to environmental databases.

Evaluation and Standardization Status

Common Names:

SAFARI

OASES

Mod or Version: SAFARI version 3.0 was documented in the 1987 User's Guide. A later upgrade to 4.0 did not include new physics but modified the code so that it would compile under Microsoft Fortran on IBM PC compatible microcomputers.

Currently, all physics changes are being incorporated into OASES, the newer, more automated version introduced in 1990. OASES is currently at version 1.4.

Implementation Type: FORTRAN.

Evaluation Event: No formal evaluation, but SACLANTCEN has run many thousands of cases in an operational mode. Also, Williams *et al.* (see Ref. below) have compared SAFARI predictions with experimental measurements of sound in a homogeneous sand sample for 20-kHz linear and parametric sources.

Results: Williams *et al.* found good agreement of SAFARI predictions with data except for severely post-critical incident grazing angles, at which the main part of the beam does not penetrate into the sand sediment.

References: K. L. Williams, L. J. Satkowiak, and D. R. Bugler, "Linear and parametric array transmission across a water-sand interface--Theory, experiment, and observation of beam displacement," J. Acoust. Soc. Am. 86, 311-325 (1989).

Evaluation (POC): No formal POC, but Terry Peebles at SACLANTCEN has been involved in the heavy operational use of SAFARI.

Evaluation (POC) Guides: None.

4. PHYSICS -- OVERVIEW

The purpose of this section and the two that follow is to provide an overview of the acoustic wave equation and of several relevant approaches to solving it. The review assumes some familiarity with differential equations and their solutions, and with acoustic models, but provides both footnotes and references to guide the reader toward more in-depth background material.

To set the stage, we begin in this section with a discussion of several forms of the acoustic wave equation and various problems to be solved. Practical problems in underwater sound lead to key differences in the type of wave equation problem, such as: time dependent or not, stochastic or deterministic, 3D or 2D, with range-dependent data or range-independent data. The latter is so important a determinant in the mathematical treatment that the discussion on solutions to the wave equation is broken into two parts: Section 5 for range-independent environments, and Section 6 for range-dependent.

4.1 The scalar time-dependent acoustic wave equation

It is beyond the scope of this short overview to provide a complete discussion of the fundamental physics of underwater sound propagation or the derivation of the various wave equations describing it. For the reader interested in studying these topics further, we note that there are a large number of textbooks and published papers on the subject, including:

- Boyles (1984) - The first chapter of this textbook gives an in-depth derivation of the acoustic wave equation from the hydrodynamic equations.
- Rayleigh (1896) - An early view of the governing equations of sound generation and propagation.
- Apel (1987) - Chapter 7 of this book gives a derivation of the acoustic wave equation and shows the relationship of acoustic waves with internal waves and surface waves.
- Lighthill (1978) - This very readable volume is dedicated to the study of sound, water, and internal waves.
- DeSanto (1979) - Derivation of the acoustic wave equation in the presence of gravitational and rotational effects.

We begin then with the familiar time-dependent, scalar wave equation derived under the assumptions that: there are neither gravitational nor rotational effects, only small amplitude pressures are allowed (i.e., no non-linear effects), and the water volume is static (no currents). The scalar wave equation occurs in a number of forms, the most common being:

$$\nabla^2 p(x,y,z,t) - c^{-2}(x,y,z,t)\frac{\partial^2 p}{\partial t^2} = s(x,y,z,t) \qquad (4\text{-}1)$$

where p(x,y,z,t) is the acoustic pressure as a function of time t and spatial coordinates x,y,z, c(x,y,z,t) is the sound speed, and s(x,y,z,t) is the source function. Already, in obtaining this familiar form of the scalar wave equation, we have neglected density variations often included for bottom interaction (see Note 4-1).

4.2 Numerical solutions and boundary conditions

In general and for real ocean cases of interest, Eq. (4-1) cannot be solved analytically. Underwater acoustic models thus provide numerical solutions to Eq. (4-1) or, more typically, to simpler wave equations derived from it. Solutions to these simpler wave equations can often be obtained at much less computational cost than direct solutions of Eq. (4-1).

To see why different forms of the wave equation vary profoundly in degree of complexity, recall [e.g., Chester (1971) or Garabedian (1964)] that the appropriate initial and/or boundary conditions are intimately linked to the *type* of the equation. Linear second-order partial differential equations (PDEs) can be either hyperbolic, parabolic, or elliptic, depending on whether the quadratic form associated with the second derivative terms is indefinite, semidefinite, or definite. In general, parabolic or separable elliptic (e.g., in two dimensions, range independent) equations allow the simplest boundary (and no initial) conditions. Even these equations become quite complicated, however, if *rough boundary scattering* effects are computed directly by solving the equation on an irregular boundary; an example of this approach, with computing times greater than those for a flat boundary by factors of more than 300, can be found in Dozier (1984). For this reason, boundary scattering effects are often modeled simply as an additional loss term to be imposed on the solution to a wave equation

in a domain with flat boundaries; in practice, this usually requires only a very small relative increase in computer time.

4.3 Coordinate systems

In addition to the considerations of the previous section, the other primary determinant of complexity is the number of independent variables in a wave equation; the fewer the variables, the simpler the solution. A time-independent wave equation in two spatial dimensions is the simplest form of practical significance in underwater acoustics. Indeed, such an equation was about all that could be handled by digital computers until the advent of supercomputers in the mid 1970s; even today, the vast majority of model runs, especially those carried out on small machines, solve such equations.

The real ocean, of course, has three spatial dimensions. Two types of simplifying assumptions are customarily made to reduce a wave equation from 3D to 2D:

(1) *Cylindrical symmetry about a point or line source.* Here there are only two spatial variables, range r and depth z. The ocean environment is assumed cylindrically symmetric about the source. Acoustic propagation is identical in all vertical planes containing the source. Results are usually displayed as transmission loss versus range at a fixed depth, or as a contour plot of transmission loss versus range and depth within a vertical plane.

(2) *N x 2D geometry.* Azimuthal derivatives in the wave equation (corresponding to out-of-plane refraction and scattering) are ignored, but the in-plane ocean environment is allowed to vary from one plane to the next; typically, the environment in each plane represents a radial slice through a full three-dimensional model of the environment. Thus, a different 2D wave equation is solved in each of N vertical planes, where N is chosen large enough to provide azimuthal sampling adequate for a given environment. This allows a further method of visualization of the results not available from the simple cylindrically symmetric model. We can now look down on the ocean from above and plot contours of transmission loss as a function of horizontal variables x and y at a fixed depth z. The acoustic effects of large oceanographic features, such as the Gulf Stream or the mid-Atlantic ridge, can be displayed quite effectively in this manner. Also, we can compute the degree of azimuthal decorrelation

of the acoustic field due to azimuthal variations of the environment, but neglecting out-of-plane refraction and scattering; such calculations are useful in computing bounds on array performance.

The first assumption (cylindrical symmetry) has most frequently been used for underwater acoustic models. The Nx2D models simply run 2D (cylindrically symmetric) models along a number of radials, sampling azimuth space at a density appropriate to the problem being solved. There are a few existing models that actually solve the full three-dimensional wave equation, but these are highly specialized research models not in general use and are not treated in this report.

4.4 Time-independent wave equations: approaches

A simpler (and perhaps the most frequently encountered in underwater acoustics) wave equation is obtained when we assume that the source function in Eq. (1) is a single frequency (denoted by ω), simple harmonic source, so that it is separable in space and time of the form $s(x,y,z,t) = A(x,y,z)\, e^{i\omega t}$, and that the pressure field is likewise separable, say $p(x,y,z,t) = P(x,y,z,\omega)\, e^{i\omega t}$. In that case, substitution into Eq. (1) yields the *reduced wave equation* or *Helmholtz equation:*

$$\Delta P + \frac{\omega^2}{c^2} P = A \tag{4-2}$$

where typically $A(x,y,z) = \delta(x-x_s, y-y_s, z-z_s)$, representing a point source at (x_s,y_s,z_s) and Δ is the Laplacian operator (Note 4-2). This equation, however, is not at all simple to solve numerically over a large region of the ocean. Since it is elliptic, in order for the problem to be well posed, boundary conditions have to be assigned on the entire closed boundary of the spatial domain of the problem. If we imagine enclosing the region of ocean by a rectangle, we do not *a priori* know the boundary condition at the far end of the rectangle, i.e., at long range; indeed, the distant pressure field is precisely what we want to compute. From a practical point of view, we also have a computer data storage problem; numerical solvers for elliptic equations typically must fill the entire rectangle with mesh points and solve for all of the pressure values simultaneously. For an elliptic PDE boundary data are transmitted instantly and simultaneously

to all interior mesh points. Discretizing, say, 100 km in range and 5 km in depth on the scale of a fraction of an acoustic wavelength, e.g., 10 m, requires 5 million mesh points, and the numerical scheme will require several words of storage per mesh point. The storage requirements will increase rapidly with acoustic frequency, and adding a third spatial dimension makes the problem even more difficult.

These considerations cause us to appreciate all the more the elegance of the *parabolic equation* (PE) approach, introduced into underwater acoustics by Tappert (1977). The essence of this approach is to factor Eq. (4-2) into forward and backward going parts. Beginning with Eq. (4-2) in cylindrical coordinates, we remove the cylindrical spreading by setting $u = \sqrt{r}\, P$ and obtain:

$$\Delta P + \frac{\omega^2}{c^2} P = \frac{\partial^2 u}{\partial r^2} + \frac{\partial^2 u}{\partial z^2} + \frac{\omega^2}{c^2} u$$

$$= \left(\frac{\partial}{\partial r} + i \sqrt{\frac{\partial^2}{\partial z^2} + \frac{\omega^2}{c^2}} \right) \left(\frac{\partial}{\partial r} - i \sqrt{\frac{\partial^2}{\partial z^2} + \frac{\omega^2}{c^2}} \right) u \qquad (4\text{-}3)$$

Each factor then has only a first range derivative, thereby allowing a marching-in-range solution for the forward propagated part of the field,

$$\frac{\partial}{\partial r} u = i \sqrt{\frac{\partial^2}{\partial z^2} + \frac{\omega^2}{c^2}}\; u. \qquad (4\text{-}4)$$

In practice, the square root operator on the right hand side must be approximated by an operator that can be explicitly evaluated numerically--this has led to many different parabolic approximations, as will be discussed in Sections 6.5 and 6.6. For all parabolic approximations, however, a key advantage is that no boundary condition is needed on the far side of the rectangular solution domain. Another advantage of PE is its effectiveness in dealing with quite severe environmental range dependence.

The most serious limitation with PE is that it becomes inaccurate at steep angles. Although improved parabolic approximations [e.g., Thomson and Chapman (1983)] have greatly expanded the angular aperture (at least to 20 degrees from the horizontal) of "acceptable" accuracy, PE cannot give reliable answers at very short range, where steep angle paths dominate. PE will be discussed further in Sections 6.5 and 6.6.

Range-independent problems, by which we mean the environment is assumed to vary with depth but not range or azimuth, admit a numerically efficient method of solution via separation of variables, i.e., normal modes. By splitting the wave equation into two ordinary differential equations (ODEs), one in range and one in depth, each ODE can be solved much more simply than the original PDE. That is, if we substitute the factorization $P(r,z)=\psi(r)\phi(z)$ into Eq. (4-2) with $A=0$ and $c=c(z)$, we are able to separate variables and obtain:

$$\psi''(r) + \frac{1}{r}\psi'(r) + \lambda^2\psi(r) = 0 \tag{4-5}$$

$$\phi''(z) + (k^2(z)-\lambda^2)\phi(z) = 0 \tag{4-6}$$

(where λ is the separation constant--physically, it is a horizontal wavenumber).

For these ODEs, boundary conditions assigned along lines or planes for the PDE (the wave equation) now translate simply into conditions at a small set of discrete points. For example, the pressure-release boundary condition $p(r,0)=0$ assigned along the line $z=0$ becomes simply the point boundary condition $\phi(0)=0$ on the depth modes in Eq. (4-6). The normal mode technique is thus illustrative of a general mathematical approach to solving PDEs: often they can profitably be decomposed into ODEs. A major drawback is that the number of normal modes which must be computed is roughly proportional to the acoustic frequency, so that this method is most practical at relatively low frequencies. However, the computational burden is relaxed somewhat if one is willing to limit the angular aperture propagated (e.g., for long range propagation in deep water, after stripping of bottom paths has occurred). In that case, since increasing mode number corresponds roughly to increasing angle, fewer modes need to be computed. Range-independent normal modes will be discussed more fully in Sections 5.3 and 5.4.

For range-dependent problems, the modal approach can still be used, but now the ODEs are coupled and we obtain *coupled mode equations*, a system of ODEs that must be solved simultaneously, of the form

$$\frac{d}{dr}\psi_n = \sum_m b_{nm}(r)\,\psi_m \tag{4-7}$$

where the coupling coefficients b_{nm} typically involve integrals of the product of normal modes n and m (i.e., ϕ_m and ϕ_n), or perhaps their derivatives, and variational functions of the environment, such as sound speed fluctuations. Unfortunately, much of the advantage in computational efficiency of range-independent normal modes is now lost; it will depend on particular considerations of acoustic frequency, propagation phenomena being addressed (e.g., backscatter/reverberation, which standard PE cannot compute), and environmental inputs as to whether this approach is helpful in a particular situation. Short of full coupling, however, slow range dependence can be treated efficiently via *adiabatic mode theory* in which the mode shapes themselves are allowed to change with range, but there is no cross coupling of energy among the modes (i.e., energy in mode number m stays in mode number m). These ideas will be discussed more fully in Sections 6.3 and 6.4.

The direct wave equation solutions mentioned above are numerically most appropriate for low frequencies; as frequency increases, the finer and finer spatial discretization required to resolve the acoustic wavelength imposes an increasing computational burden. Fortunately, in the limit of high acoustic frequency, *ray theory* offers an asymptotic approximation to the wave equation that greatly simplifies the solution. Ray-theoretic methods will be discussed in Sections 5.1, 5.2, 6.1, and 6.2. Other methods such as the Fast Field Program (FFP) that are effective at high frequencies are discussed in Section 5.5.

4.5 Time-dependent (broadband) wave equations: approaches

The emphasis of our discussion so far has been on solutions to the time-independent (or Helmholtz) wave equation derived by assuming a harmonic (CW) source and pressure field. Both active and passive sonar applications, however, deal with time-dependent, broadband sources. That is, we need solutions to Eq. (4-1) which do *not* assume that p and s have the harmonic time dependence $e^{i\omega t}$. There are two fundamental approaches to this problem:

(1) A Fourier transform of Eq. (4-1) from time to frequency space. The transformed pressure $P(x,y,z,\omega)$ satisfies Eq. (4-2) with the right-hand side A equal to the source spectrum, i.e, the transform $S(x,y,z,\omega)$. Thus, if Eq. (4-2) is solved for an appropriate set of discrete frequencies, the results at a particular field point (x,y,z) can then be inverse transformed to recover p(x,y,z,t), the pressure time series at (x,y,z).

(2) A direct time-domain solution of Eq. (4-1), or of Eq. (4-1) with parabolic approximations for the spatial variables. Just as for the single-frequency solutions discussed in Section 4.4, a parabolic approximation allows a much more numerically efficient solution to the spatial part of the wave equation, as described, e.g., by Collins (1988, 1989). On the other hand, for accurate results near the source, where steep angles dominate, the parabolic approximation should be avoided. However, in that case it is now feasible on advanced computers to solve Eq. (4-1) directly [e.g., see Birkhoff (1985)], since only a region confined near the source must be discretized.

Theoretically, these two approaches are equivalent. In practice, however, most broadband models are of the first type, which allows a synthesis of single-frequency computer codes that have already been thoroughly tested and evaluated. Not only is the additional coding required for broadband calculations much less, but the underwater community has many years of experience with the single-frequency codes. The question remains as to which of these two general approaches is computationally more efficient.

4.6 Stochastic wave equations

The above discussion has assumed implicitly that for any application of a model to a real ocean problem, the environmental inputs are known exactly. In practice, this is never literally true, but three assumptions are made:

(1) The difference between the inputs given to the model and the real ocean environment are small at the discrete spatial (or temporal) points where inputs are given.

(2) These discretized points sample space (or time) on a scale appropriate to all of the following: (a) acoustic wavelength; (b) the rate of real environmental variation; (c) the scales

on which the important mechanisms of acoustic propagation are operating; and (d) the numerical algorithm being used by the model to solve the wave equation.

(3) The difference between the solution to the approximate problem, as given by the model, and the solution to the real-ocean problem is small.

The third assumption, given that the first is true, is intimately related to the requirement for a mathematically well-posed problem, namely, that the solution of a PDE must depend continuously on the initial and/or boundary conditions. [An example of an ill-posed problem is given on p. 74 of Chester (1971).]

While informed modelers are unlikely to formulate a problem that is literally ill-posed, significant quantitative errors in inputs to a well-posed problem can still result in significant quantitative errors in the output. These errors can occur not only because of literal measurement error at given points, but because of inadequate spatial or temporal sampling of the environment. Indeed, in many cases it is physically impossible, or impractical, to sample the environment on the scale that would be required. For example, sound speed fluctuations caused by oceanic internal waves can hardly be sampled continually (at least every few minutes) on a vertical scale of a few meters, and on a horizontal scale of at most a few hundred meters, for every propagation path along which predictions are daily desired by the community. As another example, direct measurements of subbottom properties (e.g., Deep Sea Drilling Project) are difficult and expensive to carry out, and indirect measurements have hardly been done on spatial scales, and over geographic areas, to provide model inputs required for a precise deterministic calculation.

Thus, if such environmental variations are of concern quantitatively, they must be modeled statistically. One can, of course, simply draw a single realization of the environment, run a deterministic propagation model once, and assume that the result is typical. If the variations are relatively significant, however, it is safer to perform a Monte Carlo experiment, drawing perhaps 10 or 100 realizations, running the propagation model that many times, and forming appropriate sample statistics from the outputs. Another possibility is to use a *stochastic model*, which purports to solve a modified wave equation *once*, solving directly for statistical moments of the acoustic pressure field. An example of this approach can be found

in Dozier and Tappert (1978) for propagation through random internal wave fields. It is not our purpose in this notebook to discuss stochastic models in detail, but simply to note that for some problems the stochastic approach may be required.

4.7 Notes for Section 4

Note 4-1: With density, ρ, included the wave equation becomes:

$$\rho \nabla \cdot (\frac{1}{\rho} \nabla p) - c^2 \frac{\partial^2 p}{\partial t^2} = s$$

Note 4-2: As is usual, in cartesian coordinates,

$$\nabla = (\frac{\partial}{\partial x}, \frac{\partial}{\partial y}, \frac{\partial}{\partial z})$$

represents the gradient operator and "$\nabla\cdot$" the divergence.

Then, also,

$$\Delta = \nabla \cdot \nabla = \nabla^2 = (\frac{\partial^2}{\partial x^2} + \frac{\partial^2}{\partial y^2} + \frac{\partial^2}{\partial z^2}),$$

the Laplacian operator in cartesian coordinates.

Note 4-3: Wave Equations in cartesian and cylindrical coordinates:

	Cartesian Coordinates	Cylindrical Coordinates
Acoustic Wave Equation	$\frac{\partial^2 p}{\partial x^2} + \frac{\partial^2 p}{\partial y^2} + \frac{\partial^2 p}{\partial z^2} - \frac{1}{c^2}\frac{\partial^2 p}{\partial t^2} = s$	$\frac{1}{r}\frac{\partial}{\partial r}(r\frac{\partial p}{\partial r}) + \frac{1}{r}\frac{\partial^2 p}{\partial \phi^2} + \frac{\partial^2 p}{\partial z^2} - \frac{1}{c^2}\frac{\partial^2 p}{\partial t^2} = s$
Reduced (Helmholtz) Wave Equation	$\frac{\partial^2 P}{\partial x^2} + \frac{\partial^2 P}{\partial y^2} + \frac{\partial^2 P}{\partial z^2} + \frac{\omega^2}{c^2} P = A$	$\frac{1}{r}\frac{\partial}{\partial r}(r\frac{\partial P}{\partial r}) + \frac{1}{r^2}\frac{\partial^2 P}{\partial \phi^2} + \frac{\partial^2 P}{\partial z^2} - \frac{\omega^2}{c^2} P = A$

5. PHYSICS -- RANGE-INDEPENDENT ENVIRONMENTS

This section addresses the most common methods for solving the acoustic wave equation in a special type of environment: one that does not change along the route from source to receiver. It is because of this range-independence of the environment that these solutions are possible. We first consider ray theory (and modifications of it), then mode theory, and finally fast-field and multipath-expansion approaches.

5.1 Basic Ray Theory

Because the ray approach provides a visualization for acoustic propagation, consider here some distinctive features of ray propagation. Suppose that rays are emitted from a source at the axial depth. The so-called RR (refracted--refracted) rays are emitted at angles sufficiently shallow so that by Snell's Law they repeatedly turn within the channel, hitting neither the surface nor the bottom. The RSR (refracted--surface reflected) rays leave the source at angles steep enough to hit the surface but not the bottom. Finally, the RSRBR (refracted -- surface reflected -- bottom reflected) rays hit both surface and bottom. The RSRBR rays will usually be attenuated by repeated bottom interaction and will not contribute significantly to the propagation at long range. The RR and perhaps RSR rays, however, can propagate to remarkably long range at low frequencies where volume attenuation is negligible; indeed, the field of underwater acoustics began just after World War II when axial propagation was observed experimentally at a range of several thousand km, and theory had to be developed to explain the phenomenon.

Ducted propagation can occur to long range as well. Energy emitted at small angles from a source in a surface duct is trapped in the duct because of the upward refracting positive sound speed gradient there. Rough surface scattering can scatter some of the energy into angles steep enough to escape the duct, and there is some diffractive leakage out of the duct, but overall, surface ducts are quite efficient at trapping and propagating acoustic waves.

In deep water, the RR and RSR rays from a near-surface source are focused by refractive effects to form convergence zones approximately every 30 nm, or 50 km. A dominant feature of a convergence zone is the caustic, where rays that were initially adjacent

at the source converge. Typically, the caustic, being a focal surface, is bounded on one side by a shadow zone, a low-intensity region where initially adjacent rays diverge. Thus, the ray density becomes infinite at a caustic, but is zero in shadow zones. In the limit of high frequency, the caustic forms a sharp boundary, but at any finite (physically real) frequency diffraction smears this boundary and there is leakage of acoustic intensity into the shadow zone region; this leakage typically becomes important only at relatively low frequencies, say below 200 Hz. Thus, basic ray theory, which is valid in the high frequency limit, must be modified to include diffractive effects at low frequency. We defer discussion of these diffractive corrections until the next section.

We next consider a brief mathematical review of ray theory, with the simplest case of single-frequency plane-wave propagation through an idealized, isovelocity ocean with no boundaries. If c_0 is the sound speed and ω is the acoustic (angular) frequency, then with $k_0 = \omega/c_0$ the reduced wave equation (4-2) takes the form

$$\frac{\partial^2 P}{\partial x^2} + \frac{\partial^2 P}{\partial y^2} + \frac{\partial^2 P}{\partial z^2} + k_0^2 P = 0 \qquad (5\text{-}1)$$

where there is no explicit source term on the right hand side since the plane waves do not emanate from a finite region of space. Indeed, it is easy to verify that solutions to Eq. (5-1), including now the time factor via $p(x,y,z,t) = P(x,y,z,\omega)\, e^{i\omega t}$, are

$$p(x,y,z,t) = Ae^{ik_0 S^+(x,y,z) - i\omega t} + Be^{ik_0 S^-(x,y,z) - i\omega t} \qquad (5\text{-}2)$$

$$= Ae^{ik_0(S^+ - ct)} + Be^{ik_0(S^- - ct)}$$

where S^+ and S^- are unit vectors

$$S^{\pm}(x,y,z) = \pm(\alpha x+\beta y+\gamma z) \tag{5-3}$$

with $\alpha^2+\beta^2+\gamma^2=1$. Each such solution p is a *plane wave*; its amplitude A and direction of propagation defined by (α,β,γ) are constant throughout space. The constant phase fronts are planes normal to this direction, i. e., the phase is constant for values of x,y,z,t with S-tc constant. Hence, for any fixed point in time, the wave front is described by

$$S^{\pm}(x,y,z) = \pm(\alpha x+\beta y+\gamma z) = constant\ , \tag{5-4}$$

the equation of a plane.

When two or more plane waves are added together, the result is still a solution of Eq. (5-1), since that PDE is linear. Thus, we can easily generate generalized plane wave solutions of the form

$$p(x,y,z,t) = \sum_{n=1}^{N} A_n e^{ik_0 S_n(x,y,z)-i\omega t} \tag{5-5}$$

but now the constant phase fronts are no longer planes. In fact, we can even replace the sum in Eq. (5-5) with an integral to get a continuous sum of plane waves. Such generalized integral solutions are required to describe some of the complex fields due to point sources.

It is instructive to consider spherical waves, illustrated by the case of a point source introduced into our idealized ocean with no boundaries. In three spatial dimensions, the result is a solution spherically symmetric about the source position, as can be seen by rewriting the hyperbolic wave equation (4-1) in spherical coordinates [again assuming only radial (no transverse) propagation] as

$$\frac{1}{r^2}\frac{\partial}{\partial r}r^2\frac{\partial}{\partial r}p(r,t)+k_0^2\,p\;=\;0 \qquad (5\text{-}6)$$

or

$$\frac{\partial^2 p}{\partial r^2}+\frac{2}{r}\frac{\partial p}{\partial r}+k_0^2 p\;=\;0$$

for r>0, where r is the radial coordinate. At first glance, this equation appears significantly more complicated than Eq. (5-1), because the coefficient of p' is not constant even though the sound speed c is still assumed constant. However, substituting p(r,t)=U(r,t)/r into Eq. (8) yields an elementary one-dimensional wave equation for U,

$$\frac{d^2U}{dr^2}+k_0^2U\;=\;0 \qquad (5\text{-}7)$$

which is easily solved and yields solutions for p(r,t) as

$$p(r,t)\;=\;\frac{A}{r}e^{i(k_0r-\omega t)}+\frac{B}{r}e^{-i(k_0r-\omega t)} \qquad (5\text{-}8)$$

The first term represents a wave moving out from the source (increasing r), while the second term represents a wave moving back. The constant phase fronts are spheres centered at the origin (the source point). The rays are straight radial lines emanating from the origin, but unlike the pure plane wave case above, they are no longer parallel to each other; rather, they converge toward a focus at the origin and diverge towards infinity. Also, the amplitudes are no longer constant, but vary like 1/r, becoming infinite at the origin and decaying to zero at infinity. In practice, we usually impose a *radiation condition* (an additional mathematical requirement, similar to a boundary condition) to eliminate the second term in Eq. (5-8) and include only waves emanating from the source.

The real ocean is best treated in cylindrical coordinates with boundaries at the surface and bottom. Unlike the elementary unbounded case in spherical coordinates, the cylindrical result, even for an isovelocity ocean, is not nearly so easy to write down, rather than being expressible in terms of exponentials and inverse powers of r, the result is a sum of cylindrical Bessel functions which behave like 1/r (spherical spreading) near the source, but eventually decay like $1/\sqrt{r}$ (cylindrical spreading).

The real ocean is also, of course, not isovelocity. However, we can generalize our above results if the acoustic waves, while not plane, behave locally like plane waves. In that case we can derive ray theory under the assumption that there does in fact exist a local wavefront to which the rays are orthogonal. The ray paths themselves can be traced independently of acoustic frequency, but only at relatively high acoustic frequency will the approximately plane wavefronts exist. Indeed, the existence of such wavefronts requires that the amplitude and direction of the wave remain almost constant over distances of the order of an acoustic wavelength λ; intuitively, for smaller λ (i.e., for higher frequency) it is "easier" for this requirement to be satisfied; in the limit of $\lambda=0$, or infinite frequency, it is satisfied exactly. Thus, at any finite frequency, ray theory gives an approximate solution to the wave equation that is valid asymptotically in the limit of infinite frequency.

Mathematically, we sketch the derivation below [more details can be found, for example, in Boyles (1984) or in Ahluwalia and Keller (1977)]. We assume that the acoustic pressure P (along one ray path, it will turn out) has the form [compare to Eq. (5-2)]

$$P(x,y,z) = A(x,y,z)e^{ik_0 S(x,y,z)} \tag{5-9}$$

where S(x,y,z) and A(x,y,z) vary with position and are to be found. Now substitute into the reduced wave equation, i.e., Eq. (5-1) modified to include a depth-variable sound speed c(z):

$$\frac{\partial^2 P}{\partial x^2}+\frac{\partial^2 P}{\partial y^2}+\frac{\partial^2 P}{\partial z^2}+k^2(z)P = 0 \qquad (5\text{-}10)$$

where $k(z)=\omega/c(z)$. Since A and S are assumed real, we get two equations when we separate the results into real and imaginary parts. One of the equations can be written as

$$\left(\frac{\partial S}{\partial x}\right)^2+\left(\frac{\partial S}{\partial y}\right)^2+\left(\frac{\partial S}{\partial z}\right)^2-n^2 = \frac{\lambda_0^2}{4\pi^2 A}\left[\frac{\partial^2 A}{\partial x^2}+\frac{\partial^2 A}{\partial y^2}+\frac{\partial^2 A}{\partial z^2}\right] \qquad (5\text{-}11)$$

where $c_0=\omega/k_0$ is the minimum sound speed over depth, the index of refraction $n(z)=c_0/c(z)$, and the wavelength $\lambda_0=2\pi/k_0$. Taking the infinite frequency limit $\lambda_0=0$, we obtain what is known as the *eiconal* (or *eikonal*) equation for the phase S(x,y,z):

$$\left(\frac{\partial S}{\partial x}\right)^2+\left(\frac{\partial S}{\partial y}\right)^2+\left(\frac{\partial S}{\partial z}\right)^2 = n^2 \qquad (5\text{-}12)$$

Directly from this equation can be derived the ray equations, which describe the trajectories (x(s),y(s),z(s)) of ray paths given an initial position (x_0,y_0,z_0). They are independent of frequency since we have already passed to the infinite frequency limit. Actually, up until this point our derivation would hold even for a range-dependent sound speed c=c(r,z), but the ray equations greatly simplify if we assume c=c(z) only.

The condition for the ray theory solution to yield a good approximation to the true wave equation solution can be found by analyzing the conditions needed for Eq. (5-12) to be a good approximation to Eq. (5-11). Specifically, we need the right hand side of Eq. (5-11) to be much less than the left hand side of Eq. (5-12). A somewhat lengthy derivation, which also uses the other separated equation obtained along with Eq. (5-11), leads to three conditions:

$$\lambda_0 \frac{A'}{A} < 1 \qquad (5\text{-}13)$$

$$\lambda_0 n' \ll n^2 \approx 1 \tag{5-14}$$

$$\lambda_0 S'' \ll 1 \tag{5-15}$$

where a prime means a spatial derivative. These mean, respectively, that the spatial change in ray amplitude (A), index of refraction (n), and ray curvature (S") must each be small relative to a wavelength (λ).

Let us return to the ray equations, which describe a ray path (x(s),y(s),z(s)), with s the arc length along a ray. When c=c(z), a range-independent environment, the ray equations show that ray paths cannot refract out of a vertical plane, which without loss of generality we take to be the x-z plane. Indeed, in this case the ray equations reduce to

$$\frac{d}{ds}\left(n\frac{dz}{ds}\right) = \frac{dn}{dz} \tag{5-16}$$

$$n\,\frac{dx}{ds} = constant \tag{5-17}$$

Since dx/ds=cosθ with $\theta=\theta(s)$ the local angle of the path x(s) from the horizontal (we take $\theta>0$ for angles below the horizontal, since we take z increasing downward),

$$\frac{\cos\theta}{c} = \frac{1}{c_n} = K_n \equiv constant \tag{5-18}$$

where c_n is the sound speed at the ray turning point (when $\theta=0$ and the ray is horizontal). The ray parameter K_n is constant along a given ray but varies from ray to ray. Eq. (5-18) is Snell's Law and is fundamental to any analysis of propagation effects. For example, given a sound speed profile, the depth of the water column, and a source depth, we can immediately calculate the minimum angle at which rays must leave the source in order to strike the water-sediment (or water-rock) interface. If we can design an active source which emits energy only at angles shallower than this minimum, then we can avoid local bottom reverberation

altogether. As another example, for a source in a duct underlying a rough sea surface, if we know the scattering kernel (i.e., angular scattering properties) of the surface, we can compute the minimum scattered angle needed to escape the duct, and thereby estimate how rapidly in range acoustic energy will be scattered out of the duct.

From Eq. (5-16) can be derived the relationship

$$\frac{d\theta}{ds} = -K_n \frac{dc}{dz} \tag{5-19}$$

i.e., the ray curvature $d\theta/ds$ is proportional and of opposite sign to the sound speed gradient dc/dz. This formula expresses the ray bending that traps sound in a channel or in a duct. For example, as the sound speed increases with increasing z, so that $dc/dz>0$, the ray angle is decreasing, which by our sign convention means that the ray is turning upward.

Elementary analysis of Snell's Law, Eq. (5-18), yields several quantities useful in ray interpretations of acoustic propagation; the results are obtained entirely in terms of c(z) and the ray constant K_n, i.e., one must give the angle at which a ray passes through any depth along its path. For example, the acoustic travel time along a ray path can be found by integrating the elementary expression $dt=ds/c$, and path length can be found by integrating $ds=dz/\sin\theta$. These integrals can be evaluated in closed form for certain simple c(z); e.g., a constant gradient sound speed profile yields ray paths that are arcs of circles. For this reason, many ray trace models (including MPP and ASTRAL) use a simple fit (e.g., piecewise linear, or possibly a polynomial fit) to a real sound speed profile and piece together the total ray path from segments that are elementary solutions, such as the circular arcs just mentioned. Although false caustics and other anomalies can occur using the linear fit [cf Pedersen (1961) and Pedersen and Gordon (1967)], results from using it have generally proven to be accurate when compared with experimental data. Nonlinear fits to the sound speed profile generally require a much finer discretization of the profile and a large increase in computer time that is not justified by the small increase in accuracy obtained.

It is now clear that the original formulation, Eq. (5-9), for the pressure P provides for a single ray path. To construct the ray representation of the total acoustic pressure at a field

point $\underline{x}$ according to geometrical acoustics, we must follow the steps outlined in Section 6.2 of Ahluwalia and Keller (1977):

1. Determine all of the rays (eigenrays) connecting source to receiver $\underline{x}$, including the direct path, the rays singly or multiply refracted in the sound channel, and the rays reflected any number of times at the surface and bottom. In practice, one might include only two or three bottom reflections because of loss occurring with each bottom interaction.

2. Calculate the path length S_j along each eigenray from source to receiver.

3. Calculate the amplitude A_j of the field on the j^{th} ray at the receiver. This involves reflection coefficients at the boundaries, phase changes at caustics, and conservation of energy within a ray tube. It is the most difficult part of actually obtaining the total acoustic pressure field (far harder than merely tracing rays), and necessitates modifications to ray theory discussed in the next section.

4. Finally, sum the field on each path (eigenray) to obtain the pressure field:

$$P(\underline{x}) = \sum_j A_j(\underline{x}) e^{ik_0 S_j(\underline{x})} \tag{5-20}$$

5.2 Extensions of Ray Theory

The discussion in the previous section did not include details about the computation of the ray amplitude A. It turns out that mathematically this is the most difficult part of actually obtaining the pressure field. We assume a representation for the amplitude A along any path that is valid asymptotically at high frequency (i.e., as $k_0=2\pi f/c_0 \rightarrow \infty$):

$$A(\underline{x}) = A_0(\underline{x}) + \frac{A_1(\underline{x})}{(ik_0)} + \frac{A_2(\underline{x})}{(ik_0)^2} + \ldots \tag{5-21}$$

Here the subscripts on A do not refer to ray path number, as they did in Subsection 5.1, but to the order of the coefficient in this asymptotic series. In the high frequency limit all terms in inverse powers of (ik_0) vanish, and we are left with only the leading term A_0. Next, we use this representation for A in the formulation for the pressure P along a ray path given in Eq. (5-9), and substitute into the reduced wave equation (5-10). If we then set the coefficient of each power of (ik_0) equal to zero, we obtain a hierarchy of equations for S and the A_n:

$$\nabla S \bullet \nabla S - n^2(\underline{x}) = 0 \tag{5-22}$$

$$2\nabla A_0 \bullet \nabla S + A_0 \Delta S = 0 \tag{5-23}$$

$$2\nabla A_n \bullet \nabla S + A_n \Delta S = -\Delta A_{n-1}, \quad n=1,2,\ldots \tag{5-24}$$

where, as usual, ∇ is the gradient operator and Δ the Laplacian. Eq. (5-22) is simply the eiconal equation which we derived earlier in Eq. (5-12). Eqs. (5-23) and (5-24) for the A_n are the *transport equations.* Once the phase S has been found by solving the eiconal equation (by solving the ray equations, as described in the previous section), the transport equations can be solved recursively, first for A_0 using S, then for A_1 using A_0 and S, etc.

Consider, for example, how the elementary cases which we solved in the previous section can be recovered by solving Eq. (5-23) for A_0. Substituting the plane wave phase S given by Eq. (5-4) into Eq. (5-23), since $\Delta S=0$,

$$\alpha\frac{\partial A_0}{\partial x} + \beta\frac{\partial A_0}{\partial y} + \gamma\frac{\partial A_0}{\partial z} = 0 \tag{5-25}$$

which has as a solution A_0=constant. In fact, going on to solve Eq. (5-24), each A_n, n>0, can also be taken as constant, and we recover our earlier result that plane waves with constant amplitudes are solutions of the wave equation. Similarly, for the point source in a spherically symmetric isovelocity ocean without boundaries, Eq. (5-6), since the index of refraction n=1, we have

$$\nabla S \cdot \nabla S = \left(\frac{\partial S}{\partial r}\right)^2 = n^2 = 1 \tag{5-26}$$

with solutions simply S(r) = r and S(r) = -r. Choosing the outgoing wave S(r) = r, we find that Eq. (5-23) gives for A_0,

$$2\left(\frac{\partial A_0}{\partial r}\right)(1) + A_0\left(\frac{2}{r}\right) = 0, \tag{5-27}$$

with solution A_0=a/r, where a is a constant. Then since $\Delta A=0$ for r>0, we find from Eq. (5-24) that A_n can be taken as zero for n>0, and we have recovered the first term (outgoing wave) of Eq. (5-8).

In the above two examples there is no refraction and the rays are straight lines. For real oceans with non-constant sound speeds, the ray bending introduces special phenomena, such as caustics and convergence zones, which we mentioned earlier. The caustic is a focal surface at which geometrical acoustics, as expressed by Eqs. (5-22) to (5-24) above, fails because the leading amplitude term A_0 is singular. The simplest caustic is a smooth caustic characterized by two rays, one of which has touched the caustic and a second which has not. [Higher order caustics characterized by more than two rays, e.g., the cusped caustic, can occur but will not be discussed here.] Also, on one side of the smooth caustic is a region into which no rays penetrate (the shadow zone). It is filled only by diffractive leakage, negligible except at low frequencies.

The practical problem, then, is how to compute the acoustic field at a caustic. The simple exponential function chosen for the geometrical acoustics formulation, Eq. (5-9), does not have the property of decaying sharply into a shadow zone. The remedy, then, is to choose a different functional form. First Brekhovskikh (1960) and then Kratsov (1964) and Ludwig

(1966, 1968) observed that the Airy function does have a sharp transition from oscillatory to exponentially decaying behavior, and introduced a formulation based on the Airy function which correctly models a smooth caustic. The mathematical details are beyond the scope of this notebook, but the approach is used in a number of ray models (e.g., FACT and MPP) for computation of acoustic fields near caustics. The exponential part of the Airy function models the illuminated region on one side of the caustic, and the decaying part of the Airy function models the shadow zone on the other side.

5.3 Normal Mode Theory -- Purely Discrete Spectrum

Normal mode theory was used in the earliest theoretical investigations of sound and vibration, and then in the early days of underwater acoustic research. The framework was already well laid out in 1945 in *Physics of Sound in the Sea*, and in 1948 Pekeris published a theory for a simple two-layer model of isovelocity ocean and (in general, different) isovelocity sediment. Today there are a number of very good normal mode models in use in the underwater acoustics community which adapt the original methods to more realistic and detailed descriptions of the ocean and sediment.

In Section 4.4 we mentioned that normal mode theory arises naturally from the method of separation of variables to solve the reduced wave equation. Here we briefly review this method for Eq. (5-10) written in cylindrical coordinates (r-z geometry) and assuming that p is independent of the transverse variable ϕ (see Note 4-3):

$$\frac{\partial^2 P}{\partial r^2} + \frac{1}{r}\frac{\partial P}{\partial r} + \frac{\partial^2 P}{\partial z^2} + k^2(z)\,P = 0, \quad r>0 \tag{5-28}$$

Let us assume that this equation holds in the semi-infinite strip $0<r<\infty$, $0\le z\le H$, where $z=H$ is the flat bottom of the water column and $z=0$ is the flat ocean surface. For the moment we do not include any sediment in our model and suppose that the pressure P satisfies the following boundary conditions:

1. The ocean bottom is perfectly rigid and totally reflecting:

$$\frac{\partial P}{\partial z}(r,H) = 0 \tag{5-29}$$

2. The ocean surface is pressure release:

$$P(r,0) = 0 \tag{5-30}$$

3. The acoustic wave should be outgoing from the source at r=0; i.e., P satisfies an *outgoing radiation condition* as r→∞, as referred to earlier in Section 5.1.

If we now assume that the pressure P can be factored into a function of r times a function of z,

$$P(r,z) = \psi(r)\phi(z) \tag{5-31}$$

and substitute for P in Eq. (5-28), and divide both sides by the product $\psi\phi$, we obtain

$$\frac{1}{\psi}\frac{d^2\psi}{dr^2}+\frac{1}{r}\frac{1}{\psi}\frac{d\psi}{dr} = -\left(\frac{1}{\phi}\frac{d^2\phi}{dz^2}+k^2(z)\right) = constant \tag{5-32}$$

Since the terms in ψ are a function only of r and not z, and the terms in ϕ are a function only of z, both sides of the equation must equal a constant. We have thus separated the original equation (5-28) into two ordinary differential equations, each of which can be solved much more simply than Eq. (5-28). Setting the constant in Eq. (5-32) equal to $-\lambda^2$ (physically, λ is a horizontal wavenumber), the two equations become:

$$\psi''(r) + \frac{1}{r}\psi'(r) + \lambda^2\psi(r) = 0 \tag{5-33}$$

$$\phi''(z) + (k^2(z)-\lambda^2)\phi(z) = 0 \tag{5-34}$$

The key to our ability to perform the separation of variables and simplify the PDE to two ODEs is the separability of k: $k^2(r,z)=k_2^2(r)+k_1^2(z)$, or in our case simply $k^2(r,z)=k^2(z)$. Likewise the boundary conditions must be separable, to apply to Eqs. (5-33) and/or (5-34). In this case Eqs. (5-29) and (5-30) directly yield

$$\frac{d\phi}{dz}(H) = 0 \tag{5-35A}$$

$$\phi(0) = 0 \tag{5-35B}$$

Now the outgoing radiation condition on ψ in Eq.(5-33), which is Bessel's equation of order zero, gives solutions of the form (see Note 5-1).

$$\psi(r) = H_0^{(1)}(\lambda r) \tag{5-36}$$

where H_0 is the Hankel function, with no restriction on λ.

Notice now that Eq. (5-34) with boundary conditions given by Eqs. (5-35) is a classical Sturm-Liouville eigenvalue problem (Note 5-2) in which the values of λ are restricted to a discrete set. Let

$$\gamma = 1-\frac{\lambda^2}{k_0^2}\ ; \qquad V(z) = 1-n^2(z) \tag{5-37}$$

so that Eq. (36) can be recast as

$$\phi''(z) + k_0^2[\gamma - V(z)]\,\phi(z) = 0 \tag{5-38}$$

since $k(z)=k_0n(z)$. Eq. (5-38) is self-adjoint [Note 5-3] on a finite interval, so that the spectrum (the set of eigenvalues γ for which Eq. (5-38) and the boundary conditions, Eqs. (5-35), can be satisfied) is real and discrete. Moreover, since Eq. (5-38) is a classic Sturm-Liouville equation, there are infinitely many eigenvalues $\gamma_0 < \gamma_1 < \gamma_2 < \ldots$, and $\gamma_n \to \infty$ as $n \to \infty$. For the n^{th} eigenvalue, the corresponding eigenfunction, denoted by ϕ_n, has exactly n distinct nodes

(zeros) in the interval (0,H). These oscillations will occur within subintervals of (0,H) where $\gamma - V(z) > 0$, since in those regions the eigenfunction will behave roughly like a real solution of

$$\phi''(z) + d^2\,\phi(z) = 0, \quad d=constant > 0 \tag{5-39}$$

i.e., ϕ will be oscillatory of the form

$$\phi(z) = A\cos dz + B\sin dz, \quad A,\ B\ constants \tag{5-40}$$

On the other hand, in the regions where $\gamma - V(z) < 0$, ϕ will behave roughly like a real solution of

$$\phi''(z) - d^2\,\phi(z) = 0, \quad d=constant > 0 \tag{5-41}$$

i.e., ϕ will be exponential of the form

$$\phi(z) = Ce^{dz} + De^{-dz}, \quad C,\ D\ constants \tag{5-42}$$

where either C=0 or D=0. For example, if ϕ is not oscillatory near the surface, it must increase exponentially as z increases from 0 (going down into the water), so D=0. More generally, since the exponential function does not vanish, ϕ cannot have nodes, or zero crossings, in these regions of exponential behavior.

In underwater acoustics, the eigenfunctions ϕ_n are the *normal modes.* They are solutions to a one-dimensional wave equation, Eq. (5-34) or Eq. (5-38), which is analogous to the equation of a vibrating string. The normal modes correspond directly to the discrete modes of vibration of the string. The position where the string is plucked corresponds to the source depth in the water, and that depth determines the extent to which each normal mode is excited. If a mode vanishes at the source depth, that mode is not excited at all.

There is also a strong analogy between normal modes and the ray acoustics discussed earlier in Section 5.1. Points in depth where $\gamma = V(z)$, i.e., where the behavior of ϕ changes character between exponential and oscillatory, are called *turning points*, by analogy with the ray which turns by refraction in the water column at this turning point depth. The normal mode

is exponentially decaying outside regions bounded by turning points, corresponding to the ray being unable to penetrate that region.

By equation (5-36), and the asymptotic expansion of $H_o^{(1)}$, each mode (n) propagates with horizontal wavenumber λ (n), traditionally called k_n, so that

$$k_n = k_0\sqrt{1-\gamma_n} = \lambda_n \tag{5-43}$$

Since k_n is the projection of the nth mode's wavenumber onto the horizontal, it makes sense to define an "equivalent" ray angle

$$\theta_n = \arccos\left(\frac{k_n}{k_0}\right) \tag{5-44}$$

where $k_o = \omega/c_o$ and c_o is the sound speed minimum. By Snell's law

$$\frac{\omega}{c_n} = k_n = k_o\cos\theta_n = \frac{\omega}{c_o}\cos\theta_n \tag{5-45}$$

implies that θ_n is the angle which the ray equivalent makes with the horizontal at the axis depth where $c(z)=c_o$. Likewise, the ray's turning point occurs at the depth where $c(z)=c_n$.

For only finitely many n will there be a real angle θ_n given by Eq. (5-44), since as we have seen, $\gamma_n \to \infty$ as $n \to \infty$, so that the argument of the square root in Eq. (5-43) ultimately becomes negative. Physically, this corresponds to the fact that there are only a finite number of propagating modes; the remainder are referred to as *evanescent modes*, which decay rapidly away from the source and usually are neglected. Now again by Sturm-Liouville theory, the modes form a *complete set*, meaning that the total acoustic pressure can be written as a sum over all the modes, as a generalization of Eq. (5-31). Neglecting the evanescent modes, we have

$$P(r,z) = \sum_{n=1}^{N} d_n H_0^{(1)}(k_n r)\, \phi_n(z) \qquad (5\text{-}46)$$

where we have used the specific horizontal wavenumber k_n in place of λ in substituting Eq. (5-36) into Eq. (5-31), and where the complex constants d_n depend on the source function; for a point source at depth z_s, they are proportional to the excitation $\phi_n(z_s)$ of mode n at the depth z_s. Thus, a mode which has a null at the source depth will not contribute to the total pressure at any range if the environment is range-independent (no mode coupling).

In the far field, we can use the asymptotic expansion of the Hankel function to rewrite Eq. (5-46) as

$$P(r,z) = \frac{1}{\sqrt{r}} \sum_{n=1}^{N} \frac{b_n}{\sqrt{k_n}} \phi_n(z) e^{ik_n r} \qquad (5\text{-}47)$$

where the b_n are complex constants (simple modifications of the d_n). Now the cylindrical spreading factor $r^{-1/2}$ is evident. As a technical aside, we note that the sign of k_n in the phase, implicitly taken as positive in the above discussion, should be related to the sign of ω in the suppressed time factor in such a way as to give a wave outgoing from the source. With the wavenumber $k_n > 0$, we should take the time factor as $e^{-i\omega t}$ in writing the full expression for the single-frequency pressure field, i.e., $p(r,z,t) = P(r,z)e^{-i\omega t}$.

The Sturm-Liouville theory also guarantees us that the mode functions are *orthogonal*. In a medium of constant density, this means that if the mode functions have been normalized to unity, then

$$\int_0^H \phi_n(z)\, \phi_m(z) = \delta_{m,n} = \begin{cases} 1 \text{ if } m = n \\ 0 \text{ if } m \neq n \end{cases} \qquad (5\text{-}48)$$

Hence the product of two different modes ($m \neq n$) integrates to zero. For example, if the ocean is isovelocity and of constant density, modes will take the form of Eq. (5-40) or Eq. (5-42), and it is easily seen that solutions satisfying the boundary conditions in Eqs. (5-35) will satisfy the orthogonality condition. More generally, this condition has important analytical consequences

for derivations of range-dependent extensions to normal modes, as will be discussed further in Sections 6.3 and 6.4.

For most areas of the real ocean the simple hard bottom boundary condition given in Eq. (5-29) is not accurate. A more detailed geoacoustic model of the bottom can include refraction of sound through the sediments and back into the water column, as well as bottom loss which varies as a function of angle in accordance with measured data. Such a model can be introduced into a purely discrete normal mode model as a series of stratified layers in depth, with a different range-independent sound speed, density, and attenuation in each layer. There are then two fundamental ways in which the situation is more complicated than the simple hard bottom presented initially in Eqs. (5-28) to (5-30):

(1) Attenuation is introduced as a complex part of the acoustic wavenumber k(z) in Eq. (5-29). Strictly speaking, this means that the eigenfunctions and eigenvalues (horizontal wavenumbers) satisfying Eq. (5-34) are no longer real.

(2) The problem cannot be terminated immediately below the water column by a simple hard bottom condition, as in Eq. (5-29). Boundary conditions at bottom layer interfaces are much more complicated, either two-fluid boundary conditions (continuity of pressure and the normal component of particle displacement) or fluid-solid boundary conditions, involving shear and compressional waves. In addition, the depth at which the problem should be terminated is open to question.

Attenuation is usually treated by perturbation theory, as described, for example, in Section 4.1.4 of Boyles (1984). A small imaginary component is introduced into the wavenumber k(z), which is replaced in Eq. (5-28) by

$$k(z) + i\alpha(z) , \quad 0 < \alpha << k \tag{5-49}$$

The differences between the complex and real eigenfunctions are neglected, and only the first-order corrections to the squares of the eigenvalues are kept.

The perturbation treatment of attenuation does assume that $\alpha << k$. A simple attempt to terminate the eigenvalue problem with a highly absorbing layer of finite depth can easily violate this condition. More generally, a sediment layer with extremely high attenuation likewise can cause the perturbation approximation to give poor numerical accuracy. In deep water this normally will not matter very much; the modes that are too severely attenuated do not contribute much to the pressure field anyway, since it is dominated by non-bottom-interacting modes for which the value of α is immaterial. However, in shallow water, where nearly all of the modes are bottom interacting, a large value of α can cause the perturbation correction, computed as a depth integral involving α, to be so large that most of the modes are attenuated excessively, and transmission loss decays much too rapidly with range.

In such a shallow water case (or more generally), if bottom loss as a function of grazing angle is available in tabulated form (e.g., from measured data), one can simply convert the loss directly into modal attenuation factors, using the ray-equivalent angle, as given in Eq. (5-44). This avoids the perturbation method altogether, since the modal attenuations are already known. Of course, such an approach can lead to a serious misrepresentation of the modal phase (or ray beam displacement).

Much more expensive computationally is to attempt to solve the full complex eigenvalue equation directly. Numerical schemes to solve Eq. (5-34) with complex k(z), given λ, exist as straightforward modifications of their real counterparts. However, the root-finder (which must determine for which values of λ Eq. (5-34) should be solved) must now perform a two-dimensional search over complex λ-space, rather than a simple line search on the real λ axis. Whereas robust and efficient root-finders exist for the real problem, complex root-finders are error-prone and can easily fail to converge.

Returning now to the second issue raised above, i.e., the treatment of the bottom boundary conditions, we find that fluid-fluid boundary conditions at layer boundaries are much easier to treat numerically than the full elastic fluid-solid boundary conditions. For this reason many normal mode codes do not treat shear waves which can arise at fluid-solid interfaces. A description of the fluid-fluid boundary conditions and a numerical implementation of them can be found in Section 4.1.3 of Boyles (1984) or in Stickler (1975). A discussion of the fluid-solid boundary conditions and a numerical implementation of them can be found in Section 2.5 of Porter (1991) or in Porter and Reiss (1985).

It is also possible to include the effects of boundary roughness (e.g., a corrugated surface) by modifying the boundary conditions at the surface or bottom interfaces, while leaving those interfaces smooth. For example, if a tabulated complex reflection coefficient is available as a function of grazing angle, it can be implemented as an impedance boundary condition at the interface. As discussed in Section 2.6.5 of Porter (1991), a normal mode is viewed locally near the interface as a combination of up- and down-going (i.e., incident and reflected) plane waves as in Eq. (5-42). The relation between the constants A and B is given by the complex reflection coefficient. It is then straightforward to evaluate the impedance boundary condition at the interface. At the surface, for example, this new boundary condition would replace the usual pressure-release condition.

5.4 Normal Mode Theory -- Numerical Methods and Continuous Spectra

The question remains of where and how to terminate the model's domain in depth. Physically, there is no well-defined bottom depth and, in principle, we could continue to the center of the earth. As a practical matter, we justify stopping the numerical calculations when including additional depth makes little quantitative change in the result. Physically, this corresponds to attenuation being sufficient to eliminate any bottom returns via refraction or reflection.

From the standpoint of computational expense and numerical stability, we would like to terminate the problem as soon as possible. Numerical finite difference schemes, such as employed by Porter (1985, 1991), use a number of mesh points which is directly proportional to depth. Finite element methods such as employed by Stickler (1975) and Boyles (1984) require a discretization of the environment into horizontal layers; each normal mode is then computed as a linear combination of Airy functions in each layer. Although the number of layers is not directly proportional to depth, there is a restriction on the layer thickness in relation to the sound speed gradient in each layer. Even a constant gradient layer may have to be divided into sublayers, all with the same gradient. Hence, the total depth modeled in the problem can play a large role in determining computational expense.

Numerical stability also becomes a problem, especially for modes trapped near the sound channel axis, if the problem is modeled over a huge vertical extent. Except for the small vertical region between the modal turning points (one above and one below the axis depth),

these modes are exponentially decaying away from the axis. Numerical schemes such as mentioned above solve the eigenvalue equation by numerical integration. Not only is computational power wasted integrating through many orders of magnitude of these "worthless" exponential tails, but care is required to integrate "with the grain," i.e., in the direction in which the mode is exponentially increasing. Consider Eq. (5-42) with d>0 and z>0. If one incorrectly integrates in a direction such that the true solution

$$\phi(z) = Ce^{dz} + De^{-dz}$$

is exponentially decaying, so that C=0, then because of numerical roundoff C will be small but not precisely zero, and even a small coefficient multiplied by the exponentially increasing term e^{dz} will quickly dominate the true exponentially decreasing solution. One answer to this problem is *multiple shooting* methods, in which the integration is carried out from surface to axis and bottom to axis, with a matching of the two pieces of the solution at the axis. Multiple minima profiles may require multiple match points, however. Also, for modes trapped near the axis, the depths at which boundary conditions are imposed can be moved in toward the axis from surface and bottom, to reduce the computation of meaningless exponential tails; automating this process may not be easy. In any event, all of these integration methods work better and faster to the degree that the total depth of the modeled problem can be reduced.

Most models treat the problem in such a way that numerically no mesh points or layers are used below the sediment/basalt interface. One possibility is to terminate the problem with a rigid bottom as in Eq. (5-29), but with H now representing the depth of the sediment/basalt interface. This makes sense physically if there is a strong impedance contrast at this interface, but more typically basalts exhibit a strong elastic wave speed gradient which refracts ray paths upward, back toward the water column. Except at low frequencies, say below 50 Hz, or in very thin sediment areas, such energy will be severely attenuated during its passage back through the sediments and hence can be neglected in the water column; in that case the choice of boundary condition used at the sediment/basalt interface may make little difference. For low frequencies or thin sediments, however, imposing a complex reflection coefficient at the sediment/basalt interface is more realistic than using the rigid bottom.

A convenient way to do impose this reflection coefficient is to model a semi-infinite (in depth) half-space, of uniform sound speed c_b and density ρ_b, below the sediment/basalt

interface. The general solution of the acoustic pressure in the half-space is then of the form given in Eq. (5-42), with

$$d = \sqrt{\lambda^2 - \frac{\omega^2}{c_b^2}} \tag{5-50}$$

where λ is the eigenvalue in Eq. (5-34). The impedance boundary condition imposed on the numerical solution, which is computed only in the water and sediment, is then

$$p(H) + \frac{\rho_b}{\rho_s} d\, p'(H) = 0 \tag{5-51}$$

where ρ_s is the limiting density in the sediment as z→H from above, since the pressure and normal displacement must be continuous across the sediment/basalt interface at z=H.

Now, however, we have defined an eigenvalue problem on an infinite interval. By definition the problem is *singular* and does not have the properties of Eq. (5-38), defined on a finite interval [0,H] with boundary conditions given in Eqs. (5-35). There we saw that Sturm-Liouville theory gave us an infinite set of positive, discrete eigenvalues, i.e., a purely discrete spectrum. On an infinite interval, the spectrum will be at least partially continuous. Now in the previous paragraph, we appear to have converted an infinite half-space problem back to a finite domain. Unfortunately, the boundary condition in Eq. (5-51), which replaces the boundary condition $\phi'(H)=0$ in Eq. (5-35A), involves the eigenvalue through a square root function which can be defined as a single-valued analytic function not in the entire complex λ plane, but in the plane minus a line (branch cut) connecting the points $\lambda=\omega/c_b$ and $\lambda= -\omega/c_b$, where the square root in Eq. (5-50) vanishes. Thus, the problem remains singular, and the spectrum is partially continuous.

The approach generally taken to this singular problem is to use the integral representation for the Green's function solution to the separated problem, Eqs. (5-33)-(5-34) with the modified boundary conditions as above [including Eq. (5-51)], but with the right sides of Eqs. (5-33) and (5-34) containing delta functions in range and depth, respectively, representing a point source at r=0 and $z=z_s$. As described by Titchmarsh (1951), this integral solution is a Hankel transform

$$P(r,z) = \frac{1}{4\pi} \int_{-\infty}^{\infty} G(z,z_s;\lambda) H_0^{(1)}(\lambda r) \lambda d\lambda \qquad (5\text{-}52)$$

where the Green's function $G(z,z_s;\lambda)$ is the solution of Eq. (5-34) with the right hand side replaced by $\delta(z-z_s)$. This integral is then evaluated using Cauchy's integral formula from complex variable theory for the integral around a closed contour within a simply connected domain in which the integrand is analytic (in particular, single-valued) except for isolated singularities. The formula gives a result that is proportional to the sum of the residues at the singularities of the integrand enclosed by the contour, given that none of the singularities actually lies on the contour itself. In order for the integrand to be single-valued within the contour, the contour must also avoid a branch cut (line) connecting the two points at which the square root in the integrand vanishes, as described above. At least two different choices of branch cuts have been used historically, one by Pekeris (1948) and one by Ewing, Jardetsky, and Press (1957). The latter, often referred to as the EJP branch cut, results in a representation of the pressure field which has better convergence properties [cf Stickler (1975)] and is thus generally used today. The pressure field is obtained as a discrete modal sum of the residues (which occur at the eigenvalues of the discrete spectrum), plus a branch-cut integral over the continuous spectrum. Sufficiently far from the source this integral can be neglected, but in the very near field the contribution to the pressure field from the continuous spectrum can be relatively quite significant; Stickler (1975) gives further discussions on this point.

5.5 Multipath Expansion and Fast Field Theory

There are two other approaches to the evaluation of the Hankel integral transform in Eq. (5-52) which have resulted in underwater acoustic models. The first is the *multipath expansion technique (MPE),* in which the integral transform is expanded into a sum of ray integrals. The idea dates back to the 1930s in electromagnetic theory, and provides an alternative to the derivation of ray theory presented in Sections 5.1 and 5.2. Weinberg (1975) applied the theory to underwater acoustics, with the objective of improving upon the asymptotic method of stationary phase for evaluating the ray integrals. Just as in Section 5.2, the key is developing a numerical method that is accurate even near caustics. Weinberg (1981) then developed a faster, but in theory less accurate, *effective range derivative technique* and implemented it in the *Fast Multipath Expansion (FAME)* model. This technique evaluates the

ray integrals by assuming that for high frequencies the dominant contribution to the integrals comes from a small region near the point of stationary phase, where the integrand is slowly varying. Unlike the stationary phase method itself, however, *two* subintervals of integration are used, one on either side of the stationary phase point. An effective range derivative of the phase is defined as a generalization of the usual phase derivative, which is zero at a stationary phase point. The result agrees with the stationary phase result in the high-frequency limit, but is significantly more accurate at lower frequencies. In addition, Weinberg (1981) shows that the effective range derivative prediction is accurate at caustics.

The second approach is the *Fast Field Program (FFP)* developed by Marsh *et al* (1967) and DiNapoli (1971) and described in detail by DiNapoli and Deavenport (1980). The approach here is to replace the Hankel function in Eq. (58) by its far-field asymptotic expansion, which of course includes an exponential factor $\exp(i\lambda r)$. The integral is then in a form amenable to direct evaluation by a Fast Fourier Transform (FFT). The real work in this method is the calculation of the input to the FFT, which requires computing the Green's function $G(z,z_s;\lambda)$ numerically for a number of discrete values of λ at desired receiver depths. DiNapoli and Deavenport (1980) use a matrizant (propagator) method combined with an elegant recursion technique which allows the calculation of the Green's function for a number of values of λ simultaneously. However, there is a price paid in approximation, since the sound speed must vary exponentially between tabulated points in order for the recursion to hold, and restrictions are placed on a parameter in the exponential fit in order that the values of λ be evenly spaced, as required for input to the FFT.

An alternative *direct global matrix*, or "*finite wave element*," approach to evaluation of the Green's function is taken by Schmidt in the *SAFARI* model. As described in Schmidt (1987), "the pressure field in each layer is considered as a superposition of the field produced by an arbitrary number of sources and an unknown field satisfying homogeneous wave equations. These unknown fields are then determined from the boundary conditions to be satisfied simultaneously at all interfaces. The local boundary conditions at each interface lead to a linear system of equations in the Hankel transforms of the potentials in the adjacent layers. These *local* systems of equations are then assembled into a *global* system of equations expressing the boundary conditions at all interfaces simultaneously." The resulting global coefficient matrix problem can then be solved efficiently in a numerically stable manner. It appears that this method has an advantage over the Fast Field Program in ease of handling

shear, i.e., fluid-solid boundary conditions. Other than the Green's function solution, however, the approach is still the same as FFP, in that a Fourier transform is used to evaluate the integral. It remains true that the numerical evaluation of the integral transform involves both truncation to a finite integration interval in λ, and discretization of the interval, i.e., selection of discrete values of λ within the interval at which the Green's function is evaluated. In both FFP and SAFARI, therefore, automation is difficult, since convergence of the integral to an answer largely independent of truncation and discretization can only be assured by testing by experienced users. These models would, therefore, tend to be less suitable for routine or operational use than others discussed in this notebook.

5.6 Notes For Section 5

Note 5-1: Bessel's equation of order n is:

$$z^2 w'' + zw' + (z^2-n^2) w = 0 .$$

Its solutions are the Bessel functions of the first kind $J_n(z)$, of the second kind $Y_n(z)$ (or Weber functions), and of the third kind $H_n^{(1)}$, $H_n^{(2)}$. The latter are the Hankel functions of types 1 and 2 and of order n. Important relationships among these solutions include: $H_n^{(1)}(z) = J_n(z) + i\, Y_n(z)$, $H_n^{(2)}(z) = J_n(z) - iY_n(z)$, and thus $J_n(z) = 1/2\, [H_n^{(1)}(z) + H_n^{(2)}(z)]$.

Asymptotic expansions as $z \to \infty$ are

$$H_n^{(1)}(z) \sim \sqrt{2/\pi}\, \exp(i(z - \tfrac{1}{2} n\pi - \tfrac{1}{2}\pi)) \text{ and } H_n^{(2)}(z) \sim \sqrt{2/\pi z}\, \exp(-i(z - \tfrac{1}{2} n\pi - \tfrac{1}{2}\pi))$$

Note 5-2: A Sturm-Liouville equation for w(x) has form

$$r(x)w''(x) + r'(x)w'(x) + [\lambda S(x) - q(x)]w(x) = 0$$

where r(x), p(x), and q(x) are functions of x and λ is a constant parameter. For more, see textbooks on ODEs such as the classics by Courant and Hilbert (1953) or Coddington and Levinson (1955).

Note 5-3: A second order ODE of form

$$r_1(x)w''(x) + r_2(x)w'(x) + r_3(x)w(x) = 0$$

is self-adjoint if it is the same as its adjoint equation:

$$r_1(x)w''(x) + (2r_1'(x) - r_2(x))w'(x) + (r_1''(x) - r_2'(x) + r_3(x))w(x) = 0$$

Note then that $r_2(x) = r_1'(x)$ is a sufficient condition and that the Sturm-Liouville equation in Note 5-2 is self adjoint.

6. PHYSICS -- RANGE-DEPENDENT ENVIRONMENTS

In this section we consider various approaches to solving the much harder problem of estimating propagation properties in cases where the bottom, volume, or surface conditions change significantly with range. Rays, adiabatic rays, adiabatic modes, and two types of PEs are discussed.

6.1 Direct Application of Ray Theory

In principle, a range-dependent ray model requires solving the fully three-dimensional ray equations which arise from Eq. (5-12). In practice, these equations are so complicated that the numerical complexity and computational expense make a direct solution distinctly unattractive. A typical compromise is that made by GRASS [cf Cornyn (1973)], TRIMAIN [cf Roberts (1974)], and the *Multiple Profile Ray-Tracing Program (MPP)* [cf Spofford (1973)]. The essence of the approach is to use a series of sound speed profiles, interpolated in both range and depth within triangular sectors, and to solve the range-independent ray equations, Eqs. (5-16) and (5-17), within each sector. The interpolation actually yields a sound speed linear in range and depth within each triangular sector, so that the ray segments within the sector are arcs of circles. Furthermore, the use of triangular interpolation avoids the problem of intermediate profiles that can be physically unrealistic (e.g., gradients with the wrong sign, channels appearing and disappearing). More discussion of this interpolation can be found in Wright (1970).

There are two fundamental problems that must be solved with this approach. The first is ray interpolation: because of the complicated sequence of sound speed fields and boundary properties that a ray will encounter in going from source to receiver, computing precise eigenrays is impractical. Rays are launched at certain discrete angles from the source, and traced to the range of the receiver. In general, the rays will not hit the receiver precisely, so that interpolation is necessary. However, merely because two rays pass near the receiver does not mean that it is proper to interpolate to obtain a contribution at the receiver. The first ray might be an RR ray that has not encountered either the surface or the bottom, while the second ray might have encountered the bottom several times. Thus, the history of each ray --

its surface and bottom bounces, and the number of turnings in the water column-- must be recorded as it is traced. The rays can then be divided into families, while dealing with other complications such as rays that hit the bottom only because locally the water-sediment interface was sloping -- rays that really belong to the same family may *a priori* appear as two families. Interpolation, then, must be carried out only among rays that belong to the same family.

The second problem is the same false caustic problem that we noted earlier even in the range-independent case. Sound speed gradient discontinuities between triangular sectors give rise to false caustics. Such caustics can be distinguished from real caustics by careful examination of θ-r diagrams which show ray arrival angles as a function of range, or conversely, the curve $r(\theta)$, which is known for every ray traced. The variation of the slope of the $r(\theta)$ curve in the vicinity of each extremum, i.e., each possible caustic, is the deciding factor. If the $r(\theta)$ curve is convex near an extremum, it corresponds to a false cusped caustic and that extremum is rejected out of hand. Within the set of remaining extremal points, only the points which are interior relative extrema within that set are true caustics.

TRIMAIN, GRASS and most recently Gaussian Beam models [cf Porter and Bucker (1987)] have modes of operation in which no attempt is made to interpolate rays or ray intensities. Instead, a ray's intensity is smeared in range and depth.

An alternate method interpolates the sound speed profiles only at a fixed depth but fits the sound speed profiles with cubic splines [cf Solomon *et al* (1968)] or quadratic functions. Linear interpolations in range at fixed depth between these profiles gives continuous range derivatives, and false caustics are avoided.

6.2 Adiabatic Ray Theory

In the MPP model mentioned above, Snell's constant K_n along a ray [Eq. (5-18)] in general changes as the ray passes from one triangular sector into another. Indeed, a fully range-dependent ray model should be able to accommodate such changes, even those associated with an environment varying rapidly with range.

On the other hand, adiabatic ray theory shows that if the environment varies sufficiently slowly with range, we should be able to use a range-independent ray model and yet occasionally change the sound speed profiles and boundaries in such a way that we can continue to track the evolution of a ray by means of an invariant for each ray. Strictly speaking, the theory, as originally developed by Milder (1969), states that if the sound speed varies slowly enough in range, the invariant quantity is

$$\int_{ray\ cycle} [n(z)^2 - n_t^2]^{1/2}\, dz \qquad (6\text{-}1)$$

where the integral is taken over a full ray period, and where n_t denotes the refractive index at the ray turning point depth. The invariant is proportional to the "phase integral"

$$ik_0 \int n \sin\theta\, dz \qquad (6\text{-}2)$$

of the WKB approximation and may be more easily recognized as

$$J = \int_z \frac{\sin\theta(z)}{c(z)}\, dz \qquad (6\text{-}3)$$

where $\theta(z)$ is the ray's inclination angle (from the horizontal) at depth z, and where c(z) is the speed of sound at depth z. Then ωJ, per WKB, gives an approximation to the mode number (m):

$$\omega J \sim m\pi - \pi/2 \qquad (6\text{-}4)$$

Hence, the invariance of the ray parameter J is nearly equivalent to invariance of mode number m.

The quantitative criterion for varying "slowly enough" is that in a distance of one ray period, the change in n^2 at any single depth traversed by the ray must be small relative to the change in n^2 between the axis and the ray turning point:

$$\frac{\Delta n^2}{n^2 - n_t^2} < 1 \qquad (6\text{-}5)$$

Weinberg and Burridge (1974) have re-worked the theory of geometrical acoustics outlined in Section 5.2 for the case of slow horizontal variation in the environment. The standard asymptotic development is modified to include a small parameter representing the slow rate of horizontal variation.

6.3 Adiabatic Mode Theory

Adiabatic mode theory very simply states that if the environment varies slowly enough, then a mode at one range couples to a mode at a different range when (and only when) the modes have the same mode number. Mode number is thus the invariant. If the environment is presented as a sequence of sound speed profiles in range, we compute the normal modes $\phi_n(z)$ for each profile in turn. At a range r* where a profile change occurs, we begin using the new set of modes in Eq. (5-47), but for any mode n, the new mode amplitude at r>r* is just the old amplitude adjusted for cylindrical spreading and multiplied by a phase term $\exp[ik_n(r-r^*)]$, where k_n is the eigenvalue of the new mode n. More generally, in the adiabatic approximation Eq. (5-47) is replaced by

$$P(r,z) = \sum_{n=1}^{N} \frac{b_n \phi_n(z)\, e^{\,i\int_0^r k_n(r')\,dr'}}{\sqrt{\int_0^r k_n(r')\,dr'}} \qquad (6\text{-}6)$$

where $k_n(r')$ denotes a slow but continuous variation in range.

Milder (1969) gives a quantitative criterion for the adiabatic approximation to hold for modes, analogous to Eq. (6-5) above:

$$\lambda / X \gg 2\pi \Delta n^2 / n^2 \qquad (6\text{-}7)$$

where λ is the acoustic wavelength, X is the ray-analogous cycle length, and

$$\Delta n^2 = X \int_0^H \phi_\alpha \, \phi_\beta \, \frac{\partial n^2}{\partial x} \, dz$$

for adjacent modes α and β.

6.4 Coupled Mode Theory

The adiabatic approximation can be violated in any of several ways, all necessitating explicit computation of mode coupling, as indicated in the generic Eq. (4-7) given earlier. A frequently cited example is that of rapidly changing water mass sound speed profiles, e.g., in the vicinity of a front. Even if water mass profiles do not change, however, profiles within the sediment or basement may, especially in the case of sloping or rough water-sediment, sediment layer, or sediment-basement interfaces.

There are fundamental differences between "sloping" and "rough," however. Sloping interfaces cause a continual, but steady, change in the character of the set of "local" normal modes, i.e., those which can be computed at any point in range based on the environment precisely at that range. For example, shallower water will generally trap fewer modes in the water column, and will cause increased modal attenuations as a higher percentage of modes interact with the bottom. On the other hand, if by roughness we mean oscillation of an interface about some fixed depth, its effect is better modeled as a continual coupling, or transfer, of energy among a single set of modes, e.g., those computed for the interfaces at their mean depths.

Thus, we see that the term "adiabatic" is generally concerned with whether large-scale, gross changes in the environment, e.g., in the general shape of the sound speed profile, or in the water depth, are taking place within a spatial scale on the order of a ray cycle length. Normal mode codes with adiabatic options can handle such changes if they do not occur too rapidly. Coupled mode codes, on the other hand, can be designed not only to treat rapid changes of that sort, but to carry out specialized analysis of more subtle effects, which are weaker but can add up significantly over range. This is typical of scattering due to bottom interface roughness, as mentioned above, or to surface scattering, or even to water mass

scattering caused by inhomogeneities. As an example of the latter, Dozier and Tappert (1978) derive coupled mode equations in their study of internal wave effects.

These more subtle effects are often modeled stochastically; recall our discussion of stochastic wave equations in Section 4.6. Thus, it is important to distinguish whether a coupled mode implementation is designed to solve the wave equation for a particular realization of the environment, e.g., a realization of a rough sea surface, or to solve for the average acoustic field weighted over all possible environments. The latter situation typically requires additional theoretical development, since the averaged coupled mode equations to be solved are generally not obvious. Again, a good example is given in Dozier and Tappert (1978), where these averaged equations, so-called *master equations,* are shown to be statistically good approximations to the original coupled mode equations in certain circumstances. Such equations are a computationally efficient route to the statistics of the acoustic field, but require environmental statistics (e.g.., spectral parameters) for inputs. The results, however, are often more useful to system designers who want to understand the mean and variance of acoustic fluctuations.

Regarding the term "scattering," we must be careful to specify whether forward scatter, backscatter, or both are included. The Dozier-Tappert equations just mentioned treat forward scatter only. As a more common example, the simplest way to include coupling using a standard normal mode code is to "renormalize" the acoustic field at each environmental province boundary; the acoustic field computed as a sum of the previous mode set is integrated against each of the new mode shapes to determine the initial amplitudes of the new mode set in the new province. This approach has been used to add coupling to the WRAP model [Kuperman *et al.* (1991)], in which mode sets are precomputed and stored in advance for all environmental provinces within a three-dimensional area of interest. Acoustic field calculations are carried out along vertical planes which cut through the three-dimensional area at various orientations, and within each plane, if desired, mode coupling can be included roughly as indicated above. Although such coupling includes only forward scatter, it is usually quite adequate for volume scatter, where backscatter is often negligible compared to forward scatter.

Scattering from rough boundaries, however, often leads to significant backscatter. Numerical calculation of such backscatter cannot be done by a simple one-way forward computation of mode coupling in range, as described in the previous paragraph. That

calculation has the same element of simplicity which we originally noted in Section 4.4 in our discussion of the parabolic equation; it can be solved as an initial value problem. Including backscatter leads to a two-point boundary value problem in range; the numerical methods become much more involved, and much more computationally intensive.

Boyles (1983; 1984, Chapter 7) describes an approach to the rough surface scattering problem using coupled local normal modes. This approach is, however, applicable directly only to cylindrical geometries, or to a full 3D geometry but with a surface roughness that is a function of only one horizontal coordinate. Dozier (1982) reformulated Boyles' coupled mode equations and devised an efficient algorithm for their numerical solution. A key to the success of this approach is that the boundary condition to be satisfied at the rough surface is the simple pressure-release boundary condition $p=0$.

At bottom interfaces (e.g., the water-sediment interface) the boundary conditions are more complicated and involve the normal derivative of p. Typically, the approximation is made that the normal derivative is nearly equal to the z derivative, and it is assumed that as long as the interface slopes are small, the approximation is good. However, Rutherford (1979) showed that this approximation does not conserve energy, and that this non-conservation can contribute significant error. Rutherford then derived coupled mode equations which conserve energy by applying first order perturbation theory in a consistent manner. Rutherford's equations are thus limited only by the small slope approximation. Further discussion of energy conservation for coupled-mode models may be found in Rutherford and Hawker (1981).

Another approach to conservation of energy used in the 1980s was to approximate bottom interfaces by piecewise constant stair-step representations; e.g., see Evans (1983). The argument was made that since each segment is flat, the normal and z derivatives agree precisely on the segment, and energy is conserved. Now, however, all backscattering occurs at the corners of the stair steps, where the normal derivative to the surface is not even defined, so that the boundary condition does not even hold: A further problem is that this approach describes backscattering as occurring from a series of corners rather than from a realistic representation of bottom roughness. Lack of energy conservation for stair-step bottoms in the one-way parabolic approximation, and possible improved boundary conditions, are discussed in Porter *et al.* (1991).

Recently, Fawcett (1992) derived bottom coupled mode equations based on local normal modes which individually satisfy boundary conditions based on vertical (z), not normal, derivatives at the interfaces. However, he was well aware of Rutherford's objections, described above, and the mode amplitudes are carefully constructed so that the modal sum for the pressure will indeed satisfy the correct boundary conditions. Fawcett also presents a numerical method for solving a two-point boundary value problem with his equations, and gives numerical results that compare favorably with results from a boundary integral equation solution. His method does omit any treatment of shear waves.

Clearly, coupled mode modeling is a field of ongoing research, and there is a significant amount of work yet to be done before these models advance beyond purely R&D use.

6.5 Split-step PE

The essence of the parabolic approximation was described earlier in Section 4.4. Tappert's original manuscript [Tappert (1977)] on PE discusses the numerical solution of PE only as much as to mention in Appendix A that his original PE code used the split-step Fourier algorithm. Indeed, all of the first PE codes followed Tappert's lead in this regard, and even today the Navy Standard PE code [cf Holmes and Gainey (1991)] is based on split-step, as is the University of Miami Parabolic Equation Model [Smith and Tappert (1993)]. However, since the 1980s, considerable development of alternative finite element and finite difference numerical methods for PE has also taken place, and these algorithms will be discussed in Section 6.6.

The original introduction of PE into underwater acoustics in 1972-73 attracted immediate and widespread interest because at once it became clear that PE could solve severely range-dependent problems that no previous underwater acoustic model could reasonably even attempt. For example, Tappert (1977) shows an example in his Figure 5 of a 40 dB drop in transmission loss across an oceanic front; his Figures 11-13 strikingly illustrate differences in transmission across a seamount for various propagation geometries.

All of these first PE results were obtained using the split-step Fourier algorithm. Unfortunately, a definitive manuscript on this algorithm, analogous to Tappert's 1977

manuscript, is yet to be written. Two of the best original descriptions of the algorithm were given by Jensen and Krol (1975) and Brock (1978). Following Brock, we begin with the "original" parabolic equation, which in the early years of PE development was the most widely used approximation (a simple binomial expansion) to the square root operator in Eq. (4-4):

$$\psi_r = i\,(A+B)\,\psi \tag{6-8}$$

where A is the constant-coefficient differential operator

$$A = \frac{1}{2k_0}\frac{\partial^2}{\partial z^2} \tag{6-9}$$

and where B is the variable, but only multiplicative (not differential) operator

$$B = \frac{k_0}{2}(n^2-1) \tag{6-10}$$

where $n(z)=c_0/c(z)$ and c_0 were defined following Eq. (5-11), and where $k_0=\omega/c_0$ was defined following Eq. (5-44). Equation (6-8) is also derived as Eq. (1.21) in Tappert (1977). The numerical solution of Eq. (6-8) is carried out by repeatedly advancing the solution in depth over range steps of length Δr; formally, we can represent a single range step advance by

$$\psi(r+\Delta r,z) = e^{i\Delta r(A+B)}\,\psi(r,z) \tag{6-11}$$

to third order accuracy in Δr, where A and B are evaluated at the midpoint $(r+\Delta r/2)$ of the interval $(r,r+\Delta r)$. The essence of the split-step algorithm then is twofold: first, the exponentiation of the operator involving (A+B) is approximated by a product of three exponentials involving only A and B separately:

$$\psi(r+\Delta r,z) = e^{\frac{i\Delta rB}{2}}\,e^{i\Delta rA}\,e^{\frac{i\Delta rB}{2}}\,\psi(r,z) \tag{6-12}$$

where again this approximation is shown to be third order accurate in Δr. Second, since A is a constant coefficient differential operator, the evaluation of $e^{i\Delta rA}$ is carried out by means of a fast Fourier transform. In Fourier space, the second derivative operator is simply a multiplication by $(ik)^2$. Finally, since one range step follows another, it works in practice simply to lump the final $e^{i\Delta rB/2}$ of one range step with the initial $e^{i\Delta rB/2}$ of the next, so that effectively,

after an initial application of $e^{i\Delta r B/2}$ to the source function (of depth) at the source range r=0, advancing the solution by Δr consists simply of applying $e^{i\Delta r A}$ and then $e^{i\Delta r B}$:

$$\psi(r+\Delta r, z) = e^{\frac{i\Delta r}{2} k_0 (n^2-1)} \, FFT^{-1}\left[e^{\frac{-i\Delta r K^2}{2k_0}} \, FFT(\psi(r,z)) \right] \quad (6\text{-}13)$$

where FFT is the spatial Fourier transform from z to K and FFT^{-1} is the inverse transform. Eq. (6-13) is the original split-step Fourier PE algorithm.

The pressure release boundary condition at a flat ocean surface is handled by replacing the complex FFT in Eq. (6-13) by real sine transforms and forcing the pressure to be anti-symmetric in depth z. However, due to the periodicity implicit in any use of discrete Fourier or sine transforms, the pressure field will then also satisfy a pressure release boundary condition at the maximum depth of the transform. This non-physical boundary condition is handled by inserting an absorbing layer beneath all other physical layers (water, sediment, rock) in the problem.

A significant portion of the time required to numerically evaluate Eq. (6-13) is spent computing the Fourier or sine transforms. These transforms are a staple of signal processing algorithms, and in recent years various computer hardware items, such as Digital Signal Processing (DSP) chips and array processors, have been designed specifically for fast computation of these transforms. Several implementations of PE that make use of such specialized hardware have been carried out, but even today the vast majority of PE runs done in the underwater acoustic community use only general purpose computer hardware. The rapid increase in the computing power of such general purpose hardware, and the extra cost of the specialized hardware, is probably responsible for this trend so far.

A fundamental complication in the split-step algorithm is that its solution is not independent of the choice of the reference sound speed c_0. Note that the "original" parabolic equation, Eq. (6-8), is exact for modes (rays) with a phase speed of c_0, i.e., with turning point(s) at the depth(s) where the sound speed is c_0; indeed, the operator B vanishes at those depths. Thus, the above (usual) choice of c_0 as the sound speed minimum means that the parabolic approximation is exact for the axial ray, and is accurate to within a given error criterion for rays crossing the axis at angles within an interval symmetric about the horizontal. Given that choice

of c_0, the original PE, Eq. (6-8), is generally considered to have acceptable accuracy for paths which cross the axis at angles up to about 15 degrees from the horizontal. Therefore, the original PE was applied primarily in deep water environments where angles steeper than 15 degrees would interact with the bottom and thus not be significant contributors to the acoustic field at long range.

Outside of this 15-degree aperture, paths can accumulate significant phase errors with range, as shown by Brock, Buchal, and Spofford (1977). They introduced an algorithm, known as CMOD, which attempts to correct for the phase errors by modifying the index of refraction of a given problem in such a way that the phase errors in the modified problem act as a correction, and the computed solution is, to good approximation, a solution of the original given problem. The development of CMOD is motivated by an attempt to match the ray equations of PE with modified index of refraction to the true ray equations of the Helmholtz equation. Continuing this line of research, Berman, Wright, and Baer (1989) recently introduced a parabolic equation whose rays are *exactly* those of the Helmholtz equation in a range-independent environment, and which is amenable to a split-step numerical solution.

The other fundamental approach to improving the accuracy of PE is to directly introduce a more accurate approximation to the square root operator in Eq. (4-4). Thomson and Chapman (1983) introduced such an approximation, which is amenable to a split-step numerical solution and is currently in use in a number of PE codes, including the Navy Standard PE code. Berman *et al.* (1989), whose PE modification was mentioned in the previous paragraph, show that their results compare favorably with results obtained using the Thomson-Chapman method. For most cases, the Thomson-Chapman method, compared to the original PE, yields a substantial increase in the effective aperture; some modelers state that they have observed paths at 40 degrees or even higher computed to high accuracy. Unfortunately, there are cases in which Thomson-Chapman does even worse than the original PE. Perhaps the most famous example is the "Porter duct" problem defined in Test Case 7 of the PE Workshop II [Chin-Bing *et al.* (1993)]. Work documented there, using the University of Miami Parabolic Equation Model [Smith and Tappert (1993)], shows that there exists an interval of choice for c_0 within which the Thomson-Chapman method is more accurate than the original PE, as expected; unfortunately, the standard choice of c_0 as the sound speed minimum

does not fall within this interval. Smith and Tappert (1993) discuss a scheme for automatic c_0 selection, but state that it is not foolproof. The ambiguity in the choice of c_0 is a fundamental complication that apparently can be eliminated only with a significant increase in running time, by performing a transformation of the dependent variable at each range step in a range-dependent environment [Tappert (1991)].

The split-step algorithm as described above uses a sine transform to force the solution for the pressure p to be an odd function of depth, and thus to vanish at the *flat* surface z=0. Dozier (1984) showed that this algorithm could be modified to solve PE so that the pressure vanishes on a realization z=h(r) of a *rough* sea surface. The surface is represented in piecewise linear fashion, and local conformal mappings are used to flatten each segment of the surface in turn, whereupon the solution can be advanced locally using the split-step algorithm. A year later Tappert and Nghiem-Phu (1985) duplicated Dozier's result by implementing the split-step algorithm with a full Fourier (not a sine) transform over the ocean plus its image, in such a way that a modified parabolic equation is solved in the image ocean; this modified equation is carefully constructed to force p=0 on the rough surface z=h(r).

While elegant, these solutions have two key disadvantages. First, they are computationally slow because they require the split-step algorithm to take range steps somewhat smaller than the minimum surface wavelength of interest. Whereas ordinarily range steps might be on the order of a quarter or half kilometer, resolving rough surface wavelengths may require range steps on the order of a few meters. The second disadvantage is that a Monte Carlo simulation, consisting of multiple PE runs over a statistical sampling of realizations of rough surfaces, is required to obtain a statistical average of rough surface effects on propagation. Again, this can increase computation time by an order of magnitude or more. Thus, Moore-Head *et al.* (1989) introduced an algorithm to compute surface loss in an average sense, incurring negligible additional computational expense. The additional input for this algorithm is average surface loss as a function of angle. After each range step (with length selected by standard algorithms), the pressure at a small (e.g., 8 or 16) set of depth mesh points near the surface is Fourier transformed (a "slow" Fourier transform, not an FFT which requires periodicity) to obtain the local distribution of energy with angle near the surface. The loss function evaluated at each angle, normalized by the range step relative to the cycle length for a ray at that angle, is then applied, and the inverse transform is taken.

In upward refracting environments such as surface ducts, surface loss often occurs because energy has been scattered into other small, forward propagating angles. Dozier *et al.* (1991) showed that computing only loss, and thereby discarding energy which continues to propagate, can lead to serious error. Building upon the Moore-Head *et al.* (1989) algorithm described above, they introduced a further modification of the split-step algorithm which redistributes these energies among the propagating angles and allows them to continue to propagate. The additional input required for this modification is a scattering kernel which describes statistically the scattering of energy from one angle to another for a given class of rough surfaces.

Throughout our discussion of PE in this Section, we have been talking about "one-way" PEs which propagate energy only in the forward direction (recall our original discussion of PE in Section 4.4 as arising from a factorization of the Helmholtz equation into forward and backward going parts). Thus, all of the scattering treatments described above include only forward scatter and are thus analogous only to the simplest of the coupled mode approaches described in Section 6.4. However, Tappert (1977) originally envisioned the extension of PE to include backscatter by following a forward scatter PE computation with a second one-way computation, marching backward toward the source, but where the second computation solves an inhomogeneous PE, with the inhomogeneous term containing the forward scattered solution just computed. The final result then would contain multiple forward scatter but only single backscatter; additional forward-backward cycles could be carried out in the unlikely event that higher order backscatter was required. In the last few years, Tappert and his colleagues [e.g., Tappert and Ryan (1989); Tappert and Yamamoto (1993)] have implemented his original idea as a two-way "reverberation PE." An alternative method of incorporating reverberation into the split-step algorithm, which draws upon the work of Moore-Head *et al.* (1989) and Dozier *et al.* (1991) described above, was recently published by Schneider (1993).

6.6 Finite-Difference and Finite-Element PE

Early versions of split-step PE did not handle most bottom-interacting paths accurately; either they were too steep, or the boundary conditions were not properly implemented (recall the artificial absorbing layer). Thus, some researchers [e.g., Lee *et al.*, (1981) and (1982)] turned to finite-difference methods in an attempt to obtain improved accuracy. Finite-

difference schemes proceed by directly discretizing the parabolic equation in range and depth, and solving the resulting equations for values of the solution on those range-depth mesh points. General background on finite-difference methods for PDEs may be found in Mitchell and Griffiths (1980); a survey of such methods in ocean acoustics is given in Lee and McDaniel (1988). Implicit finite-difference methods, for which imposition of boundary conditions leads to a system of equations solvable by standard matrix techniques, are generally preferred to explicit ones because the former are faster and unconditionally stable; most if not all finite difference implementations of PE in underwater acoustics use implicit schemes.

The IFDPE (Implicit Finite Difference PE) code of Lee and Botseas (1982) has been augmented for wide angle capability [Botseas *et al.* (1983)] and for enhanced treatment of boundary conditions [McDaniel and Lee (1982); Lee and McDaniel (1983)]. IFDPE was benchmarked by Jensen and Ferla (1990) and found to be accurate for angles forward scattered at up to 40 degrees from the horizontal. In addition, IFDPE was found to be 10 to 100 times faster than the coupled mode code of Evans (1983). On the other hand, IFDPE was found to be five to ten times slower than the split-step PE code known as PAREQ [Jensen and Martinelli (1985)] and developed at SACLANTCEN. PAREQ was found to be accurate only up to about 20 degrees from the horizontal, even with the Thomson-Chapman (1983) modification, but the increased accuracy of IFDPE was obtained at a severe computational price compared to split-step PE.

Greene (1984) introduced a finite-difference High-Angle PE (HAPE) using a rational linear approximation similar to that used by Claerbout (1976), but more accurate than the approximation to the square root operator used by Thomson and Chapman (1983). Rational linear approximations are more accurate than Taylor approximations [Collins (1989)] and are easier to implement than rational-polynomial approximations, for which the depth-discretization matrices are no longer tridiagonal, so that the numerical solution is not as efficient; also, these matrices contain derivatives of acoustic properties which are usually discontinuous across interfaces. Greene shows an example where HAPE is quite good for angles up to 40 degrees from the horizontal.

Recently, finite element methods have been introduced in an attempt to obtain even more accurate treatment of complicated interfaces and boundary conditions. Goldstein (1984) gives a helpful, succinct description of finite element methods, which we paraphrase here:

> The finite element method is based on replacing the given boundary-value problem by an equivalent variational problem, which can then be approximated by use of a convenient finite-dimensional space of functions. Typically, this space of functions consists of sufficiently smooth piecewise polynomials defined with respect to a partitioning of the computational domain into simple subsets called elements. The variational problem is then reduced to the solution of a finite number of linear equations. As the diameter of the largest element decreases, the approximate solution converges to the exact solution, but the number of equations to be solved increases.

Additional background on finite element methods can be found in Zienkiewicz (1971). Collins (1988) describes FEPE, a PE code which uses finite elements for depth discretization and Crank-Nicolson integration in range as described in Collins (1989). FEPE uses an efficient tridiagonal solver (not based on the standard Gaussian elimination scheme), and Collins (1990) finds that FEPE runs several times faster than IFDPE [Lee and Botseas (1982)] on a benchmark problem; FEPE appears to offer special advantages for problems involving sloping bathymetry. There is also a version of FEPE, known as FEPES, which includes shear.

The issue of energy conservation is important for PE just as for coupled mode models. Collins and Westwood (1991) present an energy-conserving finite-difference PE using higher-order Padé approximations. Still, however, sloping bottom interfaces are modeled as stair steps.

Analogous to the two-way forward and back scattering PE described at the end of Section 6.5, Collins and Evans (1992) have recently introduced a two-way PE which sweeps in each direction using the energy-conserving one-way PE just mentioned above. This two-way PE follows the approach of the two-way coupled mode model [Evans (1983)] in which range-dependent environments are approximated by a series of range-independent regions, with the two-way PE solution required to satisfy two continuity conditions at the vertical boundaries between regions.

Finally, Collins (1993) has introduced a "split-step Pade" numerical solution of the wide-angle PE [Botseas *et al.* (1983)] which is much more efficient than the Crank-Nicolson finite-difference scheme originally used. Indeed, this numerical method may be competitive with the split-step Fourier method in efficiency, while retaining all of the increased accuracy of the wide-angle PE. Also, this method is especially suitable for implementation on a computer with a small number of parallel processors.

7. REFERENCES

Ahluwalia, D. S. and Keller, J. B. (1977). *Exact and asymptotic representations of the sound field in a stratified ocean,* in Keller, J. B. and Papadakis, J. S. (eds) (1977), *WAVE PROPAGATION AND UNDERWATER ACOUSTICS*, Lecture Notes In Physics, Vol. 70, Springer-Verlag, New York.

Apel, J. R. (1987). *PRINCIPLES OF OCEAN PHYSICS,* Academic, Orlando, FL.

Bartberger, C. L., (1981). "*An investigation of the physics of the RAYMODE model,*" Report No. NADC-82009-30, NADC, Warminster, PA.

Berman, D. H., Wright, E. B., and Baer, R. N. (1989). *An optimal PE-type wave equation,* J. Acoust. Soc. Am. 86, 228-233.

Birkhoff, G. (1985). *Some mathematical problems of numerical ocean acoustics*, Comp. & Maths. with Appls. 11, 643-654.

Boden, L., Bowlin, J. B., and Spiesberger, J. L., (1991). "*Time domain analysis of normal mode, parabolic, and ray solutions of the wave equation,*" J. Acoust. Soc. Am. 90, 954-958.

Botseas, G., Lee, D., and Gilbert, K. E. (1983). *IFD: wide angle capability,* Rep. TR-6905, Naval Underwater Systems Center, New London, CT.

Boyles, C. A. (1983). *Coupled mode solution for a cylindrically symmetric oceanic waveguide with a range and depth dependent refractive index and a time varying rough sea surface,* J. Acoust. Soc. Am. 73, 800-805.

Boyles, C. A. (1984). *ACOUSTIC WAVEGUIDES*, John Wiley, New York.

Brekhovskikh, L. M. (1980). *WAVES IN LAYERED MEDIA,* Academic Press, New York.

Brock, H. K., Buchal, R. N., and Spofford, C. W. (1977). *Modifying the sound-speed profile to improve the accuracy of the parabolic equation technique,* J. Acoust. Soc. Am. 62, 543-562.

Brock, H. K. (1978). *The AESD parabolic equation model*, Nav. Ocean Res. Dvlpmt. Activity (NORDA) Technical Note 12.

Burridge, R. and Weinberg, H. (1977). *Horizontal rays and vertical modes,* in Keller, J. B. and Papadakis, J. S. (eds), *WAVE PROPAGATION AND UNDERWATER ACOUSTICS*, Lecture Notes In Physics, Vol. 70, Springer-Verlag, New York.

Chester, C. R. (1971). *TECHNIQUES IN PARTIAL DIFFERENTIAL EQUATIONS,* McGraw-Hill, New York.

Chin-Bing, S., King, D., Davis, J. and Evans, R. (editors), (1993). *PE Workshop II: Proceedings of the 2nd Parabolic Equation Workshop (May 6-9, 1991)*, NRL/BE/7181-93-0001, Naval Research Laboratory, Washington, DC.

Claerbout, J. F. (1976). *Fundamentals of Geophysical Data Processing,* McGraw-Hill, New York, p. 198.

Coddington, E. A. and Levinson, N. (1955), *THEORY OF ORDINARY DIFFERENTIAL EQUATIONS*, McGraw-Hill, New York.

Collins, M. D. (1988). *The time-domain solution of the wide-angle parabolic equation including the effects of sediment dispersion*, J. Acoust. Soc. Am. 84, 2114-2125.

Collins, M. D. (1988). *FEPE User's Guide,* NORDA TN-365, Naval Ocean Research and Development Activity, Stennis Space Center, MS.

Collins, M. D. (1989). *Applications and time-domain solution of higher-order parabolic equations in underwater acoustics*, J. Acoust. Soc. Am. 86, 1097-1102.

Collins, M. D. (1990). *Benchmark calculations for higher-order parabolic equations,* J. Acoust. Soc. Am. 87, 1535-1538.

Collins, M. D. and Westwood, E. K. (1991). *A higher-order energy-conserving parabolic equation for range-dependent ocean depth, sound speed, and density,* J. Acoust. Soc. Am. 89, 1068-1075.

Collins, M. D. and Evans, R. B. (1992). *A two-way parabolic equation for acoustic backscattering in the ocean,* J. Acoust. Soc. Am. 91, 1357-1368.

Collins, M.D. (1993). *A split-step Pade solution for the parabolic equation method,* J. Acoust. Soc. Am. 93, 1736-1742.

Cornyn, J. J., (1973). *GRASS: A digital-computer ray-tracing and transmission-loss prediction system,*" NRL Report 7621.

Courant, R. and Hilbert, D. (1953). *METHODS OF MATHEMATICAL PHYSICS,* Volume 1, Interscience, New York.

DeSanto, J. A. (1979). *Derivation of the acoustic wave equation in the presence of gravitational and rotational effects,* J. Acoust. Soc. Am. 66, 827-830.

DiNapoli, F. R. (1971). *A Fast Field Program for Multilayered Media,* NUSC Technical Report 4103.

DiNapoli, F. R. and Deavenport, R. L. (1979). *Numerical mode of underwater acoustic propagation,* in OCEAN ACOUSTICS (Ed. DeSanto), Springer-Verlag, New York.

DiNapoli, F. R. and Deavenport, R. L. (1980). *Theoretical and numerical Green's function field solution in a plane multilayered medium,* J. Acoust. Soc. Am. 67, 92-105.

Dozier, L. B. and Tappert, F. D. (1978). *Statistics of normal mode amplitudes in a random ocean. I. Theory,* J. Acoust. Soc. Am. 63, 353-365.

Dozier, L. B. and Tappert, F. D. (1978). *Statistics of normal mode amplitudes in a random ocean. II. Computations*, J. Acoust. Soc. Am. 64, 533-547.

Dozier, L. B. (1982). *Numerical Solution of Coupled Mode Equations,* Report STD-N-076 (Science Applications, Inc., McLean, VA, May 1982).

Dozier, L. B. (1984). *PERUSE: A numerical treatment of rough surface scattering for the parabolic wave equation,* J. Acoust. Soc. Am. 75, 1415-1432.

Dozier, L. B., Hanna, J. S., and Pearson, C. R. (1991). *Treatments of incoherent scattering for the parabolic equation and ASTRAL propagation models,* in *OCEAN VARIABILITY & ACOUSTIC PROPAGATION*, J. Potter and A. Warn-Varnas (eds.), Kluwer Academic Publishers, the Netherlands.

Etter, P. C. (1991). *UNDERWATER ACOUSTIC MODELING: PRINCIPLES, TECHNIQUES AND APPLICATIONS,* Elsevier, New York.

Evans, R. B. (1983). *A coupled mode solution for acoustic propagation in a waveguide with stepwise depth variations of a penetrable bottom,* J. Acoust. Soc. Am. 74, 188-195.

Ewing, W. M., Jardetzky, W. S., and Press, F. (1957). *ELASTIC WAVES IN LAYERED MEDIA,* McGraw-Hill, New York, pp. 126-151.

Fawcett, J. A. (1992). *A Derivation of the Differential Equations of Coupled-Mode Propagation,* J. Acoust. Soc. Am. 92, 290-295.

Garabedian, P. R. (1964). *PARTIAL DIFFERENTIAL EQUATIONS*, Wiley, New York.

Goldstein, C. I. (1984). *The Numerical Solution of Underwater Acoustic Propagation Problems Using Finite Difference and Finite Element Methods*, NRL Report 8820, NRL-DC.

Greene, R. R. (1984). *The rational approximation to the acoustic wave equation with bottom interaction,* J. Acoust. Soc. Am. 76, 1764-1773.

Holmes, E. S. and Gainey, L. A. (1991). *Software Product Specification for the Parabolic Equation Model Version 3.3,* OAML-SPS-22, Sept. 10, 1991.

Jensen, F. and Krol, H. (1975). *The Use of the Parabolic Equation Method in Sound Propagation Modelling,* SACLANT ASW Research Centre Memo. SM-72.

Jensen, F. and Kuperman, W. (1980). *Review of Numerical Models in Underwater Acoustics,* NATO-SACLANTCEN, LaSpezia, Italy, Report 83.

Jensen, F. and Ferla, C. M. (1990). *Numerical solutions of range-dependent benchmark problems in ocean acoustics,* J. Acoust. Soc. Am. 87, 1499-1510.

Jensen, F. B. and Martinelli, M. G. (1985). *The SACLANTCEN parabolic equation model (PAREQ),* SACLANT Undersea Research Centre, La Spezia, Italy.

Kratsov, Yu. A., (1964). "*One modification of the geometric optics method,*" Soviet Radio Physics 1, 104-111.

Kuperman, W. A. and McDonald, B. E. (1986). *Linear and Nonlinear Ocean Acoustic Models,* in *OCEAN SEISMO-ACOUSTICS* (Akal and Berkson, Eds.), NATO Conference Series, Plenum Press, New York and London.

Kuperman, W. A., Porter, M. B., Perkins, J. S., and Evans, R. B. (1991). *Rapid computation of acoustic fields in three-dimensional ocean environments,* J. Acoust. Soc. Am. 89, 125-133.

Lee, D., Botseas, G., and Papadakis, J. S. (1981). *Finite-difference solution to the parabolic wave equation,* J. Acoust. Soc. Am. 70, 795-800.

Lee, D. and Botseas, G. (1982). *IFD: An Implicit Finite-Difference Computer Model for Solving the Parabolic Equation,* NUSC Tech. Rep. 6659, Naval Underwater Systems Center, New London, CT, 27 May 1982.

Lee, D. and McDaniel, S. T. (1983). *A finite-difference treatment of interface conditions for the parabolic wave equation: The irregular interface,* J. Acoust. Soc. Am. 73, 1441-1447.

Lee, D. and McDaniel, S. T. (1988). *Ocean Acoustic Propagation by Finite Difference Methods,* Pergamon, Oxford.

Lighthill, J. (1978). *WAVES IN FLUIDS,* Cambridge U. Press, Cambridge.

Ludwig, D. (1966). *Uniform Asymptotic Expansions at a Caustic,* Comm. Pure Appl. Math 19, 215-250.

Ludwig, D. (1968). *Strength of Caustics*, J. Acoust. Soc. Am. 43, 1179-1180.

Marsh, H. W. and Elam, S. R. (1967). Internal Document, Raytheon Co., Marine Research Laboratory, New London, CT.

McDaniel, S. T. and Lee, D. (1982). *A finite-difference treatment of interface conditions for the parabolic wave equation: The horizontal interface,* J. Acoust. Soc. Am. 71, 855-858.

McGirr, R. W., King, D. B., Davis, J.A., and Campbell, J., (1985). "*An evaluation of range-dependent ray theory models,*" NORDA Report 115.

McGirr, R. W., and King, D. B., (1989). "*Review of candidate shallow water propagation loss models,*" NORDA Technical Note 346.

Milder, D. M. (1969). *Ray and Wave Invariants for SOFAR Channel Propagation*, J. Acoust. Soc. Am. 46, 1259-1263.

Mitchell, A. R. and Griffiths, D. F. (1980). *The Finite Difference Method in Partial Differential Equations,* Wiley, New York.

Moore-Head, M. E., Jobst, W., and Holmes, E. S. (1989). *Parabolic-equation modeling with angle-dependent surface loss,* J. Acoust. Soc. Am. 86, 247-251.

Papas, T. T., (1988). "*A description of the RAYMODE propagation loss program with an analysis of its frequency characteristics,*" A&T Report No., P9623-88-1 (Analysis & Technology, Arlington, VA, circa 1988).

Pedersen, M. A. (1961).*Acoustic Intensity Anomalies Introduced by Constant Velocity Gradients,* J. Acoust. Soc. Am. 33, 465-474.

Pedersen, M. A. and Gordon, D. F. (1967). *Comparison of Curvilinear and Linear Profile Approximation in the Calculation of Underwater Sound Intensities by Ray Theory,* J. Acoust. Soc. Am. 41, 419-438.

Pekeris, C. L. (1948). *Theory of propagation of explosive sound in shallow water,* in *PROPAGATION OF SOUND IN THE OCEAN*, Geol. Soc. Amer. Mem. 27.

PHYSICS OF SOUND IN THE SEA (1946). Summary Technical Report of Division 6, National Defense Research Committee, Volume 8, Washington, DC (Republished by U.S. Navy in 1969 and GPO thereafter).

Porter, M. B. and Reiss, E. L. (1985). *A numerical method for bottom interacting acoustic normal modes*, J. Acoust. Soc. Am. 77, 1760-1767.

Porter, M. B. and Bucker, H. P. (1987). *Gaussian beam tracing for computing ocean acoustic fields,* J. Acoust. Soc. Am. 82, 1349-1359.

Porter, M. B. (1991). *The KRAKEN Normal Mode Program*, SACLANT Undersea Research Centre, La Spezia, Italy.

Porter, M. B., Jensen, F. B., and Ferla, C. M. (1991). *The problem of energy conservation in one-way models,* J. Acoust. Soc. Am. 89, 1058-1067.

Rayleigh, Lord (1896). *THEORY OF SOUND* (2 vols.), 2nd edn. London: Macmillan (1896); also, New York: Dover (1945).

Roberts, B. G., Jr. (1974). *Horizontal-gradient acoustical ray trace program TRIMAIN,* NRL Report 7827.

Rutherford, S. R. (1979). *An Examination of Coupled Mode Theory as Applied to Underwater Sound Propagation,* Report ARL-TR-79-44, ARL, Univ. of Texas.

Rutherford, S. R. and Hawker, K. E. (1981). *Consistent coupled mode theory of sound propagation for a class of nonseparable problems,* J. Acoust. Soc. Am. 70, 554-564.

Schmidt, H. (1987). *SAFARI: Seismo-Acoustic Fast field Algorithm for Range Independent environments*, SACLANT ASW Research Centre, La Spezia, Italy.

Schneider, H. G. (1993). *Surface loss, scattering, and reverberation with the split-step parabolic wave equation model,* J. Acoust. Soc. Am. 93, 770-781.

Smith, K.B. and Tappert, F.D. (1993). *UMPE: The University of Miami Parabolic Equation Model, Version 1.0*, MPL Technical Memorandum 432, Univ. of California, San Diego, Scripps Inst. of Oceanography, May 1993.

Solomon, L. P., Ai, D. K. Y. and Haven, G. (1968). *Acoustic propagation in a continuously refracted medium,* J. Acoust. Soc. Am. 44, 1121-1129.

Spofford, C. W. (1973). *The Bell Laboratories Multiple-Profile Ray-Tracing Program.*

Stickler, D. C. (1975). *Normal mode program with both the discrete and branch line contributions*, J. Acoust. Soc. Am. 57, 856-861.

Tango, G. J. (1988). *Numerical Models for VLF Seismic-Acoustic Propagation Prediction: A Review,* IEEE J. Ocean. Eng. 13, 198-214.

Tappert, F. D. (1977). *The parabolic approximation method,* in Keller, J. B. and Papadakis, J. S. (eds), *WAVE PROPAGATION AND UNDERWATER ACOUSTICS*, Lecture Notes In Physics, Vol. 70, Springer-Verlag, New York.

Tappert, F. D. and Nghiem-Phu, L. (1985). *A new split-step Fourier algorithm for solving the parabolic wave equation with rough surface scattering,* J. Acoust. Soc. Am. Suppl. 1 77, S101.

Tappert, F. and Ryan, F. (1989). *Full-wave bottom reverberation modeling,* J. Acoust. Soc. Am. Suppl. 1 86, AA5 (p. S65).

Tappert, F. D. (1991). *Sensitivity to c_0 for Parabolic-Type Approximations,* unpublished lecture notes.

Tappert, F. D. and Yamamoto, T. (1993). *An issue (sediment volume fluctuations) and a nonissue (shear wave propagation) in shallow water acoustics,* J. Acoust. Soc. Am. 93, No. 4, Part 2, 1aAO5 (p. 2268).

Thomson, D. J. and Chapman, N. R. (1983). *A wide-angle split-step algorithm for the parabolic equation*, J. Acoust. Soc. Am. 74, 1848-1854.

Titchmarsh, E. C. (1951). *A Relation Between Green's Functions,* J. London Math. Soc. 26, 31-36.

Weinberg, H. and Burridge, R. (1974). *Horizontal ray theory for ocean acoustics*, J. Acoust. Soc. Am. 55, 63-79.

Weinberg, H. (1975). *Application of ray theory to acoustic propagation in horizontally stratified oceans*, J. Acoust. Soc. Am. 58, 97-109.

Weinberg, H. (1981). *Effective range derivative for acoustic propagation loss in a horizontally stratified ocean*, J. Acoust. Soc. Am. 70, 1736-1742.

Wright, E. L. (1970). *Ray-tracing with horizontal and vertical gradients*, J. Acoust. Soc. Am. 48, 92(A).

Zienkiewicz, O. C. (1971). *The Finite Element Method in Engineering Science,* McGraw-Hill, New York.

8. ACRONYMS AND ABBREVIATIONS

ABS	Activated Bottom Sensor (Model)
AEAS	ASW Environmental Acoustic Support Project (PE603785)
AESD	Acoustic Environmental Support Detachment (of ONR)
AMEC	Acoustic Model Evaluation Committee
APL-MODE	The APL/JHU Normal Mode Model
ANDES	Ambient Noise Directionality Estimation System
APL/JHU	Applied Physics Laboratory/Johns Hopkins University
APP	Acoustic Performance Prediction (Program)
ARL:UT	Applied Research Laboratory of the University of Texas
ASAPS	Advanced Sensor Acoustic Prediction System (R&D version of SPARS)
ASEPS	Automated Signal Excess Prediction System
ASW	Anti-Submarine Warfare
ASWTDA	ASW Tactical Decision Aid (Program)
ASTRAL	ASEPS Transmission Loss (Model)
A&T	Analysis and Technology (Corporation)
AUAMP	Advanced Underwater Acoustic Modeling Program
AUAMP BASELINE	The AUAMP's wide-area multistatic active model.
BBN	Bolt Beranek and Newman, Inc.
BLUG	Bottom Loss UpGrade (Predecessor to LFBL)
BLUGTB	BLUG (loss vs angle) Table
CMOD	C (sound speed) Modification
CNO	Chief of Naval Operations
CNOC	Commander, Naval Oceanography Command
COSL	Commander Ocean Systems Atlantic
COSP	Commander Ocean Systems Pacific
CST	Critical Sea Test (Program)

CW	Continuous Wave, i.e. monochromatic wave
DBDB	Digital Bathymetric Data Base
DBDBn	DBDB at a resolution of n minutes in latitude and n minutes in longitude with n=5 or n=1 or n=0.5 etc.
DBDBC, DBDBS	Classified versions of DBDB at the Confidential level and Secret level respectively.
DREA	Defence Research Establishment Atlantic (Dartmouth, Nova Scotia)
DREP	Defence Research Establishment Pacific (Victoria, British Columbia)
DSP	Digital Signal Processing (chip)
EAMOS	Environmental and Acoustic Model Operating System
EVA	Environmental Acoustic(s)
FACT	Fast Asymptotic Coherent Transmission (Model)
FAME	Fast Multipath Expansion (Model)
FEPE	Finite Element PE (Model)
FFP	Fast Field Program (Model)
FFT	Fast Fourier Transform
FNOC	Fleet Numerical Oceanographic Center
GDEM	Generalized Digital Environmental Model
GEOSED	Geoacoustic Sediment (Thickness)
GFMPL	Geophysical Fleet Mission Program Library
GRASS	Germinating Ray-Acoustics Simulation System
GSM	Generic Sonar Model
HARPO	Hamiltonian Acoustic Raytracing Program, Ocean (Model)
HGI	High Gain Initiative
HOP	Historical Ocean Profile (data base)
ICAPS	Integrated Command (previously 'Carrier') ASW Prediction System

ICECAP	Ice Capable (Model)
ICECAUMP	Ice Capable AUAMP (Baseline) (Model)
IFDPE	Implicit Finite Difference PE (Model)
JHU/APL	Johns Hopkins University/Applied Physics Laboratory
KRAKEN(C)	Name of a model (not an acronym)
LFA	Low Frequency Active
LFBL	Low Frequency Bottom Loss
LFBLTB	LFBL (loss vs angle) Table
LFM	Linear Frequency Modulation
LRAPP	Long Range Acoustic Propagation Project (predecessor to AEAS)
MEDUSA	Name of a model (Not an acronym)
MGS	Marine Geophysical Survey
MIT	Massachusetts Institute of Technology
MPE	Multipath Expansion
MPL/SIO	Marine Physical Laboratory, Scripps Institute of Oceanography
MPP	Multiple Profile Program
N-96	Oceanographer of the Navy
NADC	Naval Air Development Center (predecessor to NAWC)
NAVSEA	Naval Sea Systems Command
NAVAIR	Naval Air Systems Command
NAVOCEANO	Naval Oceanographic Office
NAWC	Naval Air Warfare Center
NCCOSC	Naval Command Control & Ocean Surveillance Center (successor to NOSC)
NJIT	New Jersey Institute of Technology
NOARL	Naval Oceanographic and Atmospheric Research Laboratory (predecessor to NRL-SSC and successor to NORDA)
NOO	NAVOCEANO
NOPF	Naval Oceanographic Processing Facility

NOSC	Naval Ocean Systems Center (Succeeded by NCCOSC)
NRaD	NCCOSC RDT&E Division
NRL	Naval Research Laboratory
NRL-DC	NRL/Washington DC
NRL-SSC	NRL/Stennis Space Center MS
NRL-MONTEREY	NRL/Monterey CA
NUSC/NLL	NUSC/New London Laboratory
NUSC	Naval Undersea Systems Center
NUWC	Naval Undersea Warfare Center (Successor to NUSC)
ODE	Ordinary Differential Equation
OAML	Oceanographic and Atmospheric Master Library
ONR	Office of Naval Research
ONR(AESD)	Acoustic Environmental Support Detachment of ONR
ONT	Office of Naval Technology
OPTAMAS	Optimization of the Performance of Theater ASW Mobile Acoustic Sensors (Model)
PAREQ	Parabolic Equation (Model)
PDE	Partial Differential Equation
PE	Parabolic Equation (approximation to the wave equation) Also, any of several models solving the parabolic approx.
PERUSE	PE Rough Surface (Model)
POSSM	Panel on Sonar System Models
RAYMODE	The RAYMODE Navy Standard Model
RBR	Refracted, Bottom-Reflected
RR	Refracted
RSR	Refracted, Surface-Reflected
SACLANT	Supreme Allied Commander, Atlantic (NATO)
SACLANTCEN	SACLANT Undersea Research Centre (LaSpezia, Italy)
SAFARI	Seismo-Acoustic Fast Field Algorithm for Range-Independent Environments

SAIC	Science Applications International Corporation
SEAS	Surveillance Environmental Acoustic Support (predecessor of AEAS)
SFMPL	Submarine Fleet Mission Program Library
SIO	Scripps Institute of Oceanography
SIMAS	Sonar In-Situ Mode Assessment System
SNAP	SACLANTCEN's Normal Mode Acoustic Propagation (Model)
SPAWAR	Space and Naval Warfare Systems Command
SPARS	System for the Prediction of the Acoustic Response of Sensors (formerly Response of SOSUS/SURTASS)
SYNBAPS	Synthetic Bathymetric Profiling System
SYSCOR	System Correction
TAEAS	Tactical ASW Environmental Acoustic Support (a predecessor of AEAS)
TDPE	Time Domain PE
TESS	Tactical Environmental Support System
TL	Transmission Loss
UNIMOD	Unified Model (for TL)
VLA	Vertical Line Array
VLF	Very Low Frequency
WC	Wright-Colborn water-mass sound-speed data base
WKB	Wentzel Kramers Brillouin
WRAP	Wide-Area Rapid Acoustic Prediction (Model)